ABSTRACT

Title of Dissertation:	TRANSLOCATION OF PROTEIN CARGO INTO *CANDIDA ALBICANS* USING CELL-PENETRATING PEPTIDES
	Sayanee Adhikari, Doctor of Philosophy, 2020
Dissertation directed by:	Professor Amy J. Karlsson, Department of Chemical and Biomolecular Engineering

Fungal infections caused by *Candida albicans* pose a serious threat to public health. The rising drug resistance towards azoles, the current first-line antifungal treatment, warrants novel approaches to designing and delivering new antifungal agents that target *C. albicans* cells.

To increase the intracellular delivery of bioactive molecular cargo, we studied the use of cell-penetrating peptides (CPPs) as delivery vehicles. CPPs have been extensively used to deliver different cargoes into mammalian cells, but limited work has focused on delivery into fungal cells. To improve understanding of CPP-mediated

delivery to *C. albicans*, we studied their ability to deliver green fluorescent protein (GFP) intracellularly.

For our work, we chose the CPPs, MPG and Hst5, that have previously shown translocation into fungal cells without cargo and recombinantly produced these CPP fusions to GFP in *Escherichia coli*. We investigated the CPP-mediated translocation of GFP using flow cytometry. Fusion of GFP to MPG resulted in translocation into 40% of *C. albicans* cells, which was significantly higher than 13% cells that demonstrate translocation of GFP without a CPP. However, Hst5 did not translocate GFP into cells, with only 5% of cells exhibiting Hst5-GFP translocation. Our results demonstrate that MPG can deliver GFP, while Hst5 is not as promising. These results are consistent with molecular dynamics simulations that show MPG enters a model membrane preferentially with the N-terminal residues, whereas Hst5 fails to enter the membrane. Our results emphasize the potential of CPPs in delivering large cargo to *C. albicans* cells and the advantage of using both experiments and simulations to study the translocation of CPPs into *C. albicans*.

To explore factors affecting translocation efficacy, we evaluated the aggregation of CPP-GFP fusion constructs. Using dynamic light scattering and interference scattering microscopy, our results identified aggregation of our fusions at high concentration as a possible limitation to translocation, motivating future studies of the causes of aggregation and its relationship to translocation efficiency.

Our work has shown that CPPs can deliver large biomolecular cargo into fungal cells and has laid the foundation for further studies to design better CPPs and to explore mechanisms limiting translocation of CPPs into fungal pathogens.

TRANSLOCATION OF PROTEIN CARGO INTO *CANDIDA ALBICANS* USING CELL-PENETRATING PEPTIDES

by

Sayanee Adhikari

Dissertation submitted to the Faculty of the Graduate School of the
University of Maryland, College Park, in partial fulfillment
of the requirements for the degree of
Doctor of Philosophy
2020

Advisory Committee:
Professor Amy J. Karlsson, Chair
Professor Jeffery B. Klauda
Professor Ganesh Sriram
Professor Taylor J. Woehl
Professor Birthe V. Kjellerup

Dedication

I dedicate my Ph.D. Dissertation to my parents Mr. Sujit Kumar Adhikari and Mrs. Basabi Adhikari, and my husband Angshuk Chakraborty. Thank you, God, for helping me become who I am today.

Acknowledgements

The past 5 years in the Karlsson Lab has been an unbelievable experience. This journey would not be possible without my advisor, Dr. Amy Karlsson. I would like to take this opportunity to express my gratitude for your constant mentoring, support and encouragement. Your faith in me has built the basis of my research projects, has helped me through many ups and downs, and helped me to become an independent researcher.

I am thankful to my committee members Dr. Jeffery Klauda, Dr. Ganesh Sriram, Dr. Taylor Woehl and Dr. Birthe Kjellerup for your guidance and support.

I am extremely grateful to be a part of the Karlsson Lab. These are a few of the nicest people in the lab that I have met. I would like to thank my previous team members and wonderful friends Dr. Zifan Gong, Dr. Svetlana Ikonomova and Dr. Parisa Moghaddam-Taaheri for supporting me in my initial years in the lab. You have always been there for me and I don't have adequate words to express my appreciation towards you. I would also like to thank Mahdi Ghorbani for being a good friend and for being a source of creative brainstorming. Thank you to Jesse Leissa for the constantly helping me in the lab and keeping the lab organized. Marzyeh Kheradmand-Hajibasi and Jiwon Wu recently joined our lab and has been instrumental in shaping up a lot of the experiments. I have been closely working with them for the past few months and they both have learned things very quickly and efficiently. They have good-naturedly listened to all my experiences in the lab and I trust that they will be very successful with all they do. Wish you both a very good luck! I would also like to take this opportunity to thank all the undergrads and the high-school students in the lab. Turki Alahamadi, Katherine Dura and

Rosemary Iwuala for all their help in the project. Thank you Dinara Konakbayeva, Wright Makambi, Katherine Sniezek, Andrea Fox, and Funke Okunrinboye for making the lab an enjoyable place.

In addition to members of the lab, I need to thank all others who have been instrumental in my PhD journey. I would like to thank Niti Agrawal who has always stood by me all these years in a journey that we started together and are at a stretch where we embark on the next phase. I want to thank Shakiba Nikfarjam who has been a great friend and helped me with my research projects. Dr. Derrick Ko and Dr. Viviana Monje-Galvan have been great friends. Thank you to Dan Lugar for being an amazing friend and listening to my grumbles.

Most essentially, I want to thank my friends and family. Thank you to my parents for the overwhelming love, inspiration, faith and pride for the past so many years; without you I would not have been here. Every bit of my success belongs to you. Thank you to my uncle for enabling me to realize my dreams and work towards achieving them. I am thankful to my sister and brother-in-law, for being there always. Thank you to my husband and my best friend, for being supportive and for trusting in my abilities. Finally, thank you to all my friends without whose friendship and constant support I wouldn't be here today.

I would also like to thank the National Science Foundation (CBET Award #1511718) for making this work possible. I would like to thank Dr. Xianbing Zeng and Kenneth Class and for their help with the flow cytometry, and Dr. Dorothy Beckett for help with CD experiments. I would also like to thank Dr. John Fisher's lab for their help in the fluorescence assays. I would also like to thank Dr. Mikhail Anisimov for his help with Dynamic light Scattering studies.

Table of contents

Dedication ii

Acknowledgements iii

Table of contents v

List of tables xi

List of figures xii

List of abbreviations xiv

Chapter 1: Background and motivation 1

1.1 Fungal pathogen C. albicans and existing treatments 2

1.2 Cell-penetrating peptides (CPPs) 5

1.3 CPPs, their classifications and mechanism of entry 6

1.4 CPP as delivery vectors 9

1.4.1 Delivery of proteins as a cargo 10

1.4.2 Delivery of nucleic acids as a cargo 11

1.4.3 Delivery of nanoparticles as cargo 12

1.4.4 Delivery of small-molecule drugs as cargo 13

1.5 Overview of thesis 14

1.6 References 16

Chapter 2: Methods to engineer peptides 27
2.1 Introduction 27
2.2 Approaches for introducing and screening diversity 29
2.2.1 Rational design 30
2.2.2 Directed evolution 32
2.2.3 Computational methods 36
2.3 Protein engineering to design peptide characteristics 38
2.3.1 Thermodynamic stability 39
2.3.2 Self-assembly 42
2.3.3 Reduced aggregation 44
2.3.4 Proteolytic stability 48
2.3.5 Binding affinity and specificity 51
2.4 Perspective on future directions for peptide engineering 54
2.5 Design strategies pertaining to present study 56
2.6 Conclusion 59
2.7 References 60
Chapter 3: Translocation of CPP-cargo protein fusions into *Candida albicans* cells 69
3.1 Introduction 70
3.2 Methods and materials 73
3.2.1 Construction of plasmids 73
3.2.2 Construction of CPP-cargo protein fusion constructs 76
3.2.3 Bacterial strains and protein expression conditions 77

3.2.4 Protein extraction and purification 77
3.2.5 Quantification of translocation into *C. albicans* 78
3.2.6 Measurement of relative fluorescence unit (RFU) using a fluorescent plate reader 80
3.2.7 Circular dichroism to study secondary structure of protein fusions ... 81
3.2.8 Simulation method to study translocation of peptides 81
3.3 Results and discussion 82
3.3.1 Detection of fusions inside *Candida albicans* cells 84
3.3.2 Fluorescence intensity measurements of purified GFP, MPG-GFP and Hst5-GFP 90
3.3.3 Simulation results to better understand experimental data 92
3.3.4 Secondary structure of proteins 95
3.3.5 Design of MPG variants to increase translocation 97
3.4 Conclusion 99
3.5 References 101
Chapter 4: Design CPP variants for translocation of CPP-cargo protein fusions into *Candida albicans* cells 105
4.1 Introduction 105
4.2 Methods for introducing design changes to peptides 110
4.2.1 Cloning of plasmids 110
4.2.2 Construction of CPP-cargo protein fusion constructs 110
4.2.3 Bacterial strains, expression conditions and purification 112

4.2.4 *C. albicans* strain and culture conditions 113
4.2.5 Quantification of translocation into *C. albicans* 114
4.3 Results and discussion 115
4.3.1 Design of MPG modifications 115
4.3.2 Expression and purification of MPG variants 117
4.3.3 Translocation of MPG variants into *C. albicans* cells 118
4.4 Discussion and conclusion 120
4.5 References 122
Chapter 5: Aggregation of fusion proteins 124
5.1 Introduction 124
5.2 Methods to study aggregation 128
5.2.1 Purification of proteins 128
5.2.2 Dynamic light scattering (DLS) to study aggregation 129
5.2.3 Interferometry to study aggregation 131
5.2.4 Study of aggregation using dynamic light scattering 133
5.2.5 Study of aggregation using interferometric scattering microscopy 137
5.2.6 Possible ways of mitigating aggregation 140
5.3 Conclusion 143
5.4 References 144
Chapter 6: Conclusion and future work 148
6.1 Detection of fusions inside Candida albicans cells for non-fluorescent cargo 149

6.1.1 Detection of fusions inside *Candida albicans* cells for non-fluorescent cargo using Western blot 149

6.1.2 Split complementation assay for assessment of functional delivery of cargo 152

6.2 Use of Directed evolution to design CPPs for enhanced translocation 155

6.3 Use of machine learning as a tool to design new and better CPPs to target fungal pathogens 156

6.4 Evaluation of CPP-mediated translocation with C-terminal attachment of cargo 159

6.5 References 161

Table A1 - Statistical analysis of Measurement of relative fluorescence unit (RFU) 165

Table A2 - Statistical analysis of Relative translocation – comparison between samples 167

Table A3 - Statistical analysis of Relative translocation – comparison between time points 169

Table A4 - Statistical analysis of Measurement of relative fluorescence unit (RFU) 171

References for Chapter 1 172

References for Chapter 2 183

References for Chapter 3 192

References for Chapter 4 196

References for Chapter 5 198

References for Chapter 6 202

List of tables

Chapter 1. Background and motivation

Table 1.1 Cell-penetrating peptides, their origin and type ……7

Chapter 3. Translocation of CPP-Cargo Protein Fusions into *Candida albicans* Cells

Table 3.1 CPPs used in the present study ……71
Table 3.2 Oligonucleotides used in this study ……74
Table 3.3 Membrane lipid composition……82

Chapter 4. Design CPP variants for translocation of CPP-Cargo Protein Fusions into *Candida albicans* Cells

Table 4.1 Oligonucleotides used in this study ……111
Table 4.2 CPPs variants used in the present study…… 116
Table 4.3 Translocation of proteins into *C. albicans* measured at 24 h …… 119

Chapter 5. Aggregation of fusion proteins

Table 5.1 Hydrodynamic radius analysis ……135

List of figures

Chapter 1. Background and motivation

Figure 1.1 *Candida albicans* in yeast and hyphal form ·····1
Figure 1.2 Antifungal drugs frequently to treat fungal infections caused by *C.albicans*····· 2
Figure 1.3 Schematic representation of reasons for resistance to azoles·····4
Figure 1.4 Cell penetrating peptides and mechanism of cell entry ·····5

Chapter 2 Literature review – methods to engineer peptides

Figure 2.1 Selection approach to design a peptide ·····30
Figure 2.2 Key properties to engineer ····· 39
Figure 2.3 Peptide engineering design on-demand ·····56

Chapter 3. Translocation of CPP-Cargo Protein Fusions into *Candida albicans* Cells

Figure 3.1 Yeast form of *Candida albicans* ·····70
Figure 3.2 Plasmid map of pNGST ····· 74
Figure 3.3 Representation of GST-CPP-cargo protein fusion construct ····· 83
Figure 3.4 Purification of GFP, Hst5-GFP and MPG-GFP ····· 84
Figure 3.5 Translocation of proteins ····· 86
Figure 3.6 Translocation studies data for 1 h – 24 h ····· 88
Figure 3.7 Cellular uptake studies ····· 89
Figure 3.8 Measurement of relative fluorescence unit (RFU) ····· 91
Figure 3.9 Comparison of full-membrane model and HMMM model ·····93
Figure 3.10 Translocation of CPPs using HMMM membrane model at various time points ·····94
Figure 3.11 Insertion of peptides into the model membrane ····· 95
Figure 3.12 CD spectra of CPPs (0.5 μM) in sodium phosphate buffer ····· 96
Figure 3.13 Interaction energies of MPG (native) residues·····98

Chapter 4. Design CPP variants for translocation of CPP-Cargo Protein Fusions into *Candida albicans* Cells

Figure 4.1 Purification of T14K-GFP ····· 118

Chapter 5. Aggregation of fusion proteins

Figure 5.1 Schematic representation of multilayered interferometric scattering microscopy sensor to describe optical scattering and interference·····127
Figure 5.2 DLS analysis for correlation function and hydrodynamic radius····· 134
Figure 5.3 Interferometry images of Hst5-GFP and MPG-GFP····· 138

Chapter 6. Conclusion and Future Work

Figure 6.1 Detection of proteins inside *C. albicans* using anti-GFP ·····150
Figure 6.2 Representation of GFP complementation assay ·····152
Figure 6.3 Protein-protein interactions ····· 153
Figure 6.4 Illustration of GFP complementation assay ·····154
Figure 6.5 Construct design for translocation into *C. albicans* ····· 160

List of abbreviations

AMP	Antimicrobial peptides
BCCP	Biotin carboxyl carrier protein
CAPDE	Computer-aided protein directed evolution
CDC	Centers for Disease Control and Prevention
CFU	Colony-forming unit
CPP	Cell-penetrating peptide
DNA	Deoxyribonucleic acid
FAM	Carboxyfluorescein
FPLC	Fast protein purification liquid chromatography
GFP	Green fluorescent protein
G_4S	Glycine-serine linker
GST	Glutathione S-transferase
Hst-5	Histatin 5
HRP	Horse-radish peroxidase
IEX	Ion exchange chromatography
IMAC	Immobilized metal affinity chromatography
IPTG	Isopropyl β-D-1-thiogalactopyranoside
ISM	Iterative saturation mutagenesis

LB	Lysogeny broth
MD	Molecular dynamics
NaCl	Sodium chloride
NaPB	Sodium phosphate buffer
OD	Optical density
PBS	Phosphate-buffered saline
PI	Propidium iodide
PCR	Polymerase chain reaction
RNA	Ribonucleic acid
SEC	Size exclusion chromatography
YPD	Yeast extract-peptone-dextrose medium
POPC	1-palmitoyl-2-oleoyl-sn-glycero-3-phosphocholine
POPG	1-palmitoyl-2-oleoyl-sn-glycero-3-phosphatidylglycerol

Chapter 1: Background and motivation

Fungal infections caused by the opportunistic pathogen *Candida albicans* (Figure 1.1) are a reason for concern for immunocompromised patients as they cause cutaneous and mucosal infections and systemic diseases[5, 6]. Infection due to *C. albicans* can be fatal, and growing drug resistance has contributed to ineffective treatment[5, 7]. Thus, new therapeutic approaches are needed. One important feature will be the ability of effectively and specifically being delivered across cell membranes to intracellular targets. *Candida albicans* is a dimorphic yeast organism (Figure 1.1) and can exist as unicellular round budding yeast cells or as multicellular elongated hyphae[8] and is a well-known human pathogen that causes infections in people with compromised immune systems. For people with HIV/AIDS, people undergoing chemotherapy, and people with diabetes, *C. albicans* can cause serious systemic infections that are difficult to treat and have a high mortality rates[9]. Although, current antifungal agents exist toxicity and the increasing drug resistance are an issue which can delay the preliminary diagnosis of fungal infections [10, 11] and motivates finding of new approaches before resistance is a bigger problem than it is currently.

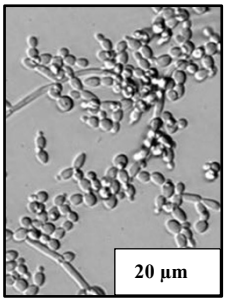

Figure 1.1. *Candida albicans* in yeast and hyphal form. The scale bars represent 20 µm. Used with permission from Dr. Amy J. Karlsson.

1.1 Fungal pathogen C. albicans *and existing treatments*

Polyenes and azoles are the primary treatment options for fungal diseases[7, 12] (Figure 1.2). Amphotericin B, a polyene, has been recognized to cause significant kidney toxicity over extended period of use[1, 12]. Amphotericin B, interacts with the membrane sterol, ergosterol and produces aqueous pores containing an annulus of eight amphotericin B molecules that are coupled hydrophobically to the membrane sterols[1, 13, 14]. This attachment forms a pore and the polyene hydroxyl residues face inward, that leads to transformed permeability, followed by escape of fundamental cytoplasmic components, and thus the death of the organism[1, 15, 16]. Polyenes have also been known to cause oxidative damage that aids in killing of *C. albicans*[1, 17].

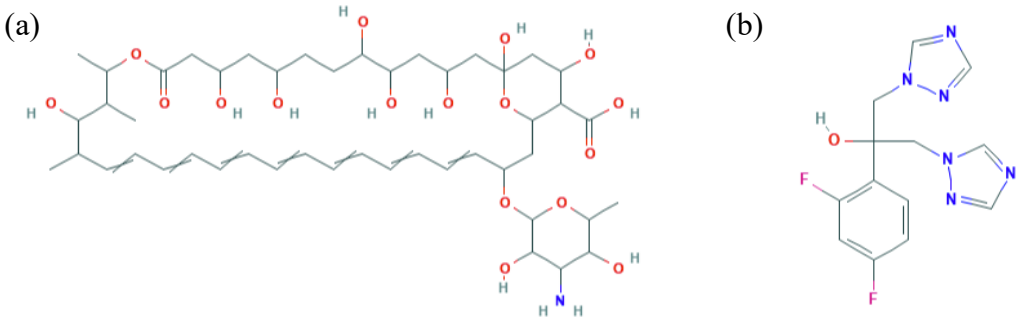

Figure 1.2. Antifungal drugs frequently to treat fungal infections caused by *C. albicans*. (a) Amphotericin B[3] (b) Fluconazole[5].

Ergosterol is the important part of a fungal cell membrane[18]. The key target of azoles is the heme protein, which co-catalyzes cytochrome P-450-dependent 14α-demethylation of lanosterol[1, 19]. When 14α-demethylase is inhibited, it leads to

reduction of ergosterol and buildup of sterol precursors, that includes 14α-methylated sterols (lanosterol, 4,14-dimethylzymosterol, and 24-methylenedihydrolanosterol), and results in the formation of a plasma membrane with transformed structure and function. The antifungal activity of the azoles, fluconazole, itraconazole, and voriconazole, can be attributed to in part the inhibition of cytochrome P-450-dependent 14α-sterol demethylase [1, 20].

The Centers for Disease Control and Prevention (CDC), listed azole-resistant *Candida* species a reason for concern[21]. *Candida* pathogens become resistant to the azoles due to various reasons (Figure 1.3). For example, (a) target enzyme is overproduced, thus the drug does not impede the biochemical reaction completely; (b) drug target is changed so that the drug does not bind to the target; (c) an efflux pump, pumps out the drug; (d) access of the drug inside is stopped at the cell membrane or wall level; (e) cell takes a bypass pathway to balances for the loss-of-function inhibition due to drug action; (f) fungal enzymes that might convert an inactive drug to its active form is inhibited; (g) cell produces enzymes into the extracellular medium, that destroy the drug.

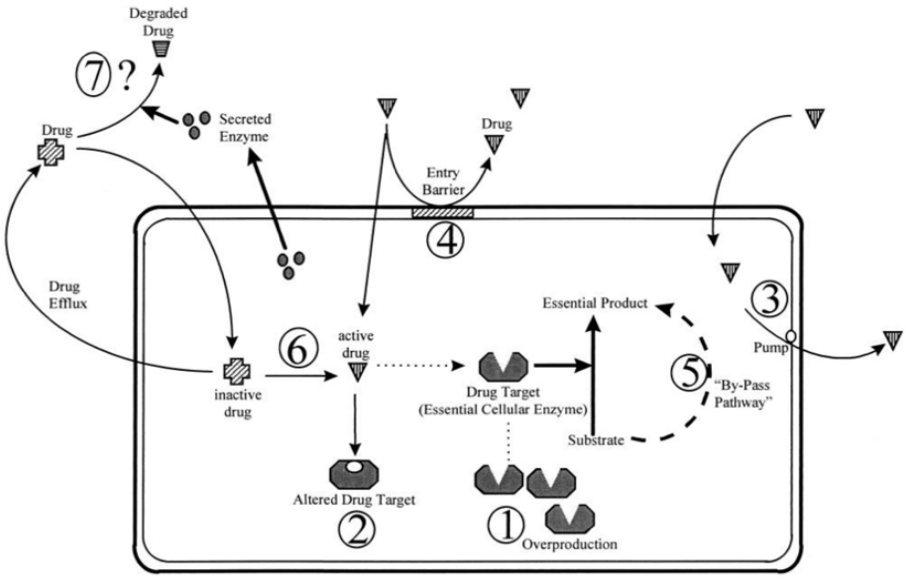

Figure 1.3. Schematic representation of reasons for resistance to azoles. The reasons include 1) Target enzyme is overproduced 2) Drug target is changed so that there is no binding 3) Efflux pump, pumps the drug 4) Entry prevented at cell membrane or cell wall 5) Compensation of loss-of-function inhibition by bypass 6) inhibition of fungal enzymes that converts inactive drug to its active form 7) Secretion of enzymes to the extracellular medium that degrades the drug. Figure reprinted with permission from Ghannoum *et al.* Copyright © 1999, American Society for Microbiology[2]

Though polyenes like amphotericin B, and azoles like fluconazole along with other drugs are efficient at treating fungal infections, their side effects and drug resistance mandate new therapeutic approaches. With continued use of these traditional treatments, the pathogen might develop more robust mechanisms to resist the fungal therapies thus increasing the risks of infection and thus fatality. This warrants the study of newer and novel drugs and drug delivery vehicles that that can cure fungal infections without causing the side-effects or drug resistance.

1.2 Cell-penetrating peptides (CPPs)

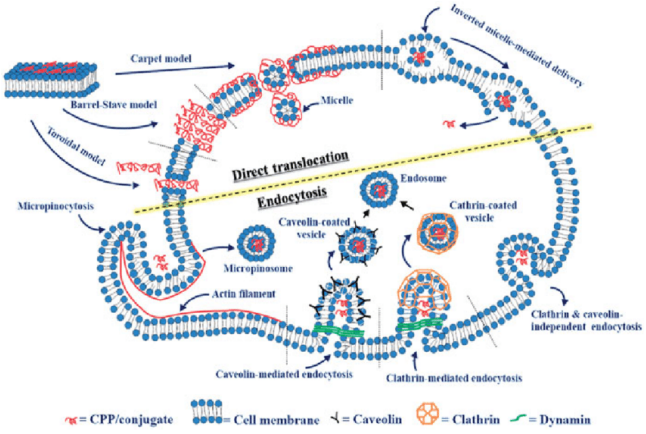

Figure 1.4. Cell penetrating peptides and mechanism of cell entry. Figure adapted from Singh et al.[6] (Open access journal. Creative commons license http://creativecommons.org/licenses/by/4.0/)

Though current antifungal treatments exist, due to problems associated with these treatments, we propose the use of cell-penetrating peptides (CPPs) as delivery vectors to transport our cargo inside the cells. As compared to other methods like microinjection, electroporation and magnetofection (biophysical methods) or use of amphipathic detergents (biochemical methods), and viral vectors[22, 23], CPPs can efficiently enter cells in a noninvasive and safe manner without destroying the integrity of the cellular membranes[23]. Consequently, this opens up newer possibilities for research in life sciences[23, 24]. Cell-penetrating peptides are short peptides, about 30 amino acids in length, mostly cationic, have the ability to cross cell membranes, and at the same time carry small biomolecular cargo across the barrier[23, 25-27] (Figure 1.4). These CPPs are also known as protein translocation domain (PTD) or Trojan horse peptides. These peptides are comparatively less toxic as compared to other drug delivery vehicles like virus vectors and can be easily synthesized, characterized and functionalized[27-30]. These CPPs have transported various cargoes like

DNA, proteins, nanoparticles and small molecules and thus can be used to target intracellular targets which is necessary for their biological activity [31-37] [37, 38,39-43].

1.3 CPPs, their classifications and mechanism of entry

CPP can be classified into different categories based on their origin or their physical-chemical character. Based on origin, CPPs can be divided into either protein-derived or synthetic; whereas based on their characteristics these CPPs can be divided into three subgroups: amphipathic, cationic and hydrophobic (Table 1 lists some examples of various CPPs)[44]. Further, they can be classified as primary amphipathic, secondary amphipathic and non-amphipathic based on their sequence, length, and association with lipids[44, 45]. Primary amphipathic peptides such as pep-1 and TP10 have hydrophobic and cationic residues segregated at the sequence level[46-50]. On the other hand, in secondary amphipathic CPPs like penetratin, cationic and hydrophobic residues are only segregated when the peptide folds into a secondary structure[51]. We are studying the use of CPPs which have the ability to cross cellular membranes by experimental and computational methods (Figure 1.4)[52,53,54,29,55]. Cationic CPPs do not interact with uncharged model membranes and does not interfere with the integrity of the plasma membrane of cells[23, 49, 50, 56]. On the contrary, primary amphipathic CPPs interact with model neutral membranes and when they interact with the plasma membrane, it interferes with the packing. This is a concentration-dependent interaction and at higher

concentrations, amphipathic CPPs stimulate the influx of Ca^{2+} ions into the cytosol. This influx triggers a repair response by the cells[44, 57].

Table 1.1 Cell-penetrating peptides, their origin and type (selected information is reproduced from Pooga et al.[44])

Sequence	Name (origin)	Type[a]	Reference
Cationic			
RKKRRQRRR	HIV-1 pTat(49–57)	N	58
RRRRNRTRRNRRRVR[b]	FHV coat	N	59,60
TRQARRNRRRRWRERQR[b]	HIV-1 Rev	N	59,127
RQIKIWFQNRRMKWKK	Penetratin	N	52
$(R)_n$[b]**; n = 6–12**	Polyarginine	S	59,46
Amphipathic			
LLIILRRRIRKQAHAHSK[b]	pVEC	N	61
KFHTFPQTAIGVGAP[b]	hCT peptide18-32	N	62
KETWWETWWTEWSQPKKKRKV[c]	Pep-1	C	63
GALFLGFLGAAGSTMGA[c]	MPG	C	33
GWTLNSAGYLLGKINLKALAALAKKIL[b]	Transportan	C	64
AGYLLGKINLKALAALAKKIL[b]	TP10 (transportan analogue)	C	65
KLALKALKALKAALKLA[b]	MAP (model amphipathic peptide)	S	66
QLALQLALQALQAALQLA	MAP17	S	67
Palmitoyl-KIHKKGMIKS	$F2Pal_{10}$	S	68
Hydrophobic			
AAVLLPVLLAAP	K-FGF	N	69
PFVYLI	C105Y	N	70
SDLWEMMMVSLACQY	Pep-7	S	71
PLILLRLLRGQF	Pept1	S	72
Anionic			
LKTLTETLKELTKTLTEL	MAP12	S	73
VELPPPVELPPPVELPPP	SAP(E)	S	74

[a]N natural, C chimeric, S synthetic; [b]C-terminal amide; [c]C-terminal cycteamide

There are different mechanisms for translocation of CPPs into cell membranes (Figure 1.4). Translocation of the peptide–cargo complex on the plasma membrane can

be through direct translocation[75], endocytic or non-endocytic routes. Endocytic routes of translocation comprise macropinocytosis, clathrin-mediated endocytosis, caveolae/lipid raft-mediated endocytosis, and clathrin/caveolae-independent endocytosis[38, 76, 77]. Endocytosis is the method by which cells take up living matter and form a vacuole. Clathrin-mediated endocytosis and caveolae-mediated pinocytosis are both receptor-mediated endocytosis processes which need membrane receptors to allow vesicles formation[78] for example receptors like receptors for growth factors and G-protein coupled receptors whereas the process of micropinocytosis, does not need a receptor[79]. An inverted micelle model, carpet model, and the pore formation model are part of the non-endocytic routes[30, 80]. For the inverted micelle model, the CPPs with hydrophobic amino acids are critical for the translocation process[80]. Electrostatic interactions between the CPP and the negatively charged membrane phospholipids leads to insertion into the membrane, and the interaction leads to formation of vesicles and capture of the CPP[81]. In the carpet model, the peptide binds to negatively charged phospholipids, is followed by rotation of the peptide that allows interaction between the hydrophobic residues of the peptide and the membrane. Subsequently, a disruption in the packing of the membrane allows internalization of the peptide[28]. The pore formation or barrel-stave model relates to development of bundles by amphipathic α-helical peptides. The barrel-stave model is typical of amphipathic α-helical peptides - the peptides form bundles after their interaction with the cellular membrane (membranes have channels in the centers)[23]. A pore forms due to the interaction between hydrophilic surfaces that face inward and the hydrophobic residues, facing

outward, with the lipid membrane[23, 28]. This interaction happens at concentration of the peptides that is higher than a threshold concentration (this concentration differs for each peptide)[28]. A toroidal model pertains to peptides that can form α-helices as they come in contact with cell membranes. In this type of model, the positive side chains of the peptide interact with the membrane phosphate groups, leading to the buildup of the peptide on the external leaflet of the membrane[23, 82]. The peptides at this point causes twisting of the lipid monolayer into the inside, that forms a hydrophilic break in the membrane, wherein the phospholipid heads and peptides are found[23, 82]. Peptides like MAP, SynB, PAF26 are transported by energy-dependent endocytic mechanisms; pVEC and penetratin employ micropinocytosis while others like MPG and Pep-1 undergo pore formation[47, 66, 83-87].

1.4 CPP as delivery vectors

The first CPP Tat was first revealed in 1989[58, 88], and since then researchers have extensively studied CPPs to utilize them as delivery vectors[34, 89]. CPPs have favorable advantages and can deliver cargoes with high efficiency and specificity[89]. CPPs can deliver a variety of biomolecules that includes DNA, siRNA, proteins, and nanoparticles[31-37 38-43]. CPPs have been seen to also deliver contrast agents for example quantum dots and metal chelates for cell imaging[90, 91]. The cargo can be linked to a

peptide when it is covalently conjugated to the peptides either by chemical reaction or recombinant expression.

1.4.1 Delivery of proteins as a cargo

Peptides and proteins can be useful as therapeutics and thus can help cure infections and diseases. Researchers have been using CPPs to transport protein cargos of variable sizes that range from 25 kDa for example scFv[41] to a size of 150 kDa that includes IgG[40]. Delivery of antibody fragments by CPPs like Tat and penetratin have shown tissue localization *in vivo* [92]. CPPs have also been shown to be effective in delivering therapeutic proteins to treat cancer and strokes for example, Tat and penetratin have delivered elastin-like polypeptides that is fused to a cyclin-dependent kinase inhibitor that inhibited the growth of cancer cells[93]. CPPs have been useful in delivering to various types of cells that include mammalian, fungal and bacterial cells[42, 94, 95] and thus can be used for drug delivery.

Penetratin has also been used to reduce blood glucose concentration. On administering insulin and penetratin simultaneously in rats, it led to a considerably higher increase in bioavailability and reduction of blood glucose, while just insulin alone did not lead to a decrease in blood glucose concentration[96, 97]. All these examples

show that on successful delivery of proteins inside cells with CPPs, many diseases can be targeted and cured.

1.4.2 Delivery of nucleic acids as a cargo

CPPs can deliver siRNA, antisense oligomers, and plasmids but intracellular transport is sometimes limited due to high molecular weight and negative charges, making the regulation of gene expression easier[98]. Recombinant lactaptin has been shown to deliver noncovalently bonded nucleic acids into cancer cells *in vitro*[99]. Various CPPs like transportan, penetratin, amphipathic peptides (for example MPG), and polyarginine have been used considerably, to deliver siRNA into animal and plant cells[32, 100-108,48,109]. When CPPs cross the cell membrane and deliver macromolecular cargoes, the process is known as protein transduction[110, 111]. Stearylation of arginine-rich CPPs have shown to drastically increase transduction efficiency of plasmid DNA[112, 113]. CPPs like Tat has been used to carry the gene for GFP into mammalian cells with a high transfection efficiency and biological activity[114]. MPG has been shown to deliver siRNA into mammalian cells, that enabled fast release of the siRNA into the cytoplasm and promoted robust down-regulation of target mRNA[105]. These examples show how CPPs, when conjugated covalently or non-covalently with nucleic acids, can be used as delivery vectors to reach target sites.

1.4.3 Delivery of nanoparticles as cargo

In general, treatment of diseases with drugs can lack specificity and can have toxic side-effects. Thus, CPPs have been studied in conjunction with nanoparticles for treatment of cancer. TGN when conjugated to poly (ethyleneglycol)-poly (lactic-co-glycolic acid) (PEG-PGLA) nanoparticles, was able to cross the blood brain barrier and transport coumarin-6 as a probe into the brain at 3.6-fold times higher than nanoparticles alone[115]. To further study the effects off CPP-conjugated nanoparticles delivery, researchers synthesized a self-assembled drug-polymer that consisted of MMP2 cleavable peptide and TAT protected by PEG and Paclitaxel. The nanostructure accrued in the tumor sites and when the cleavable MMP2 peptide was broken, it exposed the TAT that helped cell internalization followed by drug release[116, 117]. In another study, Wang et al. have used cationic antimicrobial peptides to treat multiple-drug resistant infections[118]. They studied the cholesterol-conjugated G3R6TAT (CG3R6TAT) cationic nanoparticles, and demonstrated the use of nanoparticles for treatment of *Cryptococcus neoformans* (yeast)-induced brain infections. The antifungal activity of the nanoparticles was compared with amphotericin B and fluconazole. Minimum inhibitory concentrations (MICs) of the nanoparticles were measured and they found them to be much lower than those of fluconazole but marginally higher than those of amphotericin B in some samples. The nanoparticles were shown to entirely sterilize *C. neoformans* after 3.5 h at a concentration three times the MIC. Thus, the

study showed that CG3R6TAT nanoparticles are a promising antifungal agent for treatment of brain infections.

Quantum dots (QD) have previously shown to have poor penetration in cells but researchers have been able to overcome that when attached to a CPP. This work showed that when QD was conjugated with arginine-rich CPP, they were taken up by living cells *in vitro* [119]. All the above examples show the innumerable applications of CPPs and thus these can be used to effectively deliver nanoparticles and can be used as imaging agents.

1.4.4 Delivery of small-molecule drugs as cargo

CPPs have been shown to increase the efficiency of small-molecule drugs[120, 121]. For example, to mitigate the resistance to chemotherapy, and to ensure effectiveness of anti-cancer drug treatment, a CPP-drug conjugate, with the drug cytostatic agent methotrexate (MTX) was prepared[120]. It was seen that at a concentration of 1 μM, the CPP–MTX conjugates overcame the MTX resistance and killed the cells more effectively than MTX alone[120]. In another study, polyarginine conjugates of a hydrophobic drug Paclitaxel showed improvement in water solubility and cellular uptake[121, 122]. Penetratin has delivered a photoactive drug, a pro-drug 5-aminolevulinic acid, that is changed to a photosensitizer, in the heme biosynthetic pathway[123] and this

was possible due to penetratin. These examples show that CPPs can be used to enhance properties of drugs and increase their usefulness.

The examples above outline the different applications of CPPs, but these have mostly been studied in mammalian cells, and very little information exists on translocation into other types of cells, like bacterial and fungal cells[42, 94, 124, 125]. To better understand the CPP-mediated delivery of larger biomolecular cargo and their limits in translocation, a more detailed study is required. Gong et al., recently studied the translocation mechanism of CPPs into the fungal pathogen *C. albicans.* This study gives us a better idea on designing better CPPs and ways to design the to enhance translocation[126, 127]. In the present study, we will use CPPs for delivery of proteins into the fungal pathogen, *C. albicans.*

1.5 Overview of thesis

In this dissertation, I describe my work to study CPPs and their delivery of a protein cargo into fungal cells. Current antifungal treatments can cause toxicity or the pathogens can develop resistance to the drugs and this warrants for research into newer therapeutic approaches. In this chapter, I outline characteristic features of CPPs, cell entry mechanisms of CPP-mediated cargo delivery and delivery of various types of cargo. In Chapter 2, I review protein engineering strategies and peptide properties to design efficient therapeutics. In Chapter 3, I present a study of CPPs that deliver green

fluorescent protein into *Candida albicans* cells. This chapter also talks about effect of cargo on overall secondary structure with some initial CD studies. Chapter 4 expands on the work presented in Chapter 3 by incorporating molecular dynamics simulations done by Jeffery Klauda's Lab to rationally design CPPs and test their delivery efficacy by experimental methods. In Chapter 5, I present my study on aggregation of proteins and how aggregation can affect translocation. In Chapter 6, I present some initial data on alternate methods to detect delivery of fluorescent and non-fluorescent cargo, and summarize my work and discuss future directions for research based on my studies in Chapters 3-6.

1.6 References

1. Ghannoum, M. A.; Rice, L. B., Antifungal agents: mode of action, mechanisms of resistance, and correlation of these mechanisms with bacterial resistance. *Clin Microbiol Rev* **1999,** *12* (4), 501-17.
2. Database, N. C. f. B. I. P., Amphotericin b, CID=1972. In *https://pubchem.ncbi.nlm.nih.gov/compound/Amphotericin-b (accessed on May 4, 2020)*, Pubchem: Vol. 500 x 500 pixels.
3. Database, N. C. f. B. I. P., Fluconazole, CID=3365. In *https://pubchem.ncbi.nlm.nih.gov/compound/Fluconazole (accessed on May 4, 2020)*, Pubchem.
4. Singh, T.; Murthy, A. S. N.; Yang, H. J.; Im, J., Versatility of cell-penetrating peptides for intracellular delivery of siRNA. *Drug Deliv* **2018,** *25* (1), 1996-2006.
5. Braun, K. P.; Gant, N. F.; Olson, C. M.; Parisi, V.; Forrest, K. A.; Peterson, C. M., A discriminant function for preeclampsia: case-control study of minor hemoglobins, red cell enzymes, and clinical laboratory values. *Am J Perinatol* **1997,** *14* (5), 297-302.
6. Richardson, J. P.; Moyes, D. L., Adaptive immune responses to Candida albicans infection. *Virulence* **2015,** *6* (4), 327-37.
7. Peter G. Pappas; Carol A. Kauffman; David R. Andes; Cornelius J. Clancy; Kieren A. Marr; Luis Ostrosky-Zeichner; Annette C. Reboli; Mindy G. Schuster; Jose A. Vazquez; Thomas J. Walsh; and, T. E. Z.; Sobel, J. D., Clinical Practice Guideline for the Management of Candidiasis: 2016 Update by the Infectious Diseases Society of America. *Clinical Infectious Diseases* **2016,** *62*.
8. Sánchez-Martínez, C.; Pérez-Martín, J., Dimorphism in fungal pathogens: Candida albicans and Ustilago maydis—similar inputs, different outputs. *Curr Opin Microbiol* **2001,** *4* (2), 214-221.
9. Moran, C.; Grussemeyer, C. A.; Spalding, J. R.; Benjamin, D. K., Jr.; Reed, S. D., Candida albicans and non-albicans bloodstream infections in adult and pediatric patients: comparison of mortality and costs. *Pediatr Infect Dis J* **2009,** *28* (5), 433-435.
10. Cannon, R. D.; Lamping, E.; Holmes, A. R.; Niimi, K.; Tanabe, K.; Niimi, M.; Monk, B. C., Candida albicans drug resistance another way to cope with stress. *Microbiology* **2007,** *153* (Pt 10), 3211-7.
11. White, T. C.; Marr, K. A.; Bowden, R. A., Clinical, cellular, and molecular factors that contribute to antifungal drug resistance. *Clin Microbiol Rev* **1998,** *11* (2), 382-402.

12. Pappas, P. G.; Rex, J. H.; Sobel, J. D.; Filler, S. G.; Dismukes, W. E.; Walsh, T. J.; Edwards, J. E.; Infectious Diseases Society of, A., Guidelines for treatment of candidiasis. *Clin Infect Dis* **2004,** *38* (2), 161-89.
13. Holz, R. W., The effects of the polyene antibiotics nystatin and amphotericin B on thin lipid membranes. *Ann N Y Acad Sci* **1974,** *235* (0), 469-79.
14. De Kruijff, B.; Demel, R. A., Polyene antibiotic-sterol interactions in membranes of Acholeplasma laidlawii cells and lecithin liposomes. III. Molecular structure of the polyene antibiotic-cholesterol complexes. *Biochim Biophys Acta, Biomembr* **1974,** *339* (1), 57-70.
15. D., K., The plasma membrane of C*andida albicans* and its role in the action of antifungal drugs. *The eukaryotic microbial cell* **1980**.
16. D., K., The protoplast membrane and antifungal drugs. *Fungal protoplasts: applications in biochemistry and genetics* **1985**.
17. Titsworth, E.; Grunberg, E., Chemotherapeutic activity of 5-fluorocytosine and amphotericin B against Candida albicans in mice. *Antimicrob Agents Chemother* **1973,** *4* (3), 306-8.
18. Weete, J. D.; Abril, M.; Blackwell, M., Phylogenetic distribution of fungal sterols. *PLoS One* **2010,** *5* (5), e10899.
19. Hitchcock, C. A.; Dickinson, K.; Brown, S. B.; Evans, E. G.; Adams, D. J., Interaction of azole antifungal antibiotics with cytochrome P-450-dependent 14 alpha-sterol demethylase purified from Candida albicans. *Biochem J* **1990,** *266* (2), 475-80.
20. Sanati, H.; Belanger, P.; Fratti, R.; Ghannoum, M., A new triazole, voriconazole (UK-109,496), blocks sterol biosynthesis in Candida albicans and Candida krusei. *Antimicrob Agents Chemother* **1997,** *41* (11), 2492-6.
21. Antibiotic resistance threats in the United States, 2019. **2019**.
22. Reissmann, S., Cell penetration: scope and limitations by the application of cell-penetrating peptides. *J Pept Sci* **2014,** *20* (10), 760-84.
23. Ruseska, I.; Zimmer, A., Internalization mechanisms of cell-penetrating peptides. *Beilstein J Nanotechnol* **2020,** *11*, 101-123.
24. Zhang, D.; Wang, J.; Xu, D., Cell-penetrating peptides as noninvasive transmembrane vectors for the development of novel multifunctional drug-delivery systems. *J Control Release* **2016,** *229*, 130-139.
25. Hudecz, F.; Banoczi, Z.; Csik, G., Medium-sized peptides as built in carriers for biologically active compounds. *Med Res Rev* **2005,** *25* (6), 679-736.
26. Fischer, R.; Fotin-Mleczek, M.; Hufnagel, H.; Brock, R., Break on through to the Other Side—Biophysics and Cell Biology Shed Light on Cell-Penetrating Peptides. *ChemBioChem* **2005,** *6* (12), 2126-2142.

27. Koren, E.; Torchilin, V. P., Cell-penetrating peptides:Breaking through to the other side. *Trends Mol Med* **2012,** *18* (7), 385-93.
28. Copolovici, D. M.; Langel, K.; Eriste, E.; Langel, U., Cell-penetrating peptides: design, synthesis, and applications. *ACS Nano* **2014,** *8* (3), 1972-94.
29. Mae, M.; Langel, U., Cell-penetrating peptides as vectors for peptide, protein and oligonucleotide delivery. *Curr Opin Pharmacol* **2006,** *6* (5), 509-14.
30. Madani, F.; Lindberg, S.; Langel, U.; Futaki, S.; Graslund, A., Mechanisms of cellular uptake of cell-penetrating peptides. *J Biophys* **2011,** *2011*, 414729.
31. Rousselle, C.; Clair, P.; Lefauconnier, J. M.; Kaczorek, M.; Scherrmann, J. M.; Temsamani, J., New advances in the transport of doxorubicin through the blood-brain barrier by a peptide vector-mediated strategy. *Mol Pharmacol* **2000,** *57* (4), 679-86.
32. Muratovska, A.; Eccles, M. R., Conjugate for efficient delivery of short interfering RNA (siRNA) into mammalian cells. *FEBS Lett* **2004,** *558* (1-3), 63-68.
33. Morris, M. C.; Vidal, P.; Chaloin, L.; Heitz, F.; Divita, G., A new peptide vector for efficient delivery of oligonucleotides into mammalian cells. *Nucleic Acids Res* **1997,** *25* (14), 2730-2736.
34. Morris, M. C.; Deshayes, S.; Heitz, F.; Divita, G., Cell-penetrating peptides: from molecular mechanisms to therapeutics. *Biol Cell* **2008,** *100* (4), 201-17.
35. Stetsenko, D. A.; Gait, M. J., Efficient conjugation of peptides to oligonucleotides by "native ligation". *J Org Chem* **2000,** *65* (16), 4900-8.
36. Fisher, L.; Soomets, U.; Cortes Toro, V.; Chilton, L.; Jiang, Y.; Langel, U.; Iverfeldt, K., Cellular delivery of a double-stranded oligonucleotide NFkappaB decoy by hybridization to complementary PNA linked to a cell-penetrating peptide. *Gene Ther* **2004,** *11* (16), 1264-72.
37. Shokolenko, I. N.; Alexeyev, M. F.; LeDoux, S. P.; Wilson, G. L., TAT-mediated protein transduction and targeted delivery of fusion proteins into mitochondria of breast cancer cells. *DNA Repair (Amst)* **2005,** *4* (4), 511-8.
38. Wadia, J. S.; Stan, R. V.; Dowdy, S. F., Transducible TAT-HA fusogenic peptide enhances escape of TAT-fusion proteins after lipid raft macropinocytosis. *Nat Med* **2004,** *10* (3), 310-5.
39. Olson, E. S.; Jiang, T.; Aguilera, T. A.; Nguyen, Q. T.; Ellies, L. G.; Scadeng, M.; Tsien, R. Y., Activatable cell penetrating peptides linked to nanoparticles as dual probes for in vivo fluorescence and MR imaging of proteases. *Proc Natl Acad Sci U S A* **2010,** *107* (9), 4311-6.
40. Masuda, R.; Yamamoto, K.; Koide, T., Cellular Uptake of IgG Using Collagen-Like Cell-Penetrating Peptides. *Biol Pharm Bull* **2016,** *39* (1), 130-4.

41. Lim, K. J.; Sung, B. H.; Shin, J. R.; Lee, Y. W.; Kim, D. J.; Yang, K. S.; Kim, S. C., A cancer specific cell-penetrating peptide, BR2, for the efficient delivery of an scFv into cancer cells. *PLoS One* **2013,** *8* (6), e66084.
42. Rajarao, G. K.; Nekhotiaeva, N.; Good, L., Peptide-mediated delivery of green fluorescent protein into yeasts and bacteria. *FEMS Microbiol Lett* **2002,** *215* (2), 267-72.
43. Jain, M.; Chauhan, S. C.; Singh, A. P.; Venkatraman, G.; Colcher, D.; Batra, S. K., Penetratin improves tumor retention of single-chain antibodies: a novel step toward optimization of radioimmunotherapy of solid tumors. *Cancer Res* **2005,** *65* (17), 7840-6.
44. Pooga, M.; Langel, Ü., Classes of Cell-Penetrating Peptides. In *Cell-Penetrating Peptides: Methods and Protocols*, Langel, Ü., Ed. Springer New York: New York, NY, 2015; pp 3-28.
45. Ziegler, A., Thermodynamic studies and binding mechanisms of cell-penetrating peptides with lipids and glycosaminoglycans. *Adv Drug Deliv Rev* **2008,** *60* (4-5), 580-97.
46. Mitchell, D. J.; Kim, D. T.; Steinman, L.; Fathman, C. G.; Rothbard, J. B., Polyarginine enters cells more efficiently than other polycationic homopolymers. *J Pept Res* **2000,** *56* (5), 318-25.
47. Drin, G.; Cottin, S.; Blanc, E.; Rees, A. R.; Temsamani, J., Studies on the Internalization Mechanism of Cationic Cell-penetrating Peptides. *Journal of Biological Chemistry* **2003,** *278* (33), 31192-31201.
48. Unnamalai, N.; Kang, B. G.; Lee, W. S., Cationic oligopeptide-mediated delivery of dsRNA for post-transcriptional gene silencing in plant cells. *FEBS Lett* **2004,** *566* (1-3), 307-10.
49. Gurnev, P. A.; Yang, S. T.; Melikov, K. C.; Chernomordik, L. V.; Bezrukov, S. M., Cationic cell-penetrating peptide binds to planar lipid bilayers containing negatively charged lipids but does not induce conductive pores. *Biophys J* **2013,** *104* (9), 1933-9.
50. Beloor, J.; Zeller, S.; Choi, C. S.; Lee, S. K.; Kumar, P., Cationic cell-penetrating peptides as vehicles for siRNA delivery. *Ther Deliv* **2015,** *6* (4), 491-507.
51. Kalafatovic, D.; Giralt, E., Cell-Penetrating Peptides: Design Strategies beyond Primary Structure and Amphipathicity. *Molecules* **2017,** *22* (11), 1929.
52. Derossi, D.; Joliot, A. H.; Chassaing, G.; Prochiantz, A., The 3rd helix of the antennapedia homeodomain translocates through biological-membranes. *Journal of Biological Chemistry* **1994,** *269* (14), 10444-10450.
53. Samad Mussa Farkhani, A. V., Hadi Karami, Samane Mohammadi, Nasrin Sohrabi, Fariba Badrzadeh, Cell penetrating peptides: Efficient vectors for delivery of

nanoparticles, nanocarriers, therapeutic and diagnostic molecules. *Peptides* **2014** *Volume 57* 78–94

54. Mueller, N. H.; Ammar, D. A.; Petrash, J. M., Cell penetration peptides for enhanced entry of alphaB-crystallin into lens cells. *Invest Ophthalmol Vis Sci* **2013,** *54* (1), 2-8.

55. He, H.; Ye, J.; Wang, Y.; Liu, Q.; Chung, H. S.; Kwon, Y. M.; Shin, M. C.; Lee, K.; Yang, V. C., Cell-penetrating peptides meditated encapsulation of protein therapeutics into intact red blood cells and its application. *J Control Release* **2014,** *176*, 123-132.

56. Lorents, A.; Kodavali, P. K.; Oskolkov, N.; Langel, U.; Hallbrink, M.; Pooga, M., Cell-penetrating peptides split into two groups based on modulation of intracellular calcium concentration. *J Biol Chem* **2012,** *287* (20), 16880-9.

57. Palm-Apergi, C.; Lorents, A.; Padari, K.; Pooga, M.; Hallbrink, M., The membrane repair response masks membrane disturbances caused by cell-penetrating peptide uptake. *FASEB J* **2009,** *23* (1), 214-23.

58. Vives, E.; Brodin, P.; Lebleu, B., A truncated HIV-1 Tat protein basic domain rapidly translocates through the plasma membrane and accumulates in the cell nucleus. *J Biol Chem* **1997,** *272* (25), 16010-7.

59. Futaki, S.; Suzuki, T.; Ohashi, W.; Yagami, T.; Tanaka, S.; Ueda, K.; Sugiura, Y., Arginine-rich peptides. An abundant source of membrane-permeable peptides having potential as carriers for intracellular protein delivery. *J Biol Chem* **2001,** *276* (8), 5836-40.

60. Nakase, I.; Hirose, H.; Tanaka, G.; Tadokoro, A.; Kobayashi, S.; Takeuchi, T.; Futaki, S., Cell-surface accumulation of flock house virus-derived peptide leads to efficient internalization via macropinocytosis. *Mol Ther* **2009,** *17* (11), 1868-76.

61. Elmquist, A.; Lindgren, M.; Bartfai, T.; Langel, U., VE-cadherin-derived cell-penetrating peptide, pVEC, with carrier functions. *Exp Cell Res* **2001,** *269* (2), 237-44.

62. Trehin, R.; Krauss, U.; Beck-Sickinger, A. G.; Merkle, H. P.; Nielsen, H. M., Cellular uptake but low permeation of human calcitonin-derived cell penetrating peptides and Tat(47-57) through well-differentiated epithelial models. *Pharm Res* **2004,** *21* (7), 1248-56.

63. Morris, M. C.; Depollier, J.; Mery, J.; Heitz, F.; Divita, G., A peptide carrier for the delivery of biologically active proteins into mammalian cells. *Nat Biotechnol* **2001,** *19* (12), 1173-6.

64. Pooga, M.; Hällbrink, M.; Zorko, M.; Uuml; Langel, l., Cell penetration by transportan. *The FASEB Journal* **1998,** *12* (1), 67-77.

65. Soomets, U.; Lindgren, M.; Gallet, X.; Hällbrink, M.; Elmquist, A.; Balaspiri, L.; Zorko, M.; Pooga, M.; Brasseur, R.; Langel, Ü., Deletion analogues of

transportan. *Biochimica et Biophysica Acta (BBA) - Biomembranes* **2000,** *1467* (1), 165-176.
66. Oehlke, J., A. Scheller, B. Wiesner, E. Krause, M. Beyermann, E. Klauschenz, M. Melzig, and M. Bienert, , Cellular uptake of an alpha-helical amphipathic model peptide with the potential to deliver polar compounds into the cell interior non-endocytically. *Biochimica Et Biophysica Acta-Biomembranes,* **1998,** *1414*, 127-139.
67. Scheller, A.; Oehlke, J.; Wiesner, B.; Dathe, M.; Krause, E.; Beyermann, M.; Melzig, M.; Bienert, M., Structural requirements for cellular uptake of alpha-helical amphipathic peptides. *J Pept Sci* **1999,** *5* (4), 185-94.
68. Forsman, H.; Bylund, J.; Oprea, T. I.; Karlsson, A.; Boulay, F.; Rabiet, M. J.; Dahlgren, C., The leukocyte chemotactic receptor FPR2, but not the closely related FPR1, is sensitive to cell-penetrating pepducins with amino acid sequences descending from the third intracellular receptor loop. *Biochim Biophys Acta* **2013,** *1833* (8), 1914-23.
69. Lin, Y. Z.; Yao, S. Y.; Veach, R. A.; Torgerson, T. R.; Hawiger, J., Inhibition of nuclear translocation of transcription factor NF-kappa B by a synthetic peptide containing a cell membrane-permeable motif and nuclear localization sequence. *J Biol Chem* **1995,** *270* (24), 14255-8.
70. Rhee, M.; Davis, P., Mechanism of uptake of C105Y, a novel cell-penetrating peptide. *J Biol Chem* **2006,** *281* (2), 1233-40.
71. Gao, C.; Mao, S.; Ditzel, H. J.; Farnaes, L.; Wirsching, P.; Lerner, R. A.; Janda, K. D., A cell-penetrating peptide from a novel pVII-pIX phage-displayed random peptide library. *Bioorg Med Chem* **2002,** *10* (12), 4057-65.
72. Marks, J. R.; Placone, J.; Hristova, K.; Wimley, W. C., Spontaneous membrane-translocating peptides by orthogonal high-throughput screening. *J Am Chem Soc* **2011,** *133* (23), 8995-9004.
73. Oehlke, J.; Birth, P.; Klauschenz, E.; Wiesner, B.; Beyermann, M.; Oksche, A.; Bienert, M., Cellular uptake of antisense oligonucleotides after complexing or conjugation with cell-penetrating model peptides. *Eur J Biochem* **2002,** *269* (16), 4025-32.
74. Martin, I.; Teixido, M.; Giralt, E., Design, synthesis and characterization of a new anionic cell-penetrating peptide: SAP(E). *Chembiochem* **2011,** *12* (6), 896-903.
75. Herbig, M. E.; Weller, K.; Krauss, U.; Beck-Sickinger, A. G.; Merkle, H. P.; Zerbe, O., Membrane surface-associated helices promote lipid interactions and cellular uptake of human calcitonin-derived cell penetrating peptides. *Biophys J* **2005,** *89* (6), 4056-66.
76. Conner, S. D.; Schmid, S. L., Regulated portals of entry into the cell. *Nature* **2003,** *422* (6927), 37-44.

77. Rejman, J.; Oberle, V.; Zuhorn, I. S.; Hoekstra, D., Size-dependent internalization of particles via the pathways of clathrin- and caveolae-mediated endocytosis. *Biochem J* **2004,** *377* (Pt 1), 159-69.
78. Sorkin, A.; Puthenveedu, M. A., Clathrin-Mediated Endocytosis. In *Vesicle Trafficking in Cancer*, Yarden, Y.; Tarcic, G., Eds. Springer New York: New York, NY, 2013; pp 1-31.
79. Lim, J. P.; Gleeson, P. A., Macropinocytosis: an endocytic pathway for internalising large gulps. *Immunol Cell Biol* **2011,** *89* (8), 836-43.
80. Lee, M. T.; Hung, W. C.; Chen, F. Y.; Huang, H. W., Many-body effect of antimicrobial peptides: on the correlation between lipid's spontaneous curvature and pore formation. *Biophys J* **2005,** *89* (6), 4006-16.
81. Kristensen, M.; Birch, D.; Morck Nielsen, H., Applications and challenges for use of cell-penetrating peptides as delivery vectors for peptide and protein cargos. *Int J Mol Sci* **2016,** *17* (2).
82. Bechara, C.; Sagan, S., Cell-penetrating peptides: 20 years later, where do we stand? *FEBS Lett* **2013,** *587* (12), 1693-702.
83. Derossi, D.; Calvet, S.; Trembleau, A.; Brunissen, A.; Chassaing, G.; Prochiantz, A., Cell Internalization of the Third Helix of the Antennapedia Homeodomain Is Receptor-independent. *Journal of Biological Chemistry* **1996,** *271* (30), 18188-18193.
84. Mäger, I.; Eiríksdóttir, E.; Langel, K.; El Andaloussi, S.; Langel, Ü., Assessing the uptake kinetics and internalization mechanisms of cell-penetrating peptides using a quenched fluorescence assay. *Biochimica et Biophysica Acta (BBA) - Biomembranes* **2010,** *1798* (3), 338-343.
85. Muñoz, A.; Marcos, J. F.; Read, N. D., Concentration-dependent mechanisms of cell penetration and killing by the de novo designed antifungal hexapeptide PAF26. *Molecular Microbiology* **2012,** *85* (1), 89-106.
86. López-García, B.; Pérez-Payá, E.; Marcos, J. F., Identification of novel hexapeptides bioactive against phytopathogenic fungi through screening of a synthetic peptide combinatorial library. *Applied and environmental microbiology* **2002,** *68* (5), 2453-2460.
87. Elmquist, A.; Hansen, M.; Langel, U., Structure-activity relationship study of the cell-penetrating peptide pVEC. *Biochim Biophys Acta* **2006,** *1758* (6), 721-9.
88. Green, M.; Loewenstein, P. M., Autonomous functional domains of chemically synthesized human immunodeficiency virus TAT trans-activator protein. *Cell* **1988,** *55* (6), 1179-88.
89. Stewart, K. M.; Horton, K. L.; Kelley, S. O., Cell-penetrating peptides as delivery vehicles for biology and medicine. *Org Biomol Chem* **2008,** *6* (13), 2242-55.

90. Cosgrave, L.; Devocelle, M.; Forster, R. J.; Keyes, T. E., Multimodal cell imaging by ruthenium polypyridyl labelled cell penetrating peptides. *Chem Commun (Camb)* **2010,** *46* (1), 103-5.
91. Derivery, E.; Bartolami, E.; Matile, S.; Gonzalez-Gaitan, M., Efficient delivery of quantum dots into the cytosol of cells using cell-penetrating poly(disulfide)s. *J Am Chem Soc* **2017,** *139* (30), 10172-10175.
92. Kameyama, S.; Horie, M.; Kikuchi, T.; Omura, T.; Takeuchi, T.; Nakase, I.; Sugiura, Y.; Futaki, S., Effects of cell-permeating peptide binding on the distribution of 125I-labeled Fab fragment in rats. *Bioconjug Chem* **2006,** *17* (3), 597-602.
93. Massodi, I.; Bidwell, G. L., 3rd; Raucher, D., Evaluation of cell penetrating peptides fused to elastin-like polypeptide for drug delivery. *J Control Release* **2005,** *108* (2-3), 396-408.
94. Parenteau, J.; Klinck, R.; Good, L.; Langel, U.; Wellinger, R. J.; Elela, S. A., Free uptake of cell-penetrating peptides by fission yeast. *FEBS Lett* **2005,** *579* (21), 4873-8.
95. Gong, Z.; Walls, M. T.; Karley, A. N.; Karlsson, A. J., Effect of a flexible linker on recombinant expression of cell-penetrating peptide fusion proteins and their translocation into fungal cells. *Mol Biotechnol* **2016,** *58* (12), 838-849.
96. Khafagy, E. S.; Morishita, M.; Kamei, N.; Eda, Y.; Ikeno, Y.; Takayama, K., Efficiency of cell-penetrating peptides on the nasal and intestinal absorption of therapeutic peptides and proteins. *Int. J. Pharm.* **2009,** *381* 49–55
97. Dinca, A.; Chien, W. M.; Chin, M. T., Intracellular delivery of proteins with cell-penetrating peptides for therapeutic uses in human disease. *Int J Mol Sci* **2016,** *17* (2), 263.
98. Habault, J.; Poyet, J. L., Recent advances in cell penetrating peptide-based anticancer therapies. *Molecules* **2019,** *24* (5), 927.
99. Chinak, O.; Golubitskaya, E.; Pyshnaya, I.; Stepanov, G.; Zhuravlev, E.; Richter, V.; Koval, O., Nucleic acids delivery into the cells using pro-apoptotic protein lactaptin. *Front Pharmacol* **2019,** *10* (1043), 1043.
100. Yue-Wern Huang ; Han-Jung Lee; Larry M. Tolliver; Aronstam, R. S., Delivery of Nucleic Acids and Nanomaterials by Cell-Penetrating Peptides: Opportunities and Challenges. *BioMed Research International* **2015**.
101. Eguchi, A.; Dowdy, S. F., siRNA delivery using peptide transduction domains. *Trends Pharmacol Sci* **2009,** *30* (7), 341-5.
102. Chiu, Y. L.; Ali, A.; Chu, C. Y.; Cao, H.; Rana, T. M., Visualizing a correlation between siRNA localization, cellular uptake, and RNAi in living cells. *Chem Biol* **2004,** *11* (8), 1165-75.

103. Wang, Y. H.; Hou, Y. W.; Lee, H. J., An intracellular delivery method for siRNA by an arginine-rich peptide. *J Biochem Biophys Methods* **2007,** *70* (4), 579-86.
104. Turner, J. J.; Jones, S.; Fabani, M. M.; Ivanova, G.; Arzumanov, A. A.; Gait, M. J., RNA targeting with peptide conjugates of oligonucleotides, siRNA and PNA. *Blood Cells Mol Dis* **2007,** *38* (1), 1-7.
105. Simeoni, F., Insight into the mechanism of the peptide-based gene delivery system MPG: implications for delivery of siRNA into mammalian cells. *Nucleic Acids Res* **2003,** *31* (11), 2717-2724.
106. Lundberg, P.; El-Andaloussi, S.; Sutlu, T.; Johansson, H.; Langel, U., Delivery of short interfering RNA using endosomolytic cell-penetrating peptides. *FASEB J* **2007,** *21* (11), 2664-71.
107. Meng, S.; Wei, B.; Xu, R.; Zhang, K.; Wang, L.; Zhang, R.; Li, J., TAT peptides mediated small interfering RNA delivery to Huh-7 cells and efficiently inhibited hepatitis C virus RNA replication. *Intervirology* **2009,** *52* (3), 135-40.
108. Lakshmanan, M.; Yoshizumi, T.; Sudesh, K.; Kodama, Y.; Numata, K., Double-stranded DNA introduction into intact plants using peptide–DNA complexes. *Plant Biotechnol* **2015,** *32* (1), 39-45.
109. Veldhoen, S.; Laufer, S. D.; Trampe, A.; Restle, T., Cellular delivery of small interfering RNA by a non-covalently attached cell-penetrating peptide: quantitative analysis of uptake and biological effect. *Nucleic Acids Res* **2006,** *34* (22), 6561-73.
110. Wadia, J. S.; Dowdy, S. F., Protein transduction technology. *Curr Opin Biotechnol* **2002,** *13* (1), 52-6.
111. Gump, J. M.; Dowdy, S. F., TAT transduction: the molecular mechanism and therapeutic prospects. *Trends Mol Med* **2007,** *13* (10), 443-8.
112. Futaki, S.; Ohashi, W.; Suzuki, T.; Niwa, M.; Tanaka, S.; Ueda, K.; Harashima, H.; Sugiura, Y., Stearylated arginine-rich peptides: a new class of transfection systems. *Bioconjug Chem* **2001,** *12* (6), 1005-11.
113. Wang, H. Y.; Chen, J. X.; Sun, Y. X.; Deng, J. Z.; Li, C.; Zhang, X. Z.; Zhuo, R. X., Construction of cell penetrating peptide vectors with N-terminal stearylated nuclear localization signal for targeted delivery of DNA into the cell nuclei. *J Control Release* **2011,** *155* (1), 26-33.
114. Jeong, C.; Yoo, J.; Lee, D.; Kim, Y. C., A branched TAT cell-penetrating peptide as a novel delivery carrier for the efficient gene transfection. *Biomater Res* **2016,** *20* (1), 28.
115. Li, J.; Feng, L.; Fan, L.; Zha, Y.; Guo, L.; Zhang, Q.; Chen, J.; Pang, Z.; Wang, Y.; Jiang, X.; Yang, V. C.; Wen, L., Targeting the brain with PEG-PLGA nanoparticles modified with phage-displayed peptides. *Biomaterials* **2011,** *32* (21), 4943-50.

116. Zhu, L.; Wang, T.; Perche, F.; Taigind, A.; Torchilin, V. P., Enhanced anticancer activity of nanopreparation containing an MMP2-sensitive PEG-drug conjugate and cell-penetrating moiety. *Proc Natl Acad Sci U S A* **2013,** *110* (42), 17047-52.
117. Silva, S.; Almeida, A. J.; Vale, N., Combination of cell-penetrating peptides with nanoparticles for therapeutic application: A review. *Biomolecules* **2019,** *9* (1), 22.
118. Wang, H.; Xu, K.; Liu, L.; Tan, J. P.; Chen, Y.; Li, Y.; Fan, W.; Wei, Z.; Sheng, J.; Yang, Y. Y.; Li, L., The efficacy of self-assembled cationic antimicrobial peptide nanoparticles against Cryptococcus neoformans for the treatment of meningitis. *Biomaterials* **2010,** *31* (10), 2874-81.
119. Liu, B. R.; Li, J. F.; Lu, S. W.; Leel, H. J.; Huang, Y. W.; Shannon, K. B.; Aronstam, R. S., Cellular internalization of quantum dots noncovalently conjugated with arginine-rich cell-penetrating peptides. *J Nanosci Nanotechnol* **2010,** *10* (10), 6534-43.
120. Lindgren, M.; Rosenthal-Aizman, K.; Saar, K.; Eiriksdottir, E.; Jiang, Y.; Sassian, M.; Ostlund, P.; Hallbrink, M.; Langel, U., Overcoming methotrexate resistance in breast cancer tumour cells by the use of a new cell-penetrating peptide. *Biochem Pharmacol* **2006,** *71* (4), 416-25.
121. Goun, E. A.; Pillow, T. H.; Jones, L. R.; Rothbard, J. B.; Wender, P. A., Molecular transporters: synthesis of oligoguanidinium transporters and their application to drug delivery and real-time imaging. *Chembiochem* **2006,** *7* (10), 1497-515.
122. Kirschberg, T. A.; VanDeusen, C. L.; Rothbard, J. B.; Yang, M.; Wender, P. A., Arginine-based molecular transporters: the synthesis and chemical evaluation of releasable taxol-transporter conjugates. *Org Lett* **2003,** *5* (19), 3459-62.
123. Dixon, M. J.; Bourre, L.; MacRobert, A. J.; Eggleston, I. M., Novel prodrug approach to photodynamic therapy: Fmoc solid-phase synthesis of a cell permeable peptide incorporating 5-aminolaevulinic acid. *Bioorg Med Chem Lett* **2007,** *17* (16), 4518-22.
124. Rajarao G. K.; and, N. N.; Good, L., The signal peptide NPFSD fused to ricin A chain enhances cell uptake and cytotoxicity in Candida albicans. *Biochemical and Biophysical Research Communications* **2003,** *301*, 529–534.
125. Palm, C.; Netzereab, S.; Hallbrink, M., Quantitatively determined uptake of cell-penetrating peptides in non-mammalian cells with an evaluation of degradation and antimicrobial effects. *Peptides* **2006,** *27* (7), 1710-6.
126. Gong, Z.; Ikonomova, S. P.; Karlsson, A. J., Secondary structure of cell-penetrating peptides during interaction with fungal cells. *Protein Sci* **2018,** *27* (3), 702-713.

127. Gong, Z.; Doolin, M. T.; Adhikari, S.; Stroka, K. M.; Karlsson, A. J., Role of charge and hydrophobicity in translocation of cell-penetrating peptides into Candida albicans cells. *AIChE Journal* **2019,** *65* (12).

Chapter 2: Methods to engineer peptides[1]

Peptides are a promising source of new therapeutics, but the biophysical characteristics of natural peptides, including their stability and propensity to aggregate, can limit their success. Protein engineering offers powerful tools to improve the properties of peptides for biological applications. In this chapter, we discuss rational design, directed evolution, and computational methods and how these methods can be applied to improving the characteristics of peptides. We provide a discussion of engineering the thermodynamic stability, self-assembly, reduced aggregation, proteolytic stability, and binding affinity and specificity of peptides and provide a perspective on future directions in engineering therapeutic peptides.

2.1 Introduction

Naturally-occurring peptides serve important roles in human physiology, including functioning as hormones, neurotransmitters, growth factors, and anti-infectives[2]. In these roles, peptides exhibit powerful biological activity and specificity, making them appealing for the development of potential therapeutics[2, 3]. In fact, the use and

[1] ***The various subsections (2.1, 2.2, 2.3, 2.4) of this chapter have been adapted from the AICHE special edition review 1. Adhikari, S.; Leissa, J. A.; Karlsson, A. J., Beyond function: Engineering improved peptides for therapeutic applications. AIChE Journal 2019, 66 (3), e16776. (Reproduced with permission, © 2019 American Institute of Chemical Engineers).***

development of peptide therapeutics continues to grow, with more than 60 approved in the United States and 260 peptides in active, human clinical trial development as of 2017[4]. Peptides have consistently demonstrated high levels of intrinsic safety, tolerance, and efficacy, which can lead to improved performance over small molecules in clinical trials [2, 4, 5]. Important approved peptide therapeutics include leuprolide, a gonadotropin-releasing hormone analog approved for treating advanced prostate cancer, and insulin glargine, a long-acting analog of insulin approved for treating type I and II diabetes. These peptides represent two of the most successful examples of peptide therapeutics, with the leuprolide drug Lupron® achieving US$892 million in worldwide net sales in 2018[6] and the insulin glargine drug Lantus® achieving €3.57 billion (~US$4.0 billion) in the same year [7].

Although peptides have many appealing characteristics, challenges associated with their physiochemical properties can present barriers for their use in medicine[8]. For example, peptides can be degraded *in vivo* through a multitude of endogenous proteases[3], making it difficult for the successful delivery of intact peptide to the desired site[8]. This is especially of concern for orally administered therapeutics because of the combined high proteolytic activity and low pH in the gastrointestinal tract, which intensify degradation[8]. Additionally, some natural peptides have a propensity to aggregate and are poorly soluble in water, limiting their bioavailability[2]. Because of these limitations, applying engineering approaches to explicitly address biophysical concerns such as these can help improve the therapeutic potential of peptides.

By considering these fundamental properties, novel peptides can be designed with fitness properties improved compared to natural peptides[3]. Although the peptide sequence space is limited compared to proteins, ample mutational diversity to develop improved or new peptide-based therapeutics is available through canonical amino acids, post-translational modifications, and secondary structure geometries[3]. In this chapter, we provide an overview of methods used to engineer biophysical characteristics of peptides. We focus on engineering peptides by introducing amino acid changes into the primary sequence of peptides using canonical amino acids and screening for improvements to a desired characteristic. (Recent reviews explore non-natural amino acids in peptide therapeutics and in protein engineering[9, 10].) We then discuss how these methods have been used to improve biophysical characteristics and, thus, therapeutic potential of biologically active peptides. Finally, we discuss opportunities for improving our ability to engineer peptides that have the necessary properties for therapeutic applications.

2.2 Approaches for introducing and screening diversity

A typical approach to designing therapeutic peptides involves starting with a peptide sequence with a desired biological function. Based on what is known about the structure and function of the peptide, one or more characteristics of the peptide to be improved are identified, which may include functional characteristics or characteristics

that improve the fitness and therapeutic potential of the peptide. Changes to the amino acid sequence are introduced in a specific or random manner, and these changes are evaluated to screen for modifications that lead to the desired improvement in the characteristic(s) being engineered. Experimental approaches used to introduce changes to the amino acid sequences and screen their effect on the properties of interest can be categorized as rational design or directed evolution, and these approaches can also be applied through or assisted by computational methods (Figure 2.1). When undertaking a peptide design project, considering the advantages and disadvantages of each strategy is important in selecting the route that will be used to engineer the peptide.

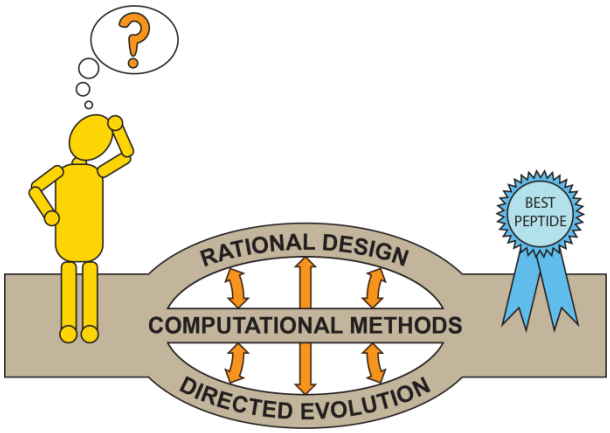

Figure 2.1. Selection of the approach to use to engineer a peptide to meet specific design criteria requires understanding the available approaches and determining which technique(s) best suit the available knowledge. Often, an engineering strategy will incorporate elements of multiple approaches (Reproduced with permission, © 2019 American Institute of Chemical Engineers).

2.2.1 Rational design

Rational design is commonly selected to engineer peptides when prior knowledge regarding structure-function relationships exists. With this knowledge, rational choices are made regarding which residues to change and to which amino acids they should be changed[3]. Rational design is typically performed with discrete mutations, generating a small library of variants. Because of the small library size, the variants often can be individually evaluated for the effect of the amino acid changes on the desired characteristic with standard, relatively low-throughput assays for the characteristic of interest. Rational design allows a deeper understanding of the importance of physiochemical interactions at a given position, as mutations that both improve and reduce fitness can be assessed because of the small library size. Additionally, information regarding structure-function trends in similar peptides or proteins can be applied through rational design to improve a peptide of interest. For example, Joshi et al. rationally designed mutations in a synthetic peptide based on current small molecule inhibitor therapeutics to map the substrate selectivity of aminopeptidase N (APN), an extracellular membrane-anchored enzyme overexpressed in cancerous cells[11]. Using a combination of crystallography and mass spectrometry, the authors analyzed variants of a substrate peptide that incorporated substitutions around the enzyme cleavage site and developed an understanding of the interactions required for substrate recognition by the enzyme. The process also identified a peptide inhibitor that is effective at inhibiting the degradation of a known APN substrate both *in vitro* and *in vivo* in prostate cancer models. This example highlights how rational design can be used to both gain

structure-function data and to use that data to design peptides for therapeutic applications.

2.2.2 Directed evolution

Directed evolution, which mimics the process of natural selection, is another important approach used to improve the properties of peptides for therapeutic applications. In directed evolution, a large library of peptide variants, which can be on the order of 10^{10}-10^{14} variants[12], is generated by introducing random or targeted variation into the gene for the peptide of interest. The library is subjected to successive rounds of screening and mutagenesis, where a promising mutant or mutants isolated from a given round are used as the foundation for mutagenesis in the next round[13]. Iterations continue until one or more mutants have the desired fitness with respect to a given property[14, 15]. Unlike rational design, where all variants are normally assessed, the focus in directed evolution is typically on those variants that show improvement in the characteristic being engineered.

In a directed evolution strategy, one of the main challenges is designing a screen for the property or properties being engineered that allows interrogation of the large number of library members required to find desired variants. The time to assay individual library members in complicated assays is typically prohibitive for the library sizes used in directed evolution. Because of this, one of the key aspects that must be

addressed in directed evolution is a screen suitable for assaying a large peptide library within a reasonable time. The screen must address two challenges: (1) it must be properly designed to effectively screen for the desired characteristic[16] and (2) it must incorporate a method to link the gene sequence of the peptide (genotype) to the quality of the characteristic being engineered (phenotype). Sometimes, a screen can simply take the form of a 96-well plate assay, where cells producing a single peptide variant are placed in each well, and the characteristic being engineered is assayed in the well. Since only a single variant is in each well, the linkage of the genotype to the phenotype is maintained through the assay. This type of screen has the advantage of being able to use any type of assay that can be performed in a 96-well plate, but, even with the use of automation, screening a sufficient number of variants in large libraries is still prohibitive. To overcome this limitation, a powerful tool called surface display can be used for screening libraries in directed evolution.

In surface display, library members are physically anchored to the surface of a cell or biological molecule, where they can be interrogated for properties of interest, including biophysical properties. The physical linkage conserves the genotype-to-phenotype linkage, allowing the properties of a selected variant to be directly traced back to the sequence that generated it to identify the amino acid changes responsible for changes in the peptide's behavior. Additionally, these systems are attractive because they are easy to use in conjunction with soluble ligands that can be used as reporters for activity or fitness, making them suitable for quantitative analysis with high-throughput techniques such as flow cytometry[17], fluorescent-associated cell sorting

(FACS),[18] and biopanning[19]. Two types of surface display technologies exist: cell-surface display and *in vitro* display. In cell-surface display, a variant is expressed by a cell and anchored to the surface of the cell through a membrane or cell-wall protein, establishing the genotype-to-phenotype linkage. Expressing the variants in a library on the surface of individual cells allows the library to be easily interrogated for desired characteristics, and the DNA encoding for a desired variant can be recovered after growing the cell or performing PCR. Several different cell-surface display systems have been used for directed evolution of peptides, including systems involving display on phage[20-22], yeast[23-25], and bacteria[26-29]. One of the main limitations of cell-surface display systems is that the library size is limited by the transformation efficiency of the cells involved in the display. Still, given the sequence space for peptides is smaller than for larger proteins, they remain very useful methods in engineering peptides[30-32].

Common *in vitro* alternatives to cell-surface display include ribosome display and mRNA display. In ribosome display, ribosome stalling is used to conserve the mRNA-ribosome-peptide complex after translation[33]. RNA display utilizes a puromycin linkage in place of the ribosome to covalently bind the mRNA and resulting translated peptide. Both methods lead to covalent linkage of peptide variants to the nucleic acids encoding their sequence, so the sequence for library variants that have desired characteristics is easily recovered. While *in vitro* systems are more expensive than cell-surface display systems, *in vitro* display can investigate a larger library size since the transformation limitation is removed[34].

Cell-surface display and *in* vitro display bring an ability to screen large numbers of variants to directed evolution, but another tactic often incorporated in directed evolution is to reduce the library size to reduce the resources needed to screen the library. Structure and function data are used to identify specific regions, residues, or residue types of interest to limit the number of residues that are varied. Saturation mutagenesis and patterned libraries are two examples of strategies that take advantage of this combination of rational design and directed evolution. In site-saturation mutagenesis, all 20 canonical amino acids are sampled at the residue(s) of importance and the resulting peptides are screened for desirable fitness. Reetz et al.'s method of iterative saturation mutagenesis (ISM) expands on this idea[35-37]. After identifying important sites containing 1-3 amino acids, the amino acid(s) in each site are subjected to site-saturation mutagenesis and the resulting libraries are each screened to identify the best mutant in each library. The best mutants from the first round are then subjected to site-saturation at each of the other sites to generate multiple new libraries based on each of the best mutants. The screening and mutagenesis continue until mutants with the desired properties are identified. While the applications of ISM have so far focused on evolving proteins, this technique also has promise for engineering peptides. Patterned libraries take advantage of the known interactions between polar and non-polar residues to limit library size while maintaining or introducing desired secondary structure of the resulting peptide library. Because the periodicity of α-helices and β-sheets is known, the location of polar and non-polar residues can be fixed, while allowing the identity of the residues to be varied[38-41]. Wilson et al. used this method to

design a peptide library containing peptides with different combinations of short α-helical and β-sheet segments and then screened for binding affinity to streptavidin with mRNA display to isolate peptides with binding affinities as low as 5 nmol/L[42]. As these library design methods illustrate, rational design and directed evolution principles often combine to yield effective experimental methods to improve peptide functions.

2.2.3 Computational methods

Rational design and directed evolution are powerful experimental approaches for peptide engineering, and improvements in structure-function knowledge and improvements in computational tools have allowed the principles of these approaches to be employed through computational design[43, 44]. Computational methods simulate experimental conditions, offer guidance for designing libraries, and help explain the influence of mutations on the characteristics of peptides. Due to these benefits, the use of computational methods continues to increase in peptide engineering and in protein engineering more generally.

Molecular dynamics (MD) simulations study physical movements of interacting atoms and molecules over time, making them valuable tools for understanding and improving properties of peptides. Atom-specific information is generated at each time-point, allowing identification of residues or domains important in a given peptide. However, these simulations are often limited in their time-scale

(typically μs)[45, 46], which is not always sufficient to observe desired biological phenomena[47, 48]. Coarse-grained simulations can be used to resolve this time-scale limitation through lower resolution and reduced atomic details, though results need to be confirmed with more sophisticated simulations to ensure predictive adequacy[49]. Course-grained and all-atom methods can also be combined to allow larger system sizes and longer time-scales compared to purely atomistic models. For example, Shelley et al. studied the aggregation of the antimicrobial peptide melittin in aqueous solution using an all-atom representation for melittin and a course-grained representation for water molecules and ions[50]. By using a course-grained representation of the solvent, the authors reduced the computational time for the simulations compared to a fully atomistic simulation, while still obtaining aggregation and structural data that aligns well with experimental observations.

Machine learning can also be used to design for improved characteristics of peptides relevant for therapeutic applications. With this method, a database of peptides with known sequences and performance with respect to the desired characteristic of interest is required. The database is used to train the model by identifying patterns in the provided peptides. After training the model, the algorithm can generate a list of promising new peptides that meet the desired criteria. In this way, machine learning mimics directed evolution by selecting peptide sequences most likely to have desirable fitness[51-54]. Fjell et al.'s work screening for potent antibiotic peptides illustrates how machine learning can be applied to peptide design[51]. The authors first evaluated the antibacterial activity of about 1400 peptides and calculated quantitative values for

descriptors of structural properties (e.g., charge, hydrophobicity) for each peptide. Using this database of peptides, the machine-learning model was then trained to determine whether a peptide has antibacterial activity by using the quantitative descriptors and the experimentally determined activity levels. After training, the model screened a virtual library of nearly 100,000 peptides based on their descriptors and successfully identified peptides with strong antibacterial activity, highlighting the power and potential of machine learning in designing peptide therapeutics.

Another method commonly used to engineer peptides is computer-aided protein directed evolution (CAPDE). In this method, computational simulation tools are utilized to assist in directed evolution. CAPDE has been used to characterize libraries that are generated by mutagenesis, to design libraries based on evolutionary and structural information of target proteins/peptides, and to predict the effect of mutations on the structure and function of the protein[55]. CAPDE and other computational methods are helpful in narrowing the set of sequences to be analyzed experimentally, which can reduce experimental time and resources and reduce or eliminate the need for high-throughput experimental methods.

2.3 Protein engineering to design peptide characteristics

When identifying or designing peptides as potential therapeutics, the biological function of the peptide is typically the first aspect considered. However, this biological

function is linked to characteristics of the peptide that govern its interactions with itself, its interactions with other molecules, and its stability (Figure 2.2). Purposefully designing peptides to address these biophysical characteristics can improve the therapeutic potential of peptides, and rational design, directed evolution, and computational tools are well suited for this design. Here, we describe how protein engineering can be used to design peptides with improved characteristics, in terms of thermodynamic stability, self-assembly, reduced aggregation, proteolytic stability, and binding affinity and specificity.

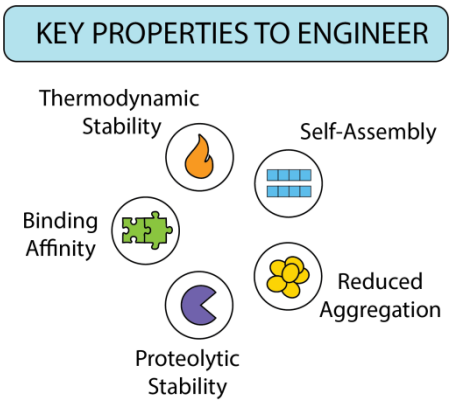

Figure 2.2. Designing peptides for therapeutic applications requires consideration and engineering biophysical characteristics, in addition to the biological function (Reproduced with permission, © 2019 American Institute of Chemical Engineers).

2.3.1 Thermodynamic stability

Thermodynamic stability is important for *in vivo* applications of peptides, as a peptide's ability to retain its structure can influence its efficacy. For example, the antimicrobial

activity and immunogenicity of peptides can rely on their ability to form and retain their secondary structures[56, 57], so engineering higher thermodynamic stability can be crucial for their *in vivo* efficacy. When engineering a peptide for thermodynamic stability, a key consideration is whether the peptide contains α-helical[58-60] or β-sheet[61-63] secondary structure, as knowledge of the intramolecular interactions in these structures assists in designing or improving peptides.

Forming an α-helical structure can stabilize a peptide[60, 64], and rational design can be used to improve the propensity to form α-helices and the stability of the helices. Using rational design, α-helicity can be engineered via intramolecular salt bridges using Glu, Asp, Arg, or Lys salt bridges to increase helicity[58, 59]. To better understand how salt-bridges affect stability, Wolny et al. designed *de novo*, single α-helix peptides with the motif AEEEXXX (X = K or R)[60]. Experimentally, they showed the sequence AEEEKRK is more helical and thermostable than AEEEKKK, suggesting that Arg increases stability compared to Lys. Molecular dynamics simulations of the peptides indicated that the improved helicity and stability of the peptide with Arg is likely due to salt bridges being formed more readily and frequently between Glu and Arg than between Glu and Lys, because Arg has a larger range of rotamer conformations and the guanidium group on the Arg side chain leads to increased interactions with Glu. This effect is not limited to small peptides. Substitution of Lys with Arg in the single α-helix of the naturally occurring protein myosin-6 increased its stability, whereas the substitution of Arg with Lys decreased stability[60], indicating the results for the single-

helix peptides can also be observed in the context of more complicated proteins or peptides.

The β-sheet structure of a peptide can also be stabilized through salt bridges and other interactions. For example, Bureau et al. compared the energetics between two small stable β-hairpin peptides, trpzip1 and chignolin using MD simulations[62]. The peptides have comparable secondary structures and hydrogen bonding profiles, but their stabilities and melting temperatures are dissimilar. Forced unfolding energetics of trpzip1 revealed the peptide is more stable than chignolin, meaning more work is required to stretch the peptide from a primarily folded state to an unfolded state. This was attributed to the presence of the E5-K8 salt bridge located near the β-hairpin turn point in trpzip1, since it was the most energetically favorable side chain interaction in the peptide and helped initiate and maintain the hairpin structure[62]. π-π stacking can also be important in stabilizing peptides by segregating the hydrophobic core from the surrounding aqueous environment. In a synthetic antimicrobial peptide utilizing repeats of the motif (WRXXRW), where XX represents the turn sequence, the Trp residues in the motif further stabilize the β-hairpin structure of the peptide through π-π stacking[61]. Stabilizing the secondary structure resulted in a higher bacterial selectivity, less salt sensitivity, and stronger activity, all of which improved with additional repeats of the motif[61]. Additionally, Capelli et al. observed that this interaction was crucial for the β-hairpin structure of the immunoglobulin-binding domain peptide GB1, as Ala screening demonstrated that the removal of Phe, Trp, and Tyr participating in π-π stacking significantly destabilized the hairpin[63].

To this point, designing peptides for thermodynamic stability has mainly used rational design, sometimes with the assistance of computational methods that apply knowledge of intramolecular interactions. Directed evolution has not played a significant role in the design of peptides for thermodynamic stability, though it is widely used for larger proteins[65-68]. The two main techniques used to improve the thermodynamic stability of proteins involve exposing a protein library to heat prior to evaluating function and screening for solubility or expression as surrogate for stability[65-68]. Bond et al. and Julian et al. employed another successful strategy, which involved using a ligand (Protein A) that binds only to library members (single-domain antibodies) when the library members are well folded[69, 70]. The methods used for larger proteins should have utility for peptides as well, and combining these techniques with assays for biological function will allow simultaneous screening for function and thermodynamic stability.

2.3.2 Self-assembly

Self-assembly produces highly ordered structures with assembly of nanoscale building blocks of all length scales. Nearly all self-assembled structures, including peptides, are thermodynamically stable compared to single unassembled structures[71], and assembly of peptides can also improve other important characteristics, including responsiveness to environmental conditions, selectivity, proteolytic resistance, and sustained activity[72,

[73]. Self-assembly of peptides into ordered nanostructures is important in various therapeutic applications, including antimicrobial activity[72], tissue grafting[74], drug delivery[75, 76], and vaccine design [74, 76-80]. In addition to modulating assembly conditions to control self-assembly[75, 76, 78], the design of the peptide sequence can also be used to tune the assembly of peptide monomers into nanoscale structures.

Molecular interactions play an important role in forming stable, self-assembled structures, so selection of the residues and sequence of a peptide affect the structures that are formed through assembly. To understand how molecular interactions lead to the self-assembly of twisted, helical, and flat nanostructures, Zhou and Deng et al. compared the self-assembly process for three different rationally designed peptides with the same amino acid composition but different sequences[81]. KE-F8 (NH_2-KEFFFFKE-$CONH_2$) and EK-F8 (NH_2-KEFFFFEK-$CONH_2$) differ only by the two C-terminal, charged residues, whereas KFE-8 (NH_2-KFEFKFEF-$CONH_2$) has the hydrophobic and charged residues uniformly distributed throughout the sequence. The sequence of each peptide was designed to elicit a specific molecular packing due to the interactions within and between β-sheets. Using transmission electron microscopy (TEM) and atomic force microscopy (AFM), the authors showed that KE-F8 form twisted ribbons, EK-F8 forms helical ribbons or tubes, and KFE-8 forms flat ribbons. MD simulations demonstrated that the variations in packing for the peptides result from differences between electrostatic and hydrophobic interactions, while variations in twisting result from differences between intra- and inter-β-sheet interactions. In another example, Zhou and Cao et al. rationally designed two self-assembling, anticancer

peptides by adding a pair of Glu and Asn residues to either the N-terminus or C-terminus of a helical, lytic peptide to generate the peptides EN (ENFLGALFKALSKLL) and NE (FLGALFKALSKLLNE)[75]. The addition of the residues changed the distribution of polar and non-polar residues of the peptide, without disrupting the helical secondary structure. TEM and AFM showed EN assembled into long, twisting nanofibrils, whereas NE formed nanomicelles[75]. The different nanostructures led to differences in biological activity; EN had the desired higher level of cytotoxicity compared to NE, though NE exhibited high stability in serum. As these examples illustrate, controlling the interactions of residues and molecular packing controls the self-assembly of the nanostructures derived from the peptides. By designing for self-assembly into specific nanostructures, the bioactivity and stability can be modulated, making self-assembly a powerful characteristic for designing improved peptides.

2.3.3 Reduced aggregation

Aggregation represents a significant limitation to the overall promise of peptide therapeutics as the formation of aggregates can limit their potency and lead to immunogenicity[82, 83]. Aggregates can be disordered globules or they can be highly ordered structures[84]. Although highly ordered aggregates may also be considered self-

assembled structures, we distinguish aggregation processes as those being undesired for the peptide of interest.

In most cases, a combination of driving forces is responsible for a given peptide's propensity to aggregate, making the task of addressing aggregation difficult. As a result, the influence of a given driving force and the key residues promoting aggregation in a given peptide should be identified to enable engineering to reduce aggregation. One way of accomplishing this is through single-mutation screening, which involves rationally designing mutations and calculating the influence of a given mutation on a peptide's propensity to aggregate through a weighted sum of the mutation's contribution to the peptide's hydrophobicity, net charge, and tendency of the peptide to form either α-helical or β-sheet structures[82, 85]. Select mutants are then validated experimentally, and the process is repeated. To address aggregation, protein engineering approaches can then be used to mitigate well-known aggregation driving forces, namely nonspecific interactions between hydrophobic regions, complementary charged regions, or aromatic π-π stacking.

Hydrophobicity is a critical property to consider when designing for reduced aggregation of peptides. Chiti et al. applied single-mutation screening to a series of medically relevant peptides, including amylin, α-synuclein, β(Aβ), tau, a human prion peptide, and leucine-rich peptides, all of which were observed to form amyloid aggregates[85]. From these experiments, it was concluded that structured, amyloid fibrillization could be best avoided with an A76E modification for α-synuclein and an I26A modification for amylin, which disrupted hydrophobic regions and attenuated the

β-sheet character that promoted nonspecific association[85]. Conversely, aggregation could be encouraged by increasing the hydrophobicity and β-sheet character, as was observed for both H111A and A117V modifications for human prion peptide[85]. Fowler et al. used a similar model to analyze hCT (residues 10-21), a polypeptide hormone involved in calcium regulation and bone dynamics that also forms amyloid fibrils in solution[82]. Based on information from the model, I27T and V29S mutations were incorporated into hCT to disrupt hydrophobic regions, and these modifications contributed to a significant reduction in aggregation[82].

In addition to the hydrophobic effect, intermolecular salt bridges formed between exposed, complementary charged regions represent another significant driving force for the aggregation of therapeutic peptides. Chiti et al. showed that salt bridges also contribute to the aggregation of leucine-rich peptides and tau and mitigated the aggregation using a D24Q mutation in leucine-rich peptides and an R5L mutation in tau to eliminate undesirable intermolecular salt bridges[85]. Similarly, this was demonstrated in a *de novo* α-helical peptide composed of $(AEEEXXX)_n$ repeats (X = K or R)[60]. The peptide was designed for improved thermostability by careful pairing of either Lys or Arg with Glu to stabilize the helix; however, the increased prevalence of Arg residues produced undesirable salt bridges that instead promoted aggregation[60], likely into amorphous aggregates. The aggregation was attributed to the respectively short salt-bridge lifetime of the Glu-Arg pairing and the presence of the additional terminal guanidinium group in Arg that encourages salt-bridge formation, but not necessarily the desired intramolecular salt-bridges that stabilize the helix[60],

highlighting the importance of considering the overall context of residues in peptide design.

A third contributing factor that may be related to aggregation is nonspecific π-π interactions, which rely on the spatial overlay of aromatic side chains commonly observed with Phe, Tyr, and Trp residues. The effect was observed by Federix et al. both through an MD simulation of all 8,000 possible natural tri-peptides with aromatic side chains and experimental comparison of the peptides with the highest propensity to aggregate in water[77]. The tri-peptide VFF exhibited the highest propensity to aggregate over other hydrophobic combinations[77]. Although not focused specifically on peptides, a computational study by Hou et al. supports these observations[86]. The study performed analysis of solubility and structures of *E. coli* proteins to identify the role of molecular interactions in solubility and identified π-π and other π-interactions as interactions that promote aggregation. The biophysical explanation for the aggregation is not clear, and, while a number of studies have shown that substitution of aromatic residues, especially Phe, reduces aggregation (for example, see references[87-90]), other work suggests that the aggregation affects presumed to be due to π-π interactions may actually be related to hydrophobic interactions. For example, in amyloid β (Aβ) peptide, mutations of both F19 and F20 to either Leu or Ile have a negligible effect on preventing amyloid fibril formation[91], and the role of the Phe residues is more likely due to hydrophobic effects[92]. With this in mind, attempts to design peptides to prevent aggregation potentially related to π-π stacking should consider that hydrophobicity of aromatic residues may be more important than the π-interactions.

2.3.4 Proteolytic stability

Proteolytic stability is a historically significant limitation for therapeutic peptides, as the potency of peptides is closely tied to the integrity of their sequence. Susceptibility to proteolytic degradation continues to be a concern for the development of therapeutic peptides due to the host of proteases encountered *in vivo*, including digestive tract enzymes[93-98] and microbial proteases from both commensal and pathogen species[97-100].

Peptides can be engineered to reduce the degradation associated with the most likely encountered proteases and retain the peptide's function. Increasing proteolytic stability is most frequently accomplished by identifying residue specificity of the relevant proteases and determining residue substitutions that can avoid degradation. Our discussion focuses on linear peptides with canonical amino acids, though proteolytic stability can also be improved through cyclization[9, 101] and incorporation of non-canonical amino acid side chains or backbones[9, 102]. To identify the residue specificity of a protease, peptide mapping can be used. This involves the incubation of the peptide substrate with the protease or biological fluids of interest and analysis of the resulting fragments to identify preferential sites of degradation. For example, McGlinchey and Lee used this strategy to elucidate the role of different cysteine cathepsins in the degradation of α-synuclein, a peptide associated with Parkinson's disease[103]. CstB and CstL were primarily responsible for the clearance of α-synuclein

in the soluble and lysosomal membrane-bound forms, while CstD was only capable of degrading the peptide while bound to the membrane[103].

Once the preferred degradation sequences for relevant enzymes are known, rational design can be used to reduce susceptibility to degradation. For example, histatin 5, a salivary peptide with antifungal potency for *Candida albicans*[104] was engineered for improved proteolytic stability in the presence of secreted aspartic proteases (Sap2 and Sap9) produced by the fungus. The enzymes preferentially degrade histatin 5 at Arg residues, especially K17, and substitution of this residue to either Leu or Arg resulted in higher stability[104]. In another example, the incorporation of Trp at four residues of the antimicrobial peptide cecropin A-melittin resulted in significantly improved stability in the presence of digestive tract enzymes by improving its helical structure and avoiding protease recognition[95]. Additionally, several synthetic antimicrobial peptides were designed based on repeats of the motif (XYPX), where X = I, L, or V and Y = R or K, which was designed to resist degradation by trypsin and chymotrypsin[105]. The peptide $(IRPR)_7$ showed strong resistance to both enzymes, while also having strong antibacterial activity. In addition to illustrating design for proteolytic stability, these examples also highlight the important link between proteolytic stability and biological activity.

When the specific sequences susceptible to proteolysis are not known, directed evolution can be used to improve proteolytic stability. For example, Howell et al. started with a cyclized 10-amino acid peptide library previously enriched for binding to the signaling protein Gαi1 and used three rounds of mRNA display to improve

stability in the presence of chymotrypsin while maintaining binding to Gαi1[106]. After production and cyclization of the peptide library as a fusion to mRNA, the library was incubated with chymotrypsin and then screened again for binding to Gαi1. The screening isolated cyclic peptides with half-lives in the presence of chymotrypsin improved by 35-fold compared to peptides isolated without the chymotrypsin selective pressure. Even more impressive, the half-lives of the linear versions of the peptides were improved 200-fold, and the amino acid sequence, not cyclization, had the stronger effect on improving proteolytic stability[106]. Although this study performed screening on cyclic peptides, the results suggest that similar approaches with linear peptides would also be successful. Sieber et al. developed another strategy that uses phage display to engineer protease-resistant proteins, which would be amenable to engineering peptides[107]. The method places the protein to be stabilized between the C2 and N2/N1 domains of the gene-3-protein (g3p) of phage and subjects the resulting construct to proteolytic degradation. The N1 domain is required for infectivity of the phage, so only phage displaying variants that resist degradation and, thus, maintain an intact N1 domain can be propagated in bacteria. The method successfully identified chymotrypsin-resistant variants of ribonuclease T1 from a large library[107]. As these examples illustrate, both *in vitro* and *in vivo* display techniques have the potential to identify proteolytically stable peptide variants that could maintain longer half-lives as therapeutics.

2.3.5 Binding affinity and specificity

While interactions of peptides with other biomolecules can be undesirable in the context of proteolytic degradation, interactions are highly desirable in other applications, including inhibiting protein function[78], detecting disease[13,76,78], and activating or modulating the immune system[77]. Selective targeting or activation of biological pathways with peptides requires considering the myriad of interactions possible *in vivo*. The identification and optimization of peptide sequences that interact specifically with desired biomolecular targets are critical aspects of developing peptide-based therapeutics.

Directed evolution is a powerful approach to engineering peptides for specific binding interactions, as it can both produce peptides with higher binding affinity and specificity for a selected target and identify recurring motifs of interest that could prove useful for rational design approaches. Because of this, directed evolution methods are commonly employed to elucidate key factors in peptide binding interactions. Jiang and Boder used yeast display to determine the side-chain specificity of the peptide FLU for a class II major histocompatibility complex (MHC-II) protein, which is responsible for CD4+ T-cell stimulation in adaptive immune response[108]. FLU was expressed as a fusion to the native yeast protein Aga2 to target it to the yeast surface. Simultaneously, MHC-II was also expressed, and the interrogation of the peptide by MHC-II occurred in the endoplasmic reticulum (ER). If the peptide was recognized and bound by MHC-II in the ER, both the peptide and MHC-II were translocated to the yeast surface for

display, while a lack of interaction prevented MHC-II from being displayed[108]. Using this method, the authors revealed the preference in the FLU peptide of an aromatic residue followed by small hydrophobic residues for association with the MHC-II[108]. Similarly, Lamla and Erdmann used ribosome display to identify peptides that bind to the protein streptavidin by fusing a randomized library of 15-amino acid peptides to the N-terminus of a carrier protein (bovine heart fatty acid-binding protein, FABP). After isolating peptides with dissociation constants as low as 4 nmol/L, a substitution analysis of the best peptide revealed the motifs important for binding to allow truncation of the 15-amino acid peptide to a 9-amino acid peptide with little loss in binding[19]. When performing directed evolution to engineer peptides with high affinity for therapeutic targets, the screen must be carefully considered to generate the desired binding and specificity, as the screening procedure influences the resulting binding specificity. For example, in a study that targeted M2 macrophages, which assist in disease proliferation in cancer, the peptide M2pep was evolved to preferentially target M2 macrophages over M1 macrophages by alternating screening steps designed to select peptides that bound to M2 macrophages and screens designed to remove peptides that bound to M1 macrophages[109]. This resulted in a 3.8-fold increase in M2pep's relative binding affinity for M2:M1 macrophages[109]. Additionally, Leal et al. used phage display to screen for peptides with high diffusive transport through a cystic fibrosis mucus model, and identified peptides with lower affinity for the mucin glycoproteins that are the major protein component of mucus[110]. The peptides have mucin-like motifs, suggesting that these motifs reduce intermolecular interactions with

mucins to facilitate transport. These examples demonstrate how directed evolution can be used to generate peptides with high affinity and specificity when detailed structure-function information is not available.

Computational tools can be used in conjunction with directed evolution to better understand the structure-function relationships for binding of variants isolated from peptide libraries. One example of combining directed evolution techniques with computational analysis is SORTCERY, which uses a combination of yeast surface display, FACS, and deep-sequencing to collect data to model the binding landscape for a given interaction[111]. An enhanced version of SORTCERY that relates FACS signals to binding energies was used to understand the binding landscape and identify *de novo* peptides with specific affinity for only one of three Bcl-2 peptides (Bcl-xL, Mcl-1, and Bfl-1) associated with regulating apoptosis in B-cell lymphoma[18]. Interestingly, this method was also capable of generating peptides that bind specifically to two of three targets (but not to the third), highlighting the strength of using a computational approach to analyze the data available for individual library members in a directed evolution experiment[18]. Employing computational tools to analyze the large sets of data from directed evolution experiments will ultimately improve the ability to apply rational design principles to *de novo* design of peptides with specific binding properties.

Directed evolution is useful to improve the binding affinity of peptides when the interaction of the peptide with the target is not well understood, but rational design can be a more effective tool when sufficient information on the binding target and important interactions in binding are available. For example, Manzo et al. demonstrated

the utility of rational design by perfecting the β-strand amphiphilicity of the antimicrobial peptide SB056[112]. The order of the N-terminal WK residues was interchanged to KW, resulting in the N-terminal amine and all cationic residues extending in the same direction. The mutation increased by 3- to 4-fold the binding affinity of SB056 for model cell membranes composed of 1-palmitoyl-2-oleoyl-sn-glycero-3-phosphocholine (POPC), a zwitterionic phosphatidylcholine, and 1-palmitoyl-2-oleoyl-sn-glycero-3-phosphatidylglycerol (POPG), an anionic phospholipid. Additionally, the mutation increased cytotoxicity toward both gram-negative and gram-positive bacteria significantly[112]. The relatively small size of many peptides makes rational design strategies like the one used in this example very appealing for engineering binding interactions, though the knowledge of the relevant interactions with the target must first be elucidated.

2.4 Perspective on future directions for peptide engineering

Biophysical properties and interactions of peptides play an important role in the biological function of the peptides and in their suitability for therapeutic applications. The long-term goal in therapeutic peptide design and engineering is to reach a point where we can simply specify the desired biological function and biophysical characteristics of a peptide and identify a *de novo* peptide sequence to meet the design goals without the need to perform experiments. Conceptually, the goal is to create a

"peptide vending machine", where the user would simply input the desired biological function and biophysical characteristics of a peptide, and a peptide that suits the application could be immediately synthesized (Figure 2.3). For example, the desired levels of binding to specific targets, as well as the necessary protease resistance, could be defined, and computational algorithms would identify the best sequence for the application. To reach this point, a continued improvement of structure-function relationships for a broad range of peptide characteristics, including both biophysical properties and biological function, is needed. While rational design, including computational methods, can provide improved understanding on a small scale, directed evolution offers the opportunity to explore a much larger region of sequence space while also improving peptide design. However, although directed evolution has been widely used for designing peptides for targeted binding interactions, the application of high-throughput directed evolution tools to address other biophysical characteristics has been limited. Developing new strategies for directed evolution and applying available methods to peptide engineering will result in improved peptides and provide information to incorporate into future rational design and computational approaches. As new methods are developed and applied, taking advantage of high-throughput sequencing techniques to evaluate the sequences that do not lead to biophysical or biological improvements, in addition to those that do lead to improvements, will provide a broader understanding of relevant structure-function relationships. Incorporation of these "negative" data into structure-function datasets will also improve the accuracy and utility of machine learning approaches, which are likely to

play an increasing role in peptide design. Ultimately, improvements in both experimental techniques and computational tools will combine to push towards the desired outcome of on-demand peptide design to meet any set of criteria needed for therapeutic applications.

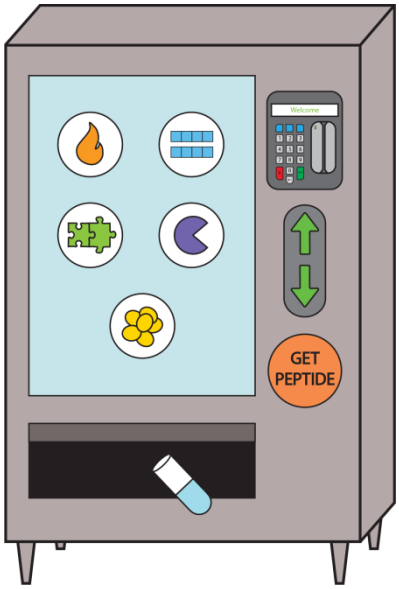

Figure 2.3. The long-term goal of peptide engineering is to enable on-demand, *de novo* design of a peptide to suit any therapeutic purpose. By simply specifying the desired biological function, along with the associated biophysical characteristics needed to achieve or maintain this function, an appropriate design for this peptide could be obtained without the need to perform experiments (Reproduced with permission, © 2019 American Institute of Chemical Engineers).

2.5 Design strategies pertaining to present study

Membrane penetration, the ability for a species to translocate into the cell through endocytosis or non-endocytosis mechanisms, is a key feature that is crucial for the therapeutic efficacy of antibacterial, antifungal and other cell penetrating peptides.

Defined by their inherent transport capability, these classes of peptides continue to be highly explored as delivery systems for poorly internalized and low-bioavailable drugs[113, 114]. Additionally, this biophysical property makes them promising novel therapeutics for the treatment of bacterial and fungal pathogens with established antibiotic-resistance[115]. However, the therapeutic potential of these peptides is limited by their selectivity[113, 114]. To mitigate this issue, rational design approaches have found the optimized use of the peptide's cationic and hydrophobic residues to impart the most beneficial results.

Cationic amino acids are thought to contribute to the penetration of cell penetrating peptides through electrostatic interactions with negatively charged phospholipid head groups and other anionic and hydrogen-bond accepting moieties in the plasma membrane[116]. Using this knowledge, the selection of cationic amino acids at key positions has been shown to significantly improve its selective translocation utilizing the diversity in the membrane composition of diverse species. This has been demonstrated through the rational design of the CPPs, penetratin and Tat (48-60), in which arginine was demonstrated to exhibit preferential translation into PC-12 tumor cells over lysine at the same positions[117]. Similarly, alteration of arginine and lysine at key positions of LL-37 has been shown to improve the selective penetration of *S. aureus* over *E. coli*[118]. Furthermore, other viable approaches to improve translocation includes increasing the net charge[119] and the number of residue repeats[120] in the peptide. Consequently, cationic residues are crucial for the association and penetration of peptides and are essential for designing selectivity.

Likewise, hydrophobic interactions with the cell membrane represent an important driving force for translocation as well. This is primarily mediated by the interaction of the hydrophobic domains of the peptide with the membrane lipids and hydrophobic core of the bilayer, driving their insertion[57]. With this in mind, the segregation of hydrophobic motifs and the orientation, the peptide adopts in relation to the surface can be key for their adsorption. Molecular dynamics simulations have been very helpful in this regard and have shown that cell-penetrating peptides preferentially associate with the membrane utilizing a parallel orientation[121, 122] and then become perpendicular before insertion[122], allowing the hydrophobic domains to pull it through. With this in mind, improving the hydrophobic moment has been shown to be an effective approach to engineering amphiphilic CPPs[123].

However, increasing the hydrophobic moment may not always help in improving translocation. Instead, strategies to find the right balance between hydrophobic and hydrophilic residues have been shown to be more beneficial[124]. However, if amphiphilic, then increasing hydrophobic moment has been shown to be useful. With this in mind, Chapter 4 of this thesis, builds on these design approaches and we have rationally designed our peptides. We have outlined possible mutations in our CPPs to enhance translocation into *Candida*. The future work section in the same chapter will provide further design strategies to enhance translocation and CPP-mediated cargo delivery.

2.6 Conclusion

The protein engineering design strategies will help us design better CPPs which can then efficiently carry biomolecular cargoes across the cell membrane barrier and can associate with cargoes in covalent or noncovalent ways. Depending on sequences, length, and interaction with cargo, the cellular entry may vary. A diversity of chemical and molecular methods has been summarized that can help design better peptides as therapeutics and delivery vectors. As studies on CPPs continue to improve our understanding about these peptides, this delivery vehicle will find extensive use in the pharmaceutical industry.

2.7 References

1. Adhikari, S.; Leissa, J. A.; Karlsson, A. J., Beyond function: Engineering improved peptides for therapeutic applications. *AIChE Journal* **2019,** *66* (3), e16776.
2. Fosgerau, K.; Hoffmann, T., Peptide therapeutics: current status and future directions. *Drug Discov Today* **2015,** *20* (1), 122-8.
3. Uhlig, T.; Kyprianou, T.; Martinelli, F. G.; Oppici, C. A.; Heiligers, D.; Hills, D.; Calvo, X. R.; Verhaert, P., The emergence of peptides in the pharmaceutical business: From exploration to exploitation. *EuPA Open Proteomics* **2014,** *4*, 58-69.
4. Lau, J. L.; Dunn, M. K., Therapeutic peptides: Historical perspectives, current development trends, and future directions. *Bioorg Med Chem* **2018,** *26* (10), 2700-2707.
5. Otvos, L., Jr.; Wade, J. D., Current challenges in peptide-based drug discovery. *Front Chem* **2014,** *2*, 62.
6. Abbvie, Abbvie Inc. Form 10-K 2018. Retrieved from U.S. Securities and Exchange Commission EDGAR: https://www.sec.gov/edgar/searchedgar/companysearch.html. Filed 2019, February 27.
7. Sanofi, Sanofi. Form 20-F 2018. Retrieved from U.S. Securities and Exchange Commission EDGAR: https://www.sec.gov/edgar/searchedgar/companysearch.html. Filed 2019, March 8.
8. Gupta, S.; Jain, A.; Chakraborty, M.; Sahni, J. K.; Ali, J.; Dang, S., Oral delivery of therapeutic proteins and peptides: a review on recent developments. *Drug Deliv* **2013,** *20* (6), 237-46.
9. Qvit, N.; Rubin, S. J. S.; Urban, T. J.; Mochly-Rosen, D.; Gross, E. R., Peptidomimetic therapeutics: scientific approaches and opportunities. *Drug Discov Today* **2017,** *22* (2), 454-462.
10. Neumann-Staubitz, P.; Neumann, H., The use of unnatural amino acids to study and engineer protein function. *Curr Opin Struct Biol* **2016,** *38*, 119-28.
11. Joshi, S.; Chen, L.; Winter, M. B.; Lin, Y. L.; Yang, Y.; Shapovalova, M.; Smith, P. M.; Liu, C.; Li, F.; LeBeau, A. M., The rational design of therapeutic peptides for aminopeptidase n using a substrate-based approach. *Sci Rep* **2017,** *7* (1), 1424.
12. Lipovsek, D.; Mena, M.; Lippow, S. M.; Basu, S.; Baynes, B. M., Library construction for protein engineering. In *Protein engineering and design*, Park, S. J.; Cochran, J. R., Eds. CRC Press: 2010.
13. Lehmann, M.; Wyss, M., Engineering proteins for thermostability: The use of sequence alignments versus rational design and directed evolution. *Curr Opin Biotech* **2001,** *12* (4), 371-375.

14. Song, J. K.; Rhee, J. S., Simultaneous enhancement of thermostability and catalytic activity of phospholipase A(1) by evolutionary molecular engineering. *Appl Environ Microbiol* **2000,** *66* (3), 890-4.
15. Yokobayashi, Y.; Weiss, R.; Arnold, F. H., Directed evolution of a genetic circuit. *Proc Natl Acad Sci U S A* **2002,** *99* (26), 16587-91.
16. Zweigerdt, R.; Braun, T.; Arnold, H. H., Faithful expression of the Myf-5 gene during mouse myogenesis requires distant control regions: a transgene approach using yeast artificial chromosomes. *Dev Biol* **1997,** *192* (1), 172-80.
17. Wittrup, K. D., Protein engineering by cell-surface display. *Curr Opin Biotechnol* **2001,** *12* (4), 395-9.
18. Jenson, J. M.; Xue, V.; Stretz, L.; Mandal, T.; Reich, L. L.; Keating, A. E., Peptide design by optimization on a data-parameterized protein interaction landscape. *Proc Natl Acad Sci U S A* **2018,** *115* (44), E10342-E10351.
19. Lamla, T.; Erdmann, V. A., Searching sequence space for high-affinity binding peptides using ribosome display. *J Mol Biol* **2003,** *329* (2), 381-388.
20. Winter, G.; Griffiths, A. D.; Hawkins, R. E.; Hoogenboom, H. R., Making antibodies by phage display technology. *Annu Rev Immunol* **1994,** *12* (1), 433-55.
21. Smith, G. P., Filamentous fusion phage: novel expression vectors that display cloned antigens on the virion surface. *Science* **1985,** *228* (4705), 1315-7.
22. Pande, J.; Szewczyk, M. M.; Grover, A. K., Phage display: concept, innovations, applications and future. *Biotechnol Adv* **2010,** *28* (6), 849-58.
23. Cherf, G. M.; Cochran, J. R., Applications of yeast surface display for protein engineering. *Methods Mol Biol* **2015,** *1319*, 155-75.
24. Boder, E. T.; Wittrup, K. D., Yeast surface display for screening combinatorial polypeptide libraries. *Nat Biotechnol* **1997,** *15* (6), 553-7.
25. Simeon, R.; Chen, Z., In vitro-engineered non-antibody protein therapeutics. *Protein Cell* **2018,** *9* (1), 3-14.
26. Charbit, A.; Boulain, J. C.; Ryter, A.; Hofnung, M., Probing the topology of a bacterial membrane protein by genetic insertion of a foreign epitope; expression at the cell surface. *EMBO J* **1986,** *5* (11), 3029-37.
27. Daugherty, P. S., Protein engineering with bacterial display. *Curr Opin Struct Biol* **2007,** *17* (4), 474-80.
28. Freudl, R.; MacIntyre, S.; Degen, M.; Henning, U., Cell surface exposure of the outer membrane protein OmpA of Escherichia coli K-12. *J Mol Biol* **1986,** *188* (3), 491-4.
29. Nicolay, T.; Vanderleyden, J.; Spaepen, S., Autotransporter-based cell surface display in Gram-negative bacteria. *Crit Rev Microbiol* **2015,** *41* (1), 109-23.
30. Lu, Z.; Murray, K. S.; Van Cleave, V.; LaVallie, E. R.; Stahl, M. L.; McCoy, J. M., Expression of thioredoxin random peptide libraries on the Escherichia coli cell surface as functional fusions to flagellin: a system designed for exploring protein-protein interactions. *Biotechnology (N Y)* **1995,** *13* (4), 366-72.

31. Mishra, B.; Reiling, S.; Zarena, D.; Wang, G., Host defense antimicrobial peptides as antibiotics: design and application strategies. *Curr Opin Chem Biol* **2017,** *38*, 87-96.
32. Lee, S. Y.; Choi, J. H.; Xu, Z., Microbial cell-surface display. *Trends Biotechnol* **2003,** *21* (1), 45-52.
33. Hanes, J.; Pluckthun, A., In vitro selection and evolution of functional proteins by using ribosome display. *Proc Natl Acad Sci U S A* **1997,** *94* (10), 4937-42.
34. He, M.; Taussig, M. J., Ribosome display: cell-free protein display technology. *Brief Funct Genomic Proteomic* **2002,** *1* (2), 204-12.
35. Reetz, M. T.; Carballeira, J. D., Iterative saturation mutagenesis (ISM) for rapid directed evolution of functional enzymes. *Nat Protoc* **2007,** *2* (4), 891-903.
36. Reetz, M. T.; Carballeira, J. D.; Vogel, A., Iterative saturation mutagenesis on the basis of B factors as a strategy for increasing protein thermostability. *Angew Chem Int Ed Engl* **2006,** *45* (46), 7745-51.
37. Reetz, M. T.; Wang, L. W.; Bocola, M., Directed evolution of enantioselective enzymes: iterative cycles of CASTing for probing protein-sequence space. *Angew Chem Int Ed Engl* **2006,** *45* (8), 1236-41.
38. Bradley, L. H., High-quality combinatorial protein libraries using the binary patterning approach. In *Protein Design: Methods and Applications*, Köhler, V., Ed. Springer New York: New York, NY, 2014; pp 117-128.
39. Kamtekar, S.; Schiffer, J. M.; Xiong, H.; Babik, J. M.; Hecht, M. H., Protein design by binary patterning of polar and nonpolar amino acids. *Science* **1993,** *262* (5140), 1680-5.
40. Bradley, L. H.; Wei, Y.; Thumfort, P.; Wurth, C.; Hecht, M. H., Protein design by binary patterning of polar and nonpolar amino acids. In *Protein Engineering Protocols*, Arndt, K. M.; Müller, K. M., Eds. Humana Press: Totowa, NJ, 2007; pp 155-166.
41. West, M. W.; Wang, W.; Patterson, J.; Mancias, J. D.; Beasley, J. R.; Hecht, M. H., De novo amyloid proteins from designed combinatorial libraries. *Proc Natl Acad Sci U S A* **1999,** *96* (20), 11211-6.
42. Wilson, D. S.; Keefe, A. D.; Szostak, J. W., The use of mRNA display to select high-affinity protein-binding peptides. *Proc Natl Acad Sci U S A* **2001,** *98* (7), 3750-5.
43. Coluzza, I., Computational protein design: A review. *J Phys Condens Matter* **2017,** *29* (14), 143001.
44. Nikiforovich, G. V., Computational molecular modeling in peptide drug design. *Int J Pept Protein Res* **1994,** *44* (6), 513-31.
45. Musiani, F.; Rossetti, G.; Capece, L.; Gerger, T. M.; Micheletti, C.; Varani, G.; Carloni, P., Molecular Dynamics Simulations Identify Time Scale of Conformational Changes Responsible for Conformational Selection in Molecular Recognition of HIV-1 Transactivation Responsive RNA. *Journal of the American Chemical Society* **2014,** *136* (44), 15631-15637.

46. Klepeis, J. L.; Lindorff-Larsen, K.; Dror, R. O.; Shaw, D. E., Long-timescale molecular dynamics simulations of protein structure and function. *Current Opinion in Structural Biology* **2009,** *19* (2), 120-127.
47. Beck, D. A.; White, G. W.; Daggett, V., Exploring the energy landscape of protein folding using replica-exchange and conventional molecular dynamics simulations. *J Struct Biol* **2007,** *157* (3), 514-23.
48. Yesylevskyy, S.; Marrink, S. J.; Mark, A. E., Alternative mechanisms for the interaction of the cell-penetrating peptides penetratin and the TAT peptide with lipid bilayers. *Biophys J* **2009,** *97* (1), 40-9.
49. Nguyen, T. H.; Rao, N. Z.; Schroeder, W. M.; Moore, P. B., Coarse-grained molecular dynamics of tetrameric transmembrane peptide bundles within a lipid bilayer. *Chem Phys Lipids* **2010,** *163* (6), 530-7.
50. Shelley, M. Y.; Selvan, M. E.; Zhao, J.; Babin, V.; Liao, C.; Li, J.; Shelley, J. C., A new mixed all-atom/coarse-grained model: Application to melittin aggregation in aqueous solution. *J Chem Theory Comput* **2017,** *13* (8), 3881-3897.
51. Fjell, C. D.; Jenssen, H.; Hilpert, K.; Cheung, W. A.; Pante, N.; Hancock, R. E.; Cherkasov, A., Identification of novel antibacterial peptides by chemoinformatics and machine learning. *J Med Chem* **2009,** *52* (7), 2006-15.
52. Khosravian, M.; Faramarzi, F. K.; Beigi, M. M.; Behbahani, M.; Mohabatkar, H., Predicting antibacterial peptides by the concept of Chou's pseudo-amino acid composition and machine learning methods. *Protein Pept Lett* **2013,** *20* (2), 180-6.
53. Sanders, W. S.; Johnston, C. I.; Bridges, S. M.; Burgess, S. C.; Willeford, K. O., Prediction of cell penetrating peptides by support vector machines. *PLoS Comput Biol* **2011,** *7* (7), e1002101.
54. Nielsen, H.; Brunak, S.; von Heijne, G., Machine learning approaches for the prediction of signal peptides and other protein sorting signals. *Protein Eng* **1999,** *12* (1), 3-9.
55. Verma, R.; Schwaneberg, U.; Roccatano, D., Computer-aided protein directed evolution: A review of web servers, databases and other computational tools for protein engineering. *Comput Struct Biotechnol J* **2012,** *2*, e201209008.
56. Camacho, C. J.; Katsumata, Y.; Ascherman, D. P., Structural and thermodynamic approach to peptide immunogenicity. *PLoS Comput Biol* **2008,** *4* (11), e1000231.
57. Sani, M. A.; Separovic, F., How membrane-active peptides get into lipid membranes. *Acc Chem Res* **2016,** *49* (6), 1130-8.
58. Sommese, R. F.; Sivaramakrishnan, S.; Baldwin, R. L.; Spudich, J. A., Helicity of short E-R/K peptides. *Protein Sci* **2010,** *19* (10), 2001-5.
59. Swanson, C. J.; Sivaramakrishnan, S., Harnessing the unique structural properties of isolated alpha-helices. *J Biol Chem* **2014,** *289* (37), 25460-7.
60. Wolny, M.; Batchelor, M.; Bartlett, G. J.; Baker, E. G.; Kurzawa, M.; Knight, P. J.; Dougan, L.; Woolfson, D. N.; Paci, E.; Peckham, M., Characterization of long and stable de novo single alpha-helix domains provides novel insight into their stability. *Sci Rep* **2017,** *7*, 44341.

61. Chou, S.; Shao, C.; Wang, J.; Shan, A.; Xu, L.; Dong, N.; Li, Z., Short, multiple-stranded beta-hairpin peptides have antimicrobial potency with high selectivity and salt resistance. *Acta Biomater* **2016,** *30*, 78-93.
62. Bureau, H. R.; Hershkovits, E.; Quirk, S.; Hernandez, R., Determining the energetics of small beta-sheet peptides using adaptive steered molecular dynamics. *J Chem Theory Comput* **2016,** *12* (4), 2028-37.
63. Capelli, R.; Villemot, F.; Moroni, E.; Tiana, G.; van der Vaart, A.; Colombo, G., Assessment of mutational effects on peptide stability through confinement simulations. *J Phys Chem Lett* **2016,** *7* (1), 126-30.
64. Yakimov, A. P.; Afanaseva, A. S.; Khodorkovskiy, M. A.; Petukhov, M. G., Design of stable alpha-helical peptides and thermostable proteins in biotechnology and biomedicine. *Acta Naturae* **2016,** *8* (4), 70-81.
65. Eijsink, V. G.; Gaseidnes, S.; Borchert, T. V.; van den Burg, B., Directed evolution of enzyme stability. *Biomol Eng* **2005,** *22* (1-3), 21-30.
66. Giver, L.; Gershenson, A.; Freskgard, P. O.; Arnold, F. H., Directed evolution of a thermostable esterase. *Proc Natl Acad Sci U S A* **1998,** *95* (22), 12809-13.
67. Socha, R. D.; Tokuriki, N., Modulating protein stability - directed evolution strategies for improved protein function. *FEBS J* **2013,** *280* (22), 5582-95.
68. Traxlmayr, M. W.; Obinger, C., Directed evolution of proteins for increased stability and expression using yeast display. *Arch Biochem Biophys* **2012,** *526* (2), 174-80.
69. Bond, C. J.; Marsters, J. C.; Sidhu, S. S., Contributions of CDR3 to VHH Domain Stability and the Design of Monobody Scaffolds for Naive Antibody Libraries. *J Mol Biol* **2003,** *332* (3), 643-655.
70. Julian, M. C.; Lee, C. C.; Tiller, K. E.; Rabia, L. A.; Day, E. K.; Schick, A. J., 3rd; Tessier, P. M., Co-evolution of affinity and stability of grafted amyloid-motif domain antibodies. *Protein Eng Des Sel* **2015,** *28* (10), 339-50.
71. Gröschel, A. H.; Müller, A. H. E., Self-assembly concepts for multicompartment nanostructures. *Nanoscale* **2015,** *7* (28), 11841-11876.
72. Tian, X.; Sun, F.; Zhou, X. R.; Luo, S. Z.; Chen, L., Role of peptide self-assembly in antimicrobial peptides. *J Pept Sci* **2015,** *21* (7), 530-9.
73. Habibi, N.; Kamaly, N.; Memic, A.; Shafiee, H., Self-assembled peptide-based nanostructures: Smart nanomaterials toward targeted drug delivery. *Nano Today* **2016,** *11* (1), 41-60.
74. Deidda, G.; Jonnalagadda, S. V. R.; Spies, J. W.; Ranella, A.; Mossou, E.; Forsyth, V. T.; Mitchell, E. P.; Bowler, M. W.; Tamamis, P.; Mitraki, A., Self-assembled amyloid peptides with arg-gly-asp (rgd) motifs as scaffolds for tissue engineering. *ACS Biomater Sci Eng* **2016,** *3* (7), 1404-1416.
75. Zhou, X. R.; Cao, Y.; Zhang, Q.; Tian, X. B.; Dong, H.; Chen, L.; Luo, S. Z., Self-assembly nanostructure controlled sustained release, activity and stability of peptide drugs. *Int J Pharm* **2017,** *528* (1-2), 723-731.

76. Zhang, H.; Park, J.; Jiang, Y.; Woodrow, K. A., Rational design of charged peptides that self-assemble into robust nanofibers as immune-functional scaffolds. *Acta Biomater* **2017,** *55*, 183-193.
77. Frederix, P. W.; Scott, G. G.; Abul-Haija, Y. M.; Kalafatovic, D.; Pappas, C. G.; Javid, N.; Hunt, N. T.; Ulijn, R. V.; Tuttle, T., Exploring the sequence space for (tri-)peptide self-assembly to design and discover new hydrogels. *Nat Chem* **2015,** *7* (1), 30-7.
78. Wang, M.; Wang, J.; Zhou, P.; Deng, J.; Zhao, Y.; Sun, Y.; Yang, W.; Wang, D.; Li, Z.; Hu, X.; King, S. M.; Rogers, S. E.; Cox, H.; Waigh, T. A.; Yang, J.; Lu, J. R.; Xu, H., Nanoribbons self-assembled from short peptides demonstrate the formation of polar zippers between beta-sheets. *Nat Commun* **2018,** *9* (1), 5118.
79. Chen, Y.; Xing, Z.; Liao, D.; Qiu, F., Neglected hydrophobicity of dimethanediyl group in peptide self-assembly: A hint from amyloid-like peptide GNNQQNY and its derivatives. *J Phys Chem B* **2018,** *122* (46), 10470-10477.
80. Rad-Malekshahi, M.; Lempsink, L.; Amidi, M.; Hennink, W. E.; Mastrobattista, E., Biomedical applications of self-assembling peptides. *Bioconjug Chem* **2016,** *27* (1), 3-18.
81. Zhou, P.; Deng, L.; Wang, Y.; Lu, J. R.; Xu, H., Different nanostructures caused by competition of intra- and inter-beta-sheet interactions in hierarchical self-assembly of short peptides. *J Colloid Interface Sci* **2016,** *464*, 219-28.
82. Fowler, S. B.; Poon, S.; Muff, R.; Chiti, F.; Dobson, C. M.; Zurdo, J., Rational design of aggregation-resistant bioactive peptides: reengineering human calcitonin. *Proc Natl Acad Sci U S A* **2005,** *102* (29), 10105-10.
83. Schellekens, H., Bioequivalence and the immunogenicity of biopharmaceuticals. *Nat Rev Drug Discov* **2002,** *1* (6), 457-62.
84. Zapadka, K. L.; Becher, F. J.; Gomes Dos Santos, A. L.; Jackson, S. E., Factors affecting the physical stability (aggregation) of peptide therapeutics. *Interface Focus* **2017,** *7* (6), 20170030.
85. Chiti, F.; Stefani, M.; Taddei, N.; Ramponi, G.; Dobson, C. M., Rationalization of the effects of mutations on peptide and protein aggregation rates. *Nature* **2003,** *424* (6950), 805-8.
86. Zhou, P.; Hou, S.; Bai, Z.; Li, Z.; Wang, H.; Chen, Z.; Meng, Y., Disrupting the intramolecular interaction between proto-oncogene c-Src SH3 domain and its self-binding peptide PPII with rationally designed peptide ligands. *Artif Cells Nanomed Biotechnol* **2018,** *46* (6), 1122-1131.
87. Esler, W. P.; Stimson, E. R.; Ghilardi, J. R.; Lu, Y. A.; Felix, A. M.; Vinters, H. V.; Mantyh, P. W.; Lee, J. P.; Maggio, J. E., Point substitution in the central hydrophobic cluster of a human beta-amyloid congener disrupts peptide folding and abolishes plaque competence. *Biochemistry* **1996,** *35* (44), 13914-21.
88. Azriel, R.; Gazit, E., Analysis of the minimal amyloid-forming fragment of the islet amyloid polypeptide. An experimental support for the key role of the phenylalanine residue in amyloid formation. *J Biol Chem* **2001,** *276* (36), 34156-61.

89. Ashburn, T. T.; Lansbury, P. T., Interspecies sequence variations affect the kinetics and thermodynamics of amyloid formation: peptide models of pancreatic amyloid. *Journal of the American Chemical Society* **1993,** *115* (23), 11012-11013.
90. Gsponer, J.; Haberthur, U.; Caflisch, A., The role of side-chain interactions in the early steps of aggregation: Molecular dynamics simulations of an amyloid-forming peptide from the yeast prion Sup35. *Proc Natl Acad Sci U S A* **2003,** *100* (9), 5154-9.
91. Armstrong, A. H.; Chen, J.; McKoy, A. F.; Hecht, M. H., Mutations that replace aromatic side chains promote aggregation of the Alzheimer's Aβ peptide. *Biochemistry* **2011,** *50* (19), 4058-67.
92. Kim, W.; Hecht, M. H., Generic hydrophobic residues are sufficient to promote aggregation of the Alzheimer's Aβ42 peptide. *Proc Natl Acad Sci U S A* **2006,** *103* (43), 15824-9.
93. McGregor, D. P., Discovering and improving novel peptide therapeutics. *Curr Opin Pharmacol* **2008,** *8* (5), 616-9.
94. Fominaya, J.; Bravo, J.; Rebollo, A., Strategies to stabilize cell penetrating peptides for in vivo applications. *Ther Deliv* **2015,** *6* (10), 1171-94.
95. Ji, S.; Li, W.; Zhang, L.; Zhang, Y.; Cao, B., Cecropin A-melittin mutant with improved proteolytic stability and enhanced antimicrobial activity against bacteria and fungi associated with gastroenteritis in vitro. *Biochem Biophys Res Commun* **2014,** *451* (4), 650-5.
96. Sun, X.; Salih, E.; Oppenheim, F. G.; Helmerhorst, E. J., Activity-based mass spectrometric characterization of proteases and inhibitors in human saliva. *Proteomics Clin Appl* **2009,** *3* (7), 810-820.
97. Soder, P. O., Proteolytic activity in the oral cavity: proteolytic enzymes from human saliva and dental plaque material. *J Dent Res* **1972,** *51* (2), 389-93.
98. Nakamura, M.; Slots, J., Salivary enzymes. Origin and relationship to periodontal disease. *J Periodontal Res* **1983,** *18* (6), 559-69.
99. Naglik, J. R.; Challacombe, S. J.; Hube, B., Candida albicans secreted aspartyl proteinases in virulence and pathogenesis. *Microbiol Mol Biol Rev* **2003,** *67* (3), 400-28, table of contents.
100. Sriranganadane, D.; Waridel, P.; Salamin, K.; Reichard, U.; Grouzmann, E.; Neuhaus, J. M.; Quadroni, M.; Monod, M., Aspergillus protein degradation pathways with different secreted protease sets at neutral and acidic pH. *J Proteome Res* **2010,** *9* (7), 3511-9.
101. Molhoek, E. M.; van Dijk, A.; Veldhuizen, E. J. A.; Haagsman, H. P.; Bikker, F. J., Improved proteolytic stability of chicken cathelicidin-2 derived peptides by D-amino acid substitutions and cyclization. *Peptides* **2011,** *32* (5), 875-880.
102. Leisle, L.; Valiyaveetil, F.; Mehl, R. A.; Ahern, C. A., Incorporation of non-canonical amino acids. *Adv Exp Med Biol* **2015,** *869*, 119-51.
103. McGlinchey, R. P.; Lee, J. C., Cysteine cathepsins are essential in lysosomal degradation of alpha-synuclein. *Proc Natl Acad Sci U S A* **2015,** *112* (30), 9322-7.
104. Ikonomova, S. P.; Moghaddam-Taaheri, P.; Jabra-Rizk, M. A.; Wang, Y.; Karlsson, A. J., Engineering improved variants of the antifungal peptide histatin 5 with

reduced susceptibility to Candida albicans secreted aspartic proteases and enhanced antimicrobial potency. *FEBS J* **2018,** *285* (1), 146-159.
105. Wang, J.; Song, J.; Yang, Z.; He, S.; Yang, Y.; Feng, X.; Dou, X.; Shan, A., Antimicrobial peptides with high proteolytic resistance for combating gram-negative bacteria. *J Med Chem* **2019,** *62* (5), 2286-2304.
106. Howell, S. M.; Fiacco, S. V.; Takahashi, T. T.; Jalali-Yazdi, F.; Millward, S. W.; Hu, B.; Wang, P.; Roberts, R. W., Serum stable natural peptides designed by mRNA display. *Sci Rep* **2014,** *4*, 6008.
107. Sieber, V.; Pluckthun, A.; Schmid, F. X., Selecting proteins with improved stability by a phage-based method. *Nat Biotechnol* **1998,** *16* (10), 955-60.
108. Jiang, W.; Boder, E. T., High-throughput engineering and analysis of peptide binding to class II MHC. *Proc Natl Acad Sci U S A* **2010,** *107* (30), 13258-63.
109. Cieslewicz, M.; Tang, J.; Yu, J. L.; Cao, H.; Zavaljevski, M.; Motoyama, K.; Lieber, A.; Raines, E. W.; Pun, S. H., Targeted delivery of proapoptotic peptides to tumor-associated macrophages improves survival. *Proc Natl Acad Sci U S A* **2013,** *110* (40), 15919-24.
110. Leal, J.; Dong, T.; Taylor, A.; Siegrist, E.; Gao, F.; Smyth, H. D. C.; Ghosh, D., Mucus-penetrating phage-displayed peptides for improved transport across a mucus-like model. *Int J Pharm* **2018,** *553* (1-2), 57-64.
111. Reich, L. L.; Dutta, S.; Keating, A. E., Sortcery-a high-throughput method to affinity rank peptide ligands. *J Mol Biol* **2015,** *427* (11), 2135-50.
112. Manzo, G.; Scorciapino, M. A.; Wadhwani, P.; Burck, J.; Montaldo, N. P.; Pintus, M.; Sanna, R.; Casu, M.; Giuliani, A.; Pirri, G.; Luca, V.; Ulrich, A. S.; Rinaldi, A. C., Enhanced amphiphilic profile of a short beta-stranded peptide improves its antimicrobial activity. *PLoS One* **2015,** *10* (1), e0116379.
113. Gallo, M.; Defaus, S.; Andreu, D., 1988-2018: Thirty years of drug smuggling at the nano scale. Challenges and opportunities of cell-penetrating peptides in biomedical research. *Arch Biochem Biophys* **2019,** *661*, 74-86.
114. Derakhshankhah, H.; Jafari, S., Cell penetrating peptides: A concise review with emphasis on biomedical applications. *Biomed Pharmacother* **2018,** *108*, 1090-1096.
115. Gomes, B.; Augusto, M. T.; Felicio, M. R.; Hollmann, A.; Franco, O. L.; Goncalves, S.; Santos, N. C., Designing improved active peptides for therapeutic approaches against infectious diseases. *Biotechnol Adv* **2018,** *36* (2), 415-429.
116. Drin, G.; Cottin, S.; Blanc, E.; Rees, A. R.; Temsamani, J., Studies on the Internalization Mechanism of Cationic Cell-penetrating Peptides. *Journal of Biological Chemistry* **2003,** *278* (33), 31192-31201.
117. Thoren, P. E.; Persson, D.; Isakson, P.; Goksor, M.; Onfelt, A.; Norden, B., Uptake of analogs of penetratin, Tat(48-60) and oligoarginine in live cells. *Biochem Biophys Res Commun* **2003,** *307* (1), 100-7.
118. Wang, G.; Epand, R. F.; Mishra, B.; Lushnikova, T.; Thomas, V. C.; Bayles, K. W.; Epand, R. M., Decoding the functional roles of cationic side chains of the major

antimicrobial region of human cathelicidin LL-37. *Antimicrob Agents Chemother* **2012,** *56* (2), 845-56.
119. Gong, Z.; Karlsson, A. J., Translocation of cell-penetrating peptides into Candida fungal pathogens. *Protein Sci* **2017,** *26* (9), 1714-1725.
120. Kimura, S.; Kawano, T.; Iwasaki, T., Short polyhistidine peptides penetrate effectively into Nicotiana tabacum-cultured cells and Saccharomyces cerevisiae cells. *Biosci Biotechnol Biochem* **2017,** *81* (1), 112-118.
121. Wei, C.; Pohorille, A., Sequence-dependent interfacial adsorption and permeation of dipeptides across phospholipid membranes. *J Phys Chem B* **2017,** *121* (42), 9859-9867.
122. Kabelka, I.; Vacha, R., Optimal hydrophobicity and reorientation of amphiphilic peptides translocating through membrane. *Biophys J* **2018,** *115* (6), 1045-1054.
123. Tian, Y.; Zeng, X.; Li, J.; Jiang, Y.; Zhao, H.; Wang, D.; Huang, X.; Li, Z., Achieving enhanced cell penetration of short conformationally constrained peptides through amphiphilicity tuning. *Chem Sci* **2017,** *8* (11), 7576-7581.
124. Kim, S.; Hyun, S.; Lee, Y.; Lee, Y.; Yu, J., Nonhemolytic cell-penetrating peptides: Site specific introduction of glutamine and lysine residues into the alpha-helical peptide causes deletion of its direct membrane disrupting ability but retention of its cell penetrating ability. *Biomacromolecules* **2016,** *17* (9), 3007-15.

Chapter 3: Translocation of CPP-cargo protein fusions into *Candida albicans* cells

Fungal infections caused by the opportunistic pathogen *Candida albicans* can cause complications in immunocompromised patients, and growing drug resistance has contributed to a need for novel therapeutic approaches. To help develop new approaches, we are studying cell-penetrating peptides (CPPs), which have the ability to cross cell membranes and carry biomolecules along with them. We fused the CPPs histatin 5 (Hst5) and MPG to green fluorescent protein (GFP) and optimized expression conditions to improve yields. We next investigated the intracellular delivery of purified Hst5-GFP and MPG-GFP into *C. albicans* compared to purified GFP with no CPP. Translocation of GFP into *C. albicans* cells was significantly higher when fused to MPG (around 40% of total cells), though Hst5 (around 5%) did not improve translocation. Molecular dynamics simulations were done in collaboration with Dr. Jeffery Klauda's lab to explain the important findings of experiments and the mechanisms employed by the CPPs to enter cells. The simulations show the utility of comparing the sequences and structures of each peptide and how their differences can lead to changes in cell entry.

3.1 Introduction

C. albicans (Figure 3.1), an opportunistic fungal pathogen, causes infections that are a reason for concern for immunocompromised patients. The pathogen can cause cutaneous and mucosal infections and systemic diseases[1]. Infection due to *C. albicans* can be fatal, and drug resistance has contributed to ineffectual treatment[1, 2]. Though current treatments exist the drugs can lead to toxicity[5] or cells are resistant to drugs[6]. In fact, in the year 2013, Centers for disease control and prevention (CDC) listed fluconazole-resistant *Candida* as a reason for concern[6]. Therefore, we need alternate treatments that specifically target and deliver biomolecular cargo into the fungal cells to treat infections caused by *C. albicans*. An essential feature of an effective therapeutic molecule is the ability to successfully deliver across cell membranes to intracellular targets. Thus, we propose the use CPPs. As mentioned in Chapter 1, CPPs are often amphipathic and cationic peptides and have the ability to carry biomolecular cargo into cells[7, 8,9-11]. We will use the CPPs, MPG and Histatin 5, to deliver our fluorescent protein cargo, GFP into the fungal cells. Both MPG and Hst-5 have previously shown delivery of cargo into cells[12-15] (Table 3.1). For example, Hst5

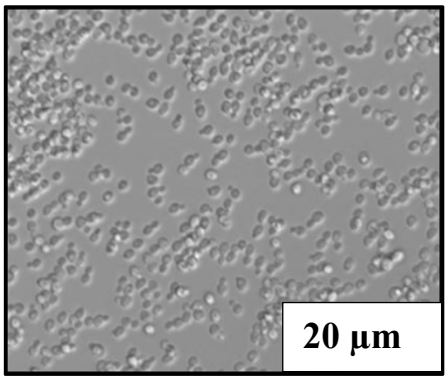

Figure 3.1. Yeast form of *Candida albicans.* The scale bars represent 20 µm.

has been shown to carry N-terminal fluorescein isothiocyanate (FITC) into cells[14], and MPG has delivered SiRNA into mammalian cells[13].

Table 3.1. CPPs used in the present study

Peptide	Sequence	Length (a.a.)	MW (Da)	Charge*	Proposed mechanism	Reference
MPG	GALFLGFLGA AGSTMGAWS QPKKKRKV	27	2807.36	+5	Endocytosis	[16]
Histatin 5	DSHAKRHHG YKRKFHEKH HSHRGY	24	3036.33	+12	Binding to cell wall, followed by translocation and then intracellular targeting	[14, 17]

*Includes charge due to amino acid side chains

MPG is a short amphipathic peptide that comprises the following domains: (1) N-terminal hydrophobic motif which is a derivative of the fusion sequence of the HIV glycoprotein 41 and is essential for effective targeting to the cell membrane and cellular uptake, (2) a hydrophilic lysine-rich domain which results from the nuclear localization sequence of SV40 (simian virus 40) large T-antigen (KKKRKV) and is critical for interaction with nucleic acids and cellular uptake, intracellular trafficking of cargo and solubility of the peptide, and (3) a linker domain (WSQP) between the two other domains, which contains a proline residue to increase flexibility and the integrity of both the hydrophobic and hydrophilic domains[16, 18, 19]. MPG (either bound to or free of cargo), has been shown to strongly interact with membrane lipids, and it spontaneously enters the lipid-phase and inserts into natural membranes[16]. Experimental circular

dichroism (CD) and Fourier-transform infrared spectroscopy (FTIR) measurements of MPG show that it adopts a random coil conformation in water and changes its conformation to β-sheet upon interacting with phospholipid vesicles made of a dioleoylphosphatidylcholine (DOPC) or dioleoylphosphatidylglycerol (DOPG) bilayer. The insertion of MPG-bcl-2 oligonucleotide structure into membrane involves a pore like structure upon formation of β-barrel type structure[20]. In this study, partial folding of the carrier peptide into β-sheet structure was observed on interaction with the cargo and on linking with the cargo, a distinct β-sheet folding was seen to be induced by the phospholipids.

Histatins, are histidine-rich peptides, and are secreted by the parotid and submandibular glands. Histatins have both antifungal activity against *C. albicans*[21, 22] and bactericidal effects[23]. The killing process includes the binding of the peptide to the cell membrane of *C. albicans* followed by transport into the cytoplasm. After the entry into the cytoplasm, targeting the mitochondria leads to membrane damage and cell death[14, 24-26]. To exert its fungicidal activity, Hst5 must cross the cell membrane, which is unlike many other antimicrobial peptides, where just membrane disruption is enough[14, 22-27]. This action makes Hst5 act like a CPP.

Translocation of CPPs through a membrane depends on a number of aspects. These include the specific sequences of the CPP, the concentration of CPP and the cell-type[28]. Additionally, the cargo that is fused to the CPP and the placement of the cargo and CPP in a CPP-cargo fusion may influence the method of translocation[29]. The localization of both peptide and cargo depends on experimental conditions and has been

also shown to depend on its sequence and thus most likely on its conformation[20, 30]. In a recent study, short arginine-rich peptide sequences have shown efficient intracellular import properties[31]. Peptides derived from the HIV Tat protein and the Antennapedia homeodomain (Antp) are examples of import sequences[31, 32]. The cargo has an additional role to play on distribution of the conjugate, as shown by PNA-Tat conjugates which were located largely isolated in endocytic vesicles[33]. Efficient cargo uptake is necessary in CPP-mediated therapeutics to deliver diverse cargoes by using various mechanisms to go through the cell's membranes[34].

3.2 Methods and materials

3.2.1 Construction of plasmids

Expression plasmid for Hst5-GFP was created using pET-21(a) (Novagen, Madison, WI, USA). This plasmid has a C-terminal 6XHis tag. A GST fusion partner was amplified from pET-42(a) (Novagen) using the primers BamHI-GST-F and GST-EcoRI-R and introduced into pET-21(a) between the BamHI and EcoRI sites. This resulted in the pNGST plasmid (Figure 3.2). Expression plasmids for GFP and MPG-GFP were made using pET-21(a) (Novagen, Madison, WI, USA).

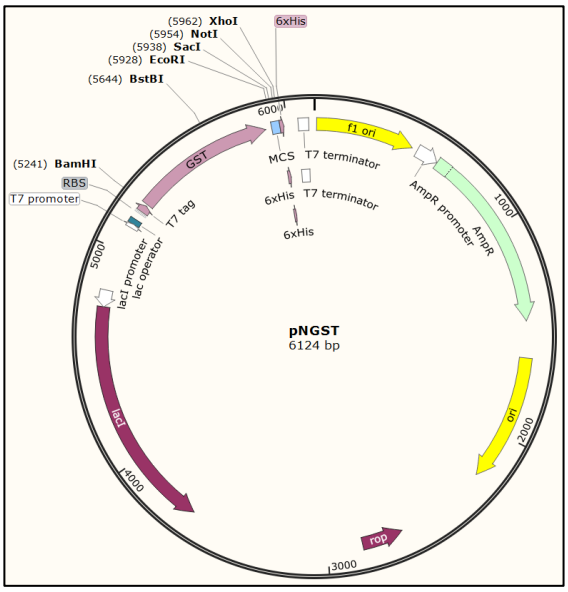

Figure 3.2. Plasmid map of pNGST**.** The pNGST plasmid was created with pET-21(a) as the backbone. GST from the pET-42a vectors was added on the N-terminus to help enhance expression followed by the cut sites for the insertion of the peptides (EcorI and SacI) and the cargoes (SacI and NotI). 6XHis tag is also displayed which has been included in the plasmid design for immobilized metal affinity chromatography.

Table 3.2 Oligonucleotides used in this study

Oligonucleotide sequence name	**Sequence (5' to 3')**	**References**
SacI-ATG-GFP-F	GCGATGGAGCTCAGTAAAGGAGAAGAACTTTTC	[4]
GFP-NotI-R	AATAAAGCGGCCGCTTTGTATAGTTCATCCATGC	[35]
EcorI-FactorXa-MPG-Top1	AATTCATTGAGGGACGCGGCGCACTTTTCTTAGGGTTCCTTGGAGCCGCCGGGAG	[4]
EcorI-FactorXa-MPG-Bottom1	CGGCGGCTCCAAGGAACCCTAAGAAAAGTGCGCCGCGTCCCTCAATG	[4]
SacI-G4S-MPG-Top2	GATGGGTGCCTGGTCCCAGCCAAAGAAGAAACGTAAAGTAGGAGGCGGTGGAAGCGAGCT	[4]

SacI-G4S-MPG-Bottom2	CGCTTCCACCGCCTCCTACTTTACGTTTCTTCTTTGGCTGGGACCAGG	[4]
SacI-G4S-Hst-5-Bottom2	CGCTTCCACCGCCTCCGTACCCGCGATGACTGTGGTGCTTTTCGTG	[4]
SacI-G4S-Hst-5-Top2	CAAGTTCCACGAAAAGCACCACAGTCATCGCGGGTACGGAGGCGGTGGAAGCGAGCT	[4]
EcorI-FactorXa-Hst-5-Bottom1	GAACTTGCGCTTATACCCGTGATGGCGTTTTGCATGAGAATCGCGTCCCTCAATG	[4]
EcorI-FactorXa-Hst-5-Top1	AATTCATTGAGGGACGCGATTCTCATGCAAAACGCCATCACGGGTATAAGCG	[4]
Xa-SynB-top-1	AATTCATTGAGGGACGCCGCGGGGGGCGGCTTAGCTATTCAAGACGGC	[4]
Xa-SynB-bottom-1	GTCTTGAATAGCTAAGCCGCCCCCCGCGGCGTCCCTCAATG	[4]
Xa-SynB-top-2	GGTTCTCCACTTCCACGGGCCGTGAGCT	[4]
Xa-SynB-bottom-2	CACGGCCCGTGGAAGTGGAGAACCGCC	[4]
Xa-SynB-G4S-top	GGTTCTCCACTTCCACGGGCCGTGGAGGCGGTGGAAGCGAGCT	[4]
Xa-SynB-G4S-bottom	CGCTTCCACCGCCTCCACGGCCCGTGGAAGTGGAGAACCGCC	[4]
EcoRI-SynB-F	AATAAGAATTCATGCGCGGGGGGCGGCTTAGCTATTCAAG	[4]
BamHI-GST-F	GCGATGGGATCCATGTCCCCTATACTAGGTTATTG	[4]
GST-EcoRI-R	AATAAAGAATTCACCAGAACCACTAGTTGAAC	[4]
NotI-FLAG-HindIII-F	GGCCGCAGATTACAAGGATGACGACGATAAGA	[4]
NotI-FLAG-HindIII-R	AGCTTCTTATCGTCGTCATCCTTGTAATCTGC	[4]
HindIII-TEV-KpnI-F	AGCTTGAGAACCTGTACTTCCAGGGCGGTAC	[4]
HindIII-TEV-KpnI-R	CGCCCTGGAAGTACAGGTTCTCA	[4]
NotI-Ala-KpnI-GST-F	ATTAGCGGCCGCAGCTGGTACCATGTCCCCTATACTAGGTTATTGG	[4]
GST-XhoI-R	ATTTCTCGAGTTTTGGAGGATGGTCGCCAC	[4]

3.2.2 Construction of CPP-cargo protein fusion constructs

The peptides (MPG and Hst5) were introduced into the pNGST plasmid for expression by using pairs of annealed oligonucleotides that were commercially manufactured (IDT, Skokie, IL, USA). These pairs of oligonucleotides comprised the coding sequence for the CPPs, and the coding sequence for a Factor Xa proteolytic cleavage site (ATTGAGGGACGC). The Factor Xa site was introduced to allow the removal of GST in downstream studies (for constructs that contained GST). Oligonucleotide pairs were annealed to form double-stranded DNA inserts to code for the CPPs and Factor Xa cleavage site with EcoRI and SacI sticky ends for incorporation into pNGST. As an example, the oligonucleotide pairs EcoRI-FactorXa-Hst5-Top1 and EcoRI-FactorXa-Hst5-Bottom1 and the pairs SacI-G_4S-Hst5-Top2 and SacI-G_4S-Hst5-Bottom2 were annealed to form the two dimers that joined to encode for Hst5. These dimers were then introduced between the EcoRI and SacI sites of pNGST (Figure 3.2).

DNA encoding the cargo GFP was PCR-amplified from template plasmids in our laboratory stocks using the oligonucleotides SacI-GFP-F and GFP-NotI-R. The resultant yields were introduced between the SacI and NotI sites of pNGST. Oligonucleotide sequences are given in Table 3.2.

3.2.3 Bacterial strains and protein expression conditions

Subsequent to plasmid construction, all plasmids were transformed into *E. coli* DH5α (Novagen) cells and sequenced. After successful plasmid construction, the plasmids were transformed into *E. coli* BL21 (DE3; Novagen) for protein expression.

Overnight culture of 20 mL for each fusion construct was subcultured into 1000 mL of fresh Luria-Bertani broth (10 mg/mL tryptone, 5 mg/mL yeast extract, and 5 mg/mL NaCl) with ampicillin (100 µg/ml) at an optical density of OD_{600} = 0.05 and was grown at 37 °C for 2.5 h. Isopropyl β-D-1-thiogalactopyranoside (IPTG) was added to each culture aliquot at a final concentration of 0.1 mM to induce the expression of the fusion proteins. The constructs were then incubated at 37 °C for 6 h.

3.2.4 Protein extraction and purification

GFP and CPP-GFP were purified to study translocation into *C. albicans*. The constructs were expressed in *E. coli* BL21 (DE3) cells at 37 °C for 6 h as they were good conditions of expression of constructs in *E. coli*[4]. The cells were harvested by centrifugation and the cells were further lysed using a homogenizer cell disruption system (Avestin). Lysates were pelleted by centrifugation and the supernatants containing soluble fraction of the cell lysates were collected and passed through a 0.2 µm sterile filter to remove cell debris. GST-Hst5-GFP has a Factor Xa enzyme

cleavage site between the GST and the Hst5, so Factor Xa was used to remove GST (Figure 3.4). Following GST removal, the sample was applied to a Profinity Nickel-nitrilotriacetic acid (Ni-NTA) resin column (Bio-Rad) and was eluted using 20 mM sodium phosphate (pH 7.4), 0.5 M potassium chloride, and 500 mM imidazole. Soluble lysate, flow-through, washes and elutes were collected to further run a gel. Coomassie stain was used to estimate the purity of the proteins. MPG-GFP (96 % purity) and GFP were purified using IMAC, similar to Hst5-GFP (90%) using an IMAC column. Both MPG-GFP and GFP lacked a GST on the N-terminus as they were well expressed even without a soluble partner.

3.2.5 Quantification of translocation into *C. albicans*

Translocation of the protein fusions into *C. albicans* cells was measured using flow cytometry. For each sample, 100 µl of protein solution (200 µM) was made in 10 mM sodium phosphate buffer and mixed with 100 µl of *C. albicans* cell suspension containing 5×10^5 cells (in 10 mM sodium phosphate buffer). The cells and fusions were incubated at 30 °C for 1 - 72 h, depending on the experiment. Cells were pelleted by centrifugation at 5,000 x g for 10 min at 4 °C. The cell pellet was then washed with 10 mM sodium phosphate buffer and again pelleted at 5,000 x g for 10 min at 4 °C. The cell pellet was further resuspended in 200 µl of 0.025% (wt/vol) trypsin (Invitrogen, Waltham, MA) and incubated at 37 °C for 30 min to remove surface-bound

proteins[36]. Following trypsin treatment, cells were washed with sodium phosphate buffer and pelleted, and then resuspended in 250 µl of 10 mM phosphate buffer to analyze by flow cytometry. To examine the effect of fusions on the *C. albicans* cells, propidium iodide (PI, 1 mg/ml; Invitrogen) was added at 0.2 mg/ml to each sample immediately before flow cytometry. Cell suspensions were studied for GFP and PI fluorescence using a BD FACSCanto II flow cytometer (BD Biosciences, San Jose, CA). Single cells were chosen for analysis, and the data was analyzed using the FlowJo software (FlowJo, LLC, Ashland, OR). Three separate biological replicates (three sets of each protein from different sources with three different *C. albicans* cell cultures) were used to perform the experiments. was completed using GraphPad Prism (La Jolla, GA, USA). A two-way ANOVA ($\alpha = 0.05$) followed by Tukey's multiple comparisons test was conducted to compare between different constructs (Figure 3.6, 3.7), and the significance of incubation time and on the translocation of various constructs. Summaries of the statistical analyses are provided in the appendices (Appendix A, Table A2 – A4). A p-value of $p < .05$ was considered significant, and the level of significance is indicated in the tables by the number of asterisks (ns for not significant, * for $p < .05$, ** for $p < .01$, *** for $p < .001$, and **** for $p < .0001$).

3.2.6 Measurement of relative fluorescence unit (RFU) using a fluorescent plate reader

GFP, MPG-GFP and Hst5-GFP were purified using a Ni-NTA profinity immobilized metal affinity column by procedure listed in Section 3.2.4 and then concentrated to 200 μM. 110 μl of 200 μM protein samples were loaded a 96-well plate (Corning, NY, USA) and the samples were thoroughly mixed. Serial dilutions (10-fold) were done to get a range of concentrations from 200 μM to 0.02 μM. RFU was measured on SpectraMax M2 plate reader (Molecular Devices, CA, USA) to compare between the proteins. The fluorescence in each well was measured for a wavelength range from 450 nm to 600 nm and the analysis was done at room temperature. Statistical analysis was done using GraphPad Prism (La Jolla, GA, USA). A two-way ANOVA ($\alpha = 0.05$) followed by Tukey's multiple comparisons test was conducted to compare between different constructs. Summaries of the statistical analyses are provided in Appendix A, Table A1. A p-value of $p < .05$ was considered significant, and the level of significance is indicated in the tables by the number of asterisks (ns for not significant, * for $p < .05$, ** for $p < .01$, *** for $p < .001$, and **** for $p < .0001$).

3.2.7 Circular dichroism to study secondary structure of protein fusions

CD spectra were collected for GFP, MPG-GFP and Hst5-GFP at room temperature using a micro-cuvette quartz cell with a 10 mm path length (Fisher Scientific). The CD spectrometer J-810 (Jasco) was set to scanning mode with a 195-300 nm range, 50 nm/min scanning speed, 1 nm bandwidth, and 1.0 nm data pitch. For proteins in solutions, the measurement was performed with 400 µL of 0.5 µM proteins solution in Na_2HPO_4 buffer. The signal was converted to molar ellipticity $[\theta]$ using

$$[\theta] = \frac{100 \times \theta}{C \times l} \qquad \text{(Equation 4.1)}$$

where, θ is the ellipticity in degrees, C is the molar concentration, and l is the quartz cell pathlength.

3.2.8 Simulation method to study translocation of peptides

The membrane was modeled by Jeffery Klauda and Mahdi Ghorbani with the highly mobile membrane-mimetic[3] (HMMM) model. This model had its membrane core was replaced with an organic solvent and short tailed lipids were used as headgroups. This was done to enhance the lipid dynamics while conserving atomistic detail of protein-lipid interaction. In HMMM model, a lipid area scaling factor of 1.2 was used along with a 6-carbon lipid chain model. Temperature was set at 298K. This system closely mimicked a yeast plasma membrane composition as described below (Table 3.3) and

consists of 150 lipid per leaflet. Each study was run for 300ns using NAMD with a time step of 2 fs. After 300ns the CHARMM server was used to translate the HMMM model to a full membrane model and the simulation was run for additional 100ns.

Table 3.3. Membrane lipid components from yeast membrane

Lipid	**PM**
ERG	60
YOPA	7
DYPC	18
POPE	20
POPI	18
POPS	27
Lipids per leaflet	150

3.3 Results and discussion

We produced CPP-cargo fusions (Figure 3.3) recombinantly in *E. coli.* The genetic fusions of CPPs to protein cargoes were linked covalently via a flexible glycine serine linker[4, 35]. Glutathione S-transferase (GST), a soluble partner, was added to the N-terminus of the construct to enhance production[37, 38]. A Factor Xa cleavage (ATTGAGGGACGC) site was added between the soluble partner and the CPP. This cleavage site would allow for the removal of GST before purification. We evaluated the expression of combinations of SynB, Hst5, and their fusions to biotin carboxyl carrier protein (BCCP), green fluorescent protein (GFP) and maltose binding protein (MBP)[4]. We observed that both the CPP and the cargo protein affected expression, and expression at 37°C for 6 or 10 h led to the highest level of expression for most fusion

proteins[4]. These results allowed improved production of the constructs considered and are a promising starting point for the expression of new CPP-cargo fusions. We further chose Hst5 and MPG as our CPPs, which have already shown the translocation into different cell types. In this study, we used green fluorescent protein (GFP) as our cargo. GFP is a protein with 238 amino acid residues (26.9 kDa) that absorbs blue light at 395 nm and exhibits bright green fluorescence at 509 nm[39, 40]. The green fluorescence is stable and almost no photo bleaching is seen[40]. This protein has been selected due to its fluorescence property, which will help us to study the translocation into cells when it is fused to an appropriate CPP. At the same time, since it is bigger in size compared to BCCP but smaller than MBP, it is an appropriate size to study effect of size on translocation.

Figure 3.3. Representation of GST-CPP-cargo protein fusion construct. CPPs are linked to the protein cargos via a G_4S peptide linker. GST was included on the N-terminus, as an expression partner to improve expression, and a 6XHis tag was incorporated on the C-terminus for detection of construct expression. A Factor Xa cleavage site was attached between GST and CPP to allow for removal of the GST in downstream processes. The genetic construct that encodes for the fusion proteins was designed with restriction enzyme sites that flanked the CPP and cargo protein to help the insertion of different CPPs and cargos.

3.3.1 Detection of fusions inside *Candida albicans* cells

GFP and CPP-GFP were purified to study translocation into *C. albicans*. The constructs were expressed in *E. coli* BL21 (DE3) cells at 37 °C for 6 h as they were good conditions of expression of constructs in *E. coli*[4]. Following cell lysis and extraction of the proteins GFP, MPG-GFP and Hst5-GFP were purified using IMAC.

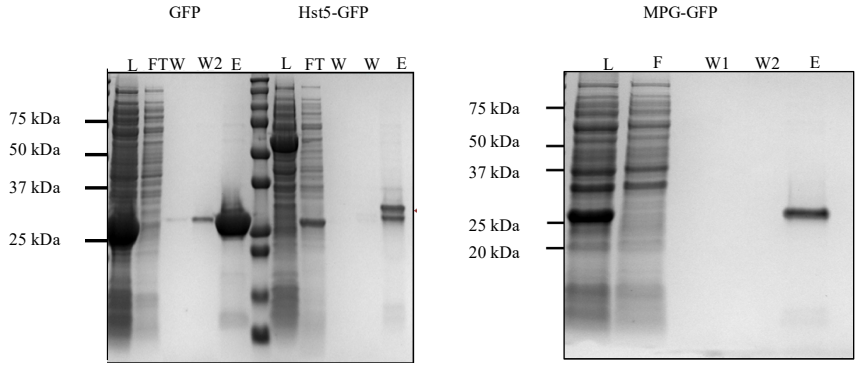

Figure 3.4. Purification of GFP, Hst5-GFP and MPG-GFP. CPP fused to GFP and unconjugated GFP were expressed in BL21 (DE3) cells at 37 C for 6 h with 0.01 mM IPTG. GST was removed prior to purification. Coomassie stain was used to estimate the purity of fusion proteins. Crude soluble lysates (L), flowthrough (FT), washes (W1, W2) and elution (E) from immobilized metal affinity chromatography are shown. Cleavage with Factor Xa to remove GST from Hst5-GFP was done before purification (A). MPG-GFP was purified using IMAC (B). The crude soluble lysate contains the whole construct; flow through does not bind to the column and so flows through; elutes are obtained using a gradient of 50% imidazole. Molecular weight: GFP = 27 kDa, Hst5-GFP = 30.1 kDa, MPG-GFP = 30.5 kDa.

Subsequent to purification, we studied the intracellular delivery of the purified proteins into the fungal pathogen *C. albicans*. To evaluate the CPPs for translocation into *Candida* species, *C. albicans* strain SC5314 was incubated with Hst5-GFP, MPG-GFP and GFP lacking a CPP. We studied and quantified translocation of the proteins using flow cytometry (Figure 3.5). Single *C. albicans* cells were chosen, and the

percentage of fluorescence-positive (GFP-positive) cells was used to evaluate the GFP delivery efficacy. The protein fusions were incubated with trypsin for different times over a range of time points that ranged from 0 mins, 5 mins, 15 mins, 30 mins, 45 mins and 60 mins out of which 30 mins represented the best time for incubation.

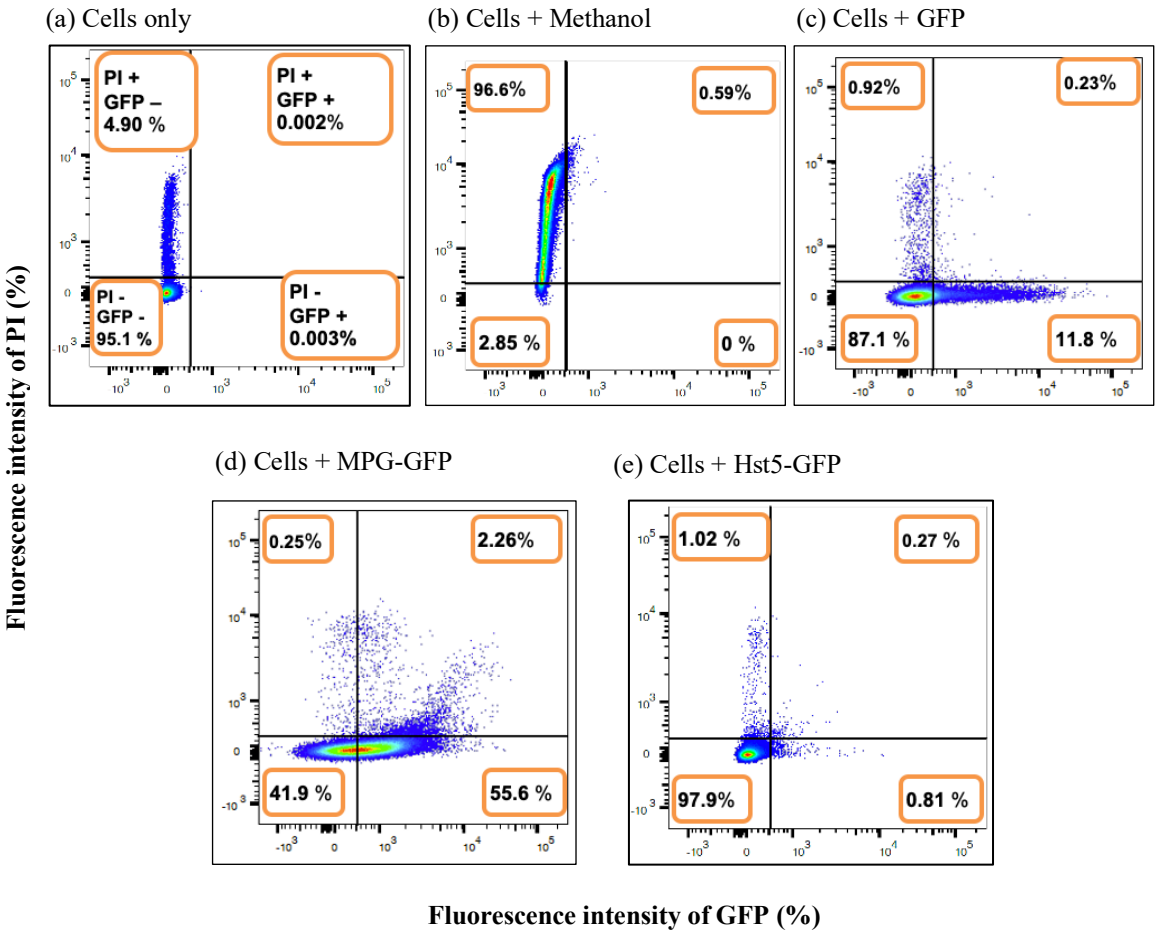

Figure 3.5. Translocation of proteins. Flow cytometry was used to quantify translocation and membrane permeabilization in *C. albicans* for (a) cells incubated with buffer only and PI, (b) cells incubated with methanol (c) cells incubated with GFP and PI, (d) cells incubated with MPG-GFP and PI, and (e) cells incubated with Hst5-GFP and PI. The translocation studies were done for multiple replicates but a, b, c, d and e are a representative set of data. Only single cells were selected for analysis. In each plot, quadrant Q1 represents cell that are PI +/GFP -, Q2 represents those that are PI +/GFP +, Q3 represents those that are PI -/GFP +, and Q4 represents those that are PI -/GFP -. The numbers under each quadrant label provide the percentage of cells in the experiment that fall into each quadrant. The quadrant boundaries were chosen with cells only. Each cell in the sample is represented by a dot, and the color on the dot plots indicate the density of cells (red represents high density and blue represents low density).

About 40% of the fungal cells exhibited a green fluorescence signal (Figure 3.6, 3.7) when treated with a final concentration of 100 µM purified GFP (Figure 3.5 (c)), MPG-GFP (Figure 3.5 (d)) and Hst5-GFP (Figure 3.5 (e)). (This concentration reflects the

total protein concentration of the sample and does not take the purity into consideration). MPG-GFP showed significantly higher translocation as compared to both GFP and Hst5-GFP ($p \leq 0.001$ and $p \leq 0.0001$, respectively) (Figure 3.7). To further investigate the effect of the fusion proteins on *C. albicans*, we evaluated the permeability of the cells using PI. Cells are usually impermeable to PI, but PI fluorescence can be found inside cells with destabilized membranes. Destabilization can occur either due to cell death or due to pore formation on the membrane[41, 42.] Our results show that there is significantly low, <2% PI-positive cells following incubation with MPG-GFP and Hst5-GFP, indicating the fusion protein does not significantly affect the membrane integrity. This was analogous to the level of toxicity of GFP alone (Figure 3.7 b).

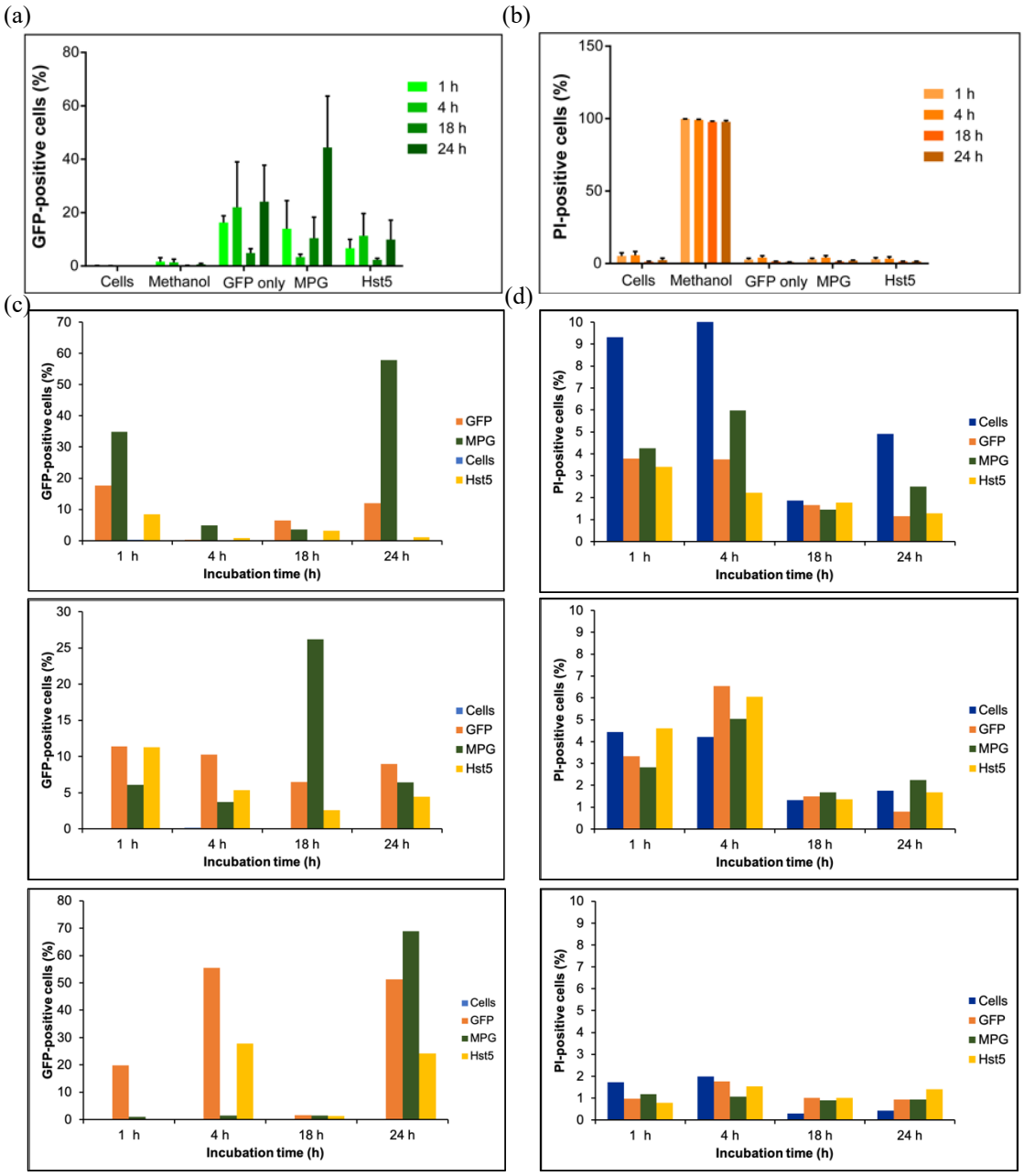

Figure 3.6. Translocation studies data for 1 h – 24 h. Flow cytometry was used to quantify translocation and membrane permeabilization in *C. albicans*. Single *C. albicans* cells were selected, and the percentage of fluorescence-positive cells was used to evaluate the GFP delivery efficacy. The permeability of the cells was evaluated after treatment with the fusion protein using propidium iodide (PI). (a) Cells were incubated with the fusions for 1 h, 4 h, 18 h and 24 h to select the best incubation time. 24 h showed significantly higher translocation compared to the others (b) Propidium iodide uptake for the same times were recorded with no significant uptake of PI (c, d) Raw data for each replicate (c) GFP positive and (d) PI positive with no methanol, to compare between different purified samples and their effect on translocation Error bars represent standard error mean of 3 replicates for figures (a, b). Refer to Appendix A, Table A2, A3 for detailed statistical analysis.

Figures 3.6 (c) and (d) represent the data for each replicate, which shows the contribution of a single replicate to translocation. Each replicate represents three different batches of purified protein samples which were incubated with three separate cell cultures. As seen from Figure 3.6 (c), replicates 1 and 3 behave similarly and show >50% GFP positive cells at 24 h whereas replicate 2 has higher translocation at 18 h. This points to either an issue with the purified protein in replicate 2 or with the cells cultured. From these data we can learn that translocation is heavily dependent on each data set and the average of data sets might not always represent the correct measurable quantity.

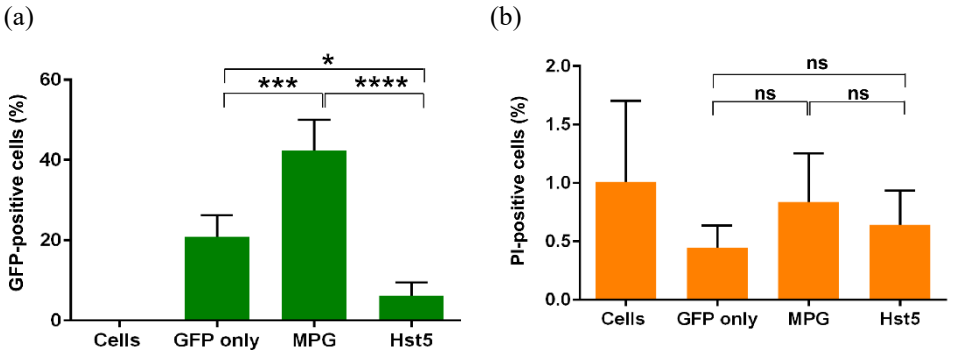

Figure 3.7. Cellular uptake studies. The flow cytometry data for 24 h incubation samples were analyzed further for 7 replicates to quantify the translocation and membrane permeabilization in *C. albicans*. The percentage of fluorescence-positive cells was used to evaluate the GFP delivery efficacy. The permeability of the cells was evaluated after treatment with the fusion protein using propidium iodide (PI). (a) Translocation data at 24 h for 7 replicates showed significantly higher uptake of MPG-GFP compared to both GFP and Hst5-GFP (b) Propidium iodide uptake for the same times were recorded with no significant uptake of PI. Error bars represent standard error of the mean for 7 replicates for panels (a, b). Refer to Appendix A, Table A4 for detailed statistical analysis.

Another fact to consider is the translocation of GFP only. GFP usually does not translocate into cells but further studies might be needed to evaluate the reasons for translocation of GFP without a CPP. Although trypsin treatment was done to remove

surface-bound proteins, it might not have been effective in removing all of the GFP and alternate approaches can be used for example fluorescence quenching groups[43]. One thing to note for the experiments outlined above is that these were done based on mass of sample and differences in purity and fluorescence activity of GFP could affect results.

As discussed previously, MPG enters cells by formation of a pore. This is consistent with the results of this study too, where MPG likely delivers GFP by making a pore without causing cell death. The pore is repaired, and, thus, we do not detect any PI fluorescence, since PI can be detected only when membranes are destabilized due to pore formation or cell death.

3.3.2 Fluorescence intensity measurements of purified GFP, MPG-GFP and Hst5-GFP

To understand if the difference in translocation of purified proteins is due to the fluorescence activity of each fluorescent molecule, we used a fluorescent plate reader (SpectraMax M2) to measure the relative fluorescent units of GFP, Hst5-GFP and MPG-GFP (Figure 3.8).

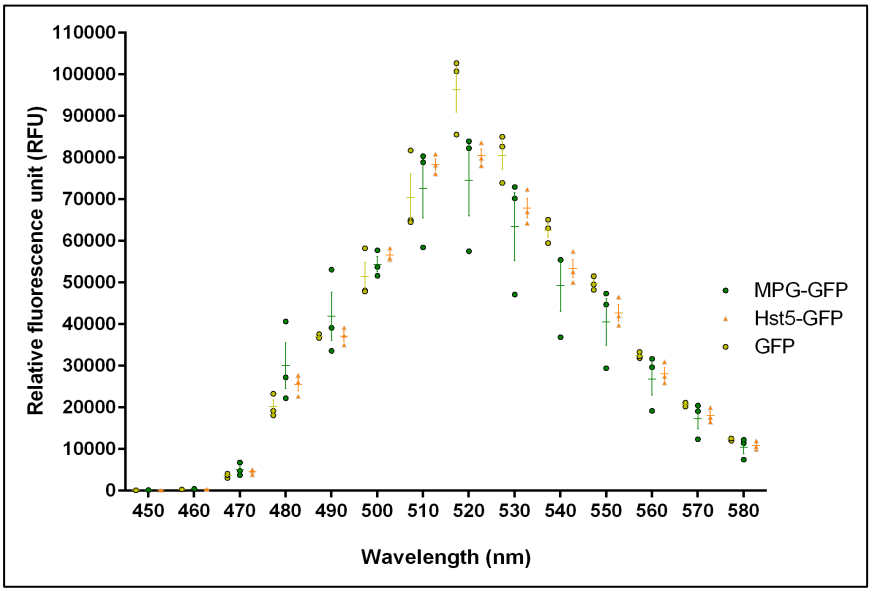

Figure 3.8. Measurement of relative fluorescence unit (RFU). The fluorescence intensity data for 200 µM of GFP, MPG-GFP and Hst5-GFP were analyzed to compare between the fluorescence activities. (a) Scattered dot plot of representing RFU's at different wavelengths for GFP, MPG-GFP and Hst5-GFP. Error bars represent standard error of the mean of 3 biological replicates. Refer to the appendix A, Table A1 for detailed statistical analysis.

The analysis showed that at the same conditions of mass concentration and temperature, the constructs had comparable fluorescence intensity at the lower wavelengths. However, at higher wavelengths, for example, 520 nm there was a significantly higher fluorescence intensity of GFP as compared to MPG-GFP and Hst5-GFP ($p \leq 0.0001$ and $p \leq 0.01$, respectively). GFP has an emission spectrum at 509 nm and these results at 520 nm molecules show that effectively GFP molecules are fluorescently more active than either MPG-GFP (purity 96%) or Hst5-GFP (purity 90%) at a concentration of 200 µM. Given that the purities of each protein are different, fluorescence activity could be affected. This result in turn can be compared to the

translocation data presented in Section 3.3.2. The difference in fluorescence activity could better explain the limited fluorescence signal observed in flow cytometry (GFP positive cells), for MPG-GFP and correlated to the translocation results.

3.3.3 Simulation results to better understand experimental data

To better understand the molecular interactions between the CPPs and the cell membrane, Jeffery Klauda and Mahdi Ghorbani to ran multiple simulations on the peptides MPG and Hst5 using a HMMM[3] model. Simulations included the peptides only and not the fusion construct as whole, as we anticipate that any changes in the peptide will help to enhance translocation. Also, addition of the cargo would make the simulation calculations computationally expensive. The structure of the peptides was predicted to be α-helical in aqueous phase using a peptide structure prediction webserver (PEPFOLD3)[44]. The HMMM model (Figure 3.9) closely mimicked a yeast model to help us study the interaction between CPPs and the membrane.

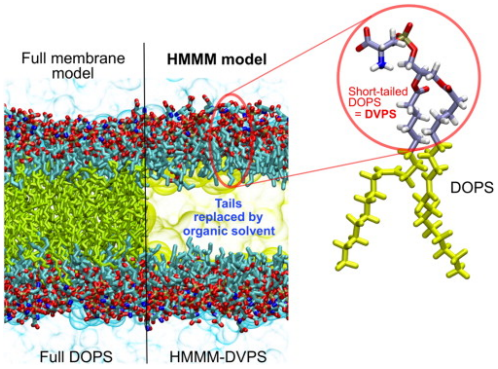

Figure 3.9. Comparison of full-membrane model and HMMM model. In a HMMM model, yellow acyl tails (sticks) of the lipids is substituted by an organic solvent (yellow area in HMMM model representation). In this paper, a full DOPS lipid molecule (inset) was denoted by a short-tailed DVPS molecule (circled part of the molecule). Red: oxygen atoms, Blue: nitrogen, Gold: phosphorus, and Ice blue: carbon (except the C6–C18 in yellow), Light blue: bulk water molecules. Figure taken from Ohkubo et al. Accelerating Membrane Insertion of Peripheral Proteins with a Novel Membrane Mimetic Model[7]. *Copyright © 2012 Biophysical Society*. Published by Elsevier Inc.

Bias in the system was avoided using three different orientation with respect to membrane plane. Each run was for 300ns and we saw the insertion of MPG into the membrane after 300ns whereas Hst5 failed to insert into the membrane (Figure 3.10). After 300 ns, the distances of each residue were measured from the membrane plane (Figure 3.11) to help understand the contribution of each residue to translocation.

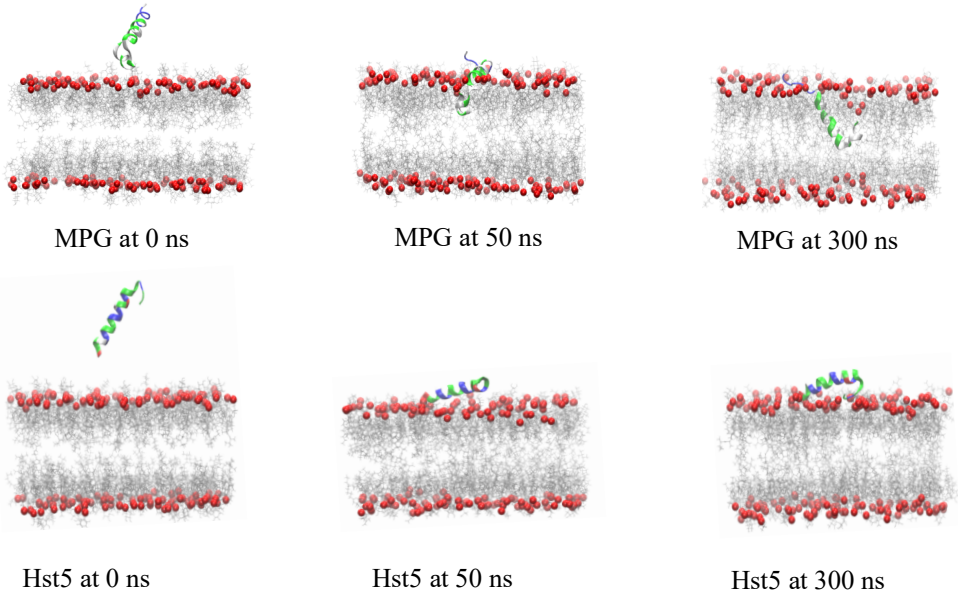

Figure 3.10. Translocation of CPPs using HMMM membrane model at various time points. MPG inserts after 300 ns into the membrane whereas Hst5 does not go in even after 300 ns (Data courtesy of Dr. Jeffery Klauda and Mahdi Ghorbani).

As seen in figure 3.10, MPG enters the membrane through its hydrophobic N-terminus (blue color representation in heat map in Figure 3.10 (a)) whereas Hst5 fails to enter the membrane. The hydrophobic end of MPG helps in insertion, while much of the charged residues are farther away from the plane. Our experimental construct design has GFP attached to the C-terminus and the simulation results support our experimental results which show MPG can deliver a biomolecular cargo, which is fused at the peptide's C-terminus. As mentioned above, MPG probably employs pore formation to enter the cell membrane. On the other hand, Hst5 is highly charged and has charge distributed all through the sequence. The positively-charged peptide thus sticks to the membrane and this electrostatic interaction prevents insertion into the

membrane.

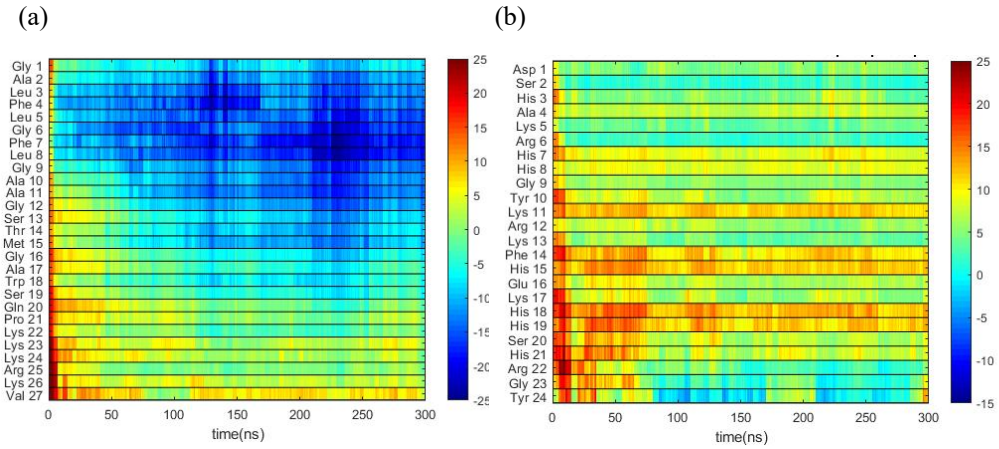

Figure 3.11. Insertion of peptides into the model membrane. The distance of each residue from the membrane plane was measured. (a) Distance of MPG residues after 300 ns into the membrane (b) Distance of Hst5 residues after 300 ns into the membrane (Collaborators: Dr. Jeffery Klauda and Mahdi Ghorbani; picture courtesy: Mahdi Ghorbani).

These data show that both experiments and simulations can be used in collaboration to study the translocation of peptides into membranes. The consistent results obtained from both simulation and experiments, show that simulation can be used as a useful tool in designing better experiments. We will need further studies to use simulations to design better peptides that can enhance translocation.

3.3.4 Secondary structure of proteins

We further wanted to know the contribution of the peptide or the protein on the secondary structure. Studies have been done to analyze the structure of CPPs but not much is known about structures of peptide-cargo fusions. To explain for this

complexity, we evaluated the secondary structure of CPP-cargo fusion by using CD (Figure 3.12). The baseline CD spectrum for buffer was subtracted from spectra of GFP and the CPP-GFP fusions.

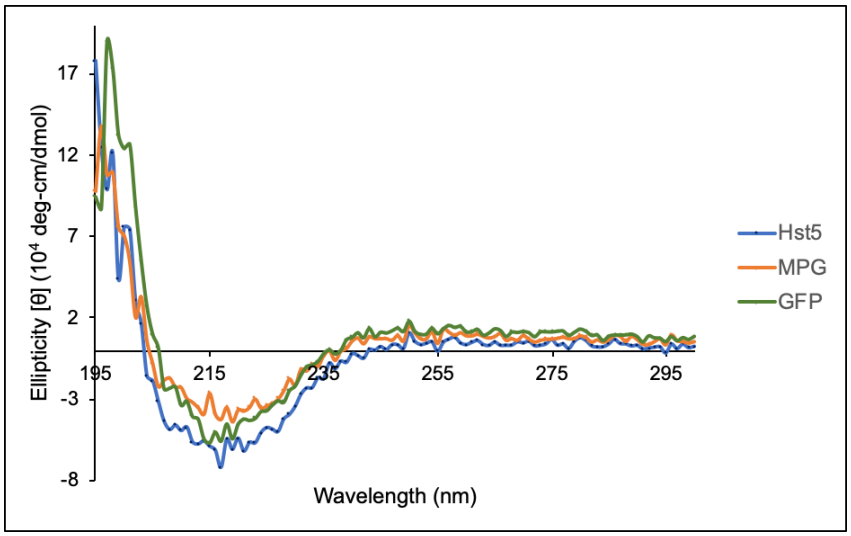

Figure 3.12. CD spectra of CPPs (0.5 µM) in sodium phosphate buffer. GFP (green), MPG-GFP (orange) and Hst5-GFP (blue) were suspended in pure buffer (10 mM Na_2HPO_4).

We report our results in ellipticity (θ x10^4 deg-cm^2/dmol). Due to substantial noise at far-UV range, which could be attributed to high absorbance, we used a lower protein concentration of 0.5 µM. Buffer alone spectra was subtracted from each spectrum for each peptide. MPG alone has a characteristic random coil structure[45] but the proteins in this experiment showed a ß-sheet conformation which is characteristic of GFP.

Further experiments with cells will provide knowledge on the conformation of fusions when the proteins are combined with the *C. albicans* cells. Studies of CPP-membrane interactions with model lipid vesicles and structure information using CD,

fail to consider the complexity of the cell matrix[46, 47]. Gong et al. evaluated the interaction between peptides and *C. albicans* cells by using CD[48]. Some peptides maintained their structures while others did not for example, peptides like MPG and penetratin maintained their random coil structure whereas MAP and cecropin B shifted to α-helical structure from random coil. Experiments of protein fusions with *Candida* will provide better knowledge of secondary structure of fusions that can help understand translocation.

3.3.5 Design of MPG variants to increase translocation

MPG can deliver biomolecular cargo, GFP into *C. albicans* with very little killing (Section 3.3.1). These results encourage the extension of the study towards residue substitutions. For an improved understanding on the behavior of the residues and their contribution towards translocation, we collaborated with Dr. Jeffery Klauda and his lab and calculated the interaction energy of each residues of native MPG with the membrane (Figure 3.13). We calculated the distance of each residue from the top membrane plane of the model membrane. The interaction energies helped us to identify residues that do not contribute to translocation of the peptide into the membrane, and modifying which could help increase translocation. These studies include MPG only and not the fusion construct. We assume that the peptide improvements will help

enhance translocation and presence of the cargo would make the computations expensive.

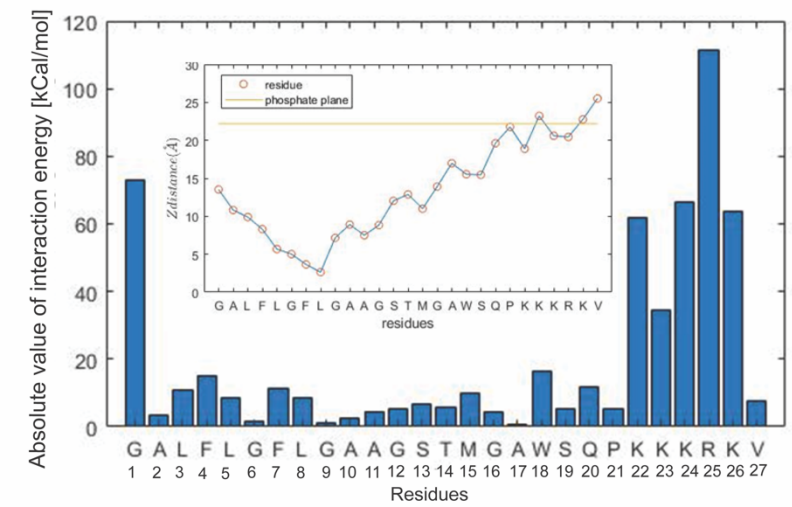

Figure 3.13. Interaction energies of MPG (native) residues. Interaction energy (kCal/mol) of each residue of MPG from the phosphate plane of a yeast model membrane and the distance (A°) of each residue (inset) from the yeast membrane.

MPG enters the membrane model from its hydrophobic end (Figure 3.13). The residues S13 and T14 are both hydrophilic uncharged residues that do not appear to contribute to translocation, and we propose to modify them to residues lysine (K) and arginine (R), which are charged hydrophilic groups. Inclusion of these residues' in the mid-region will help the attachment of the peptide to the membrane and transport of the peptide to the other side. CPPs in general tend to have charges in the mid-region of the sequences[9], and, thus, altering the mid-region residues to hydrophilic charged residues would aid in increasing translocation. Arg and Lys will help preserve the hydrophilic nature at the respective sites.

Charged residues at the C-terminus stick to the membrane and do not enter the membrane. Although these charges possibly help attachment of the peptide to the

membrane, MPG-GFP with GFP attached at the C-terminus of MPG, needs to enter the cells. Altering the charged residues to hydrophobic residues is likely to help and introduction of W19 in place of S19 could show the effect of this mutation on translocation.

3.4 Conclusion

We are using peptides to design alternate drug delivery systems to translocate cargo into the fungal pathogen *C. albicans.* We were able to study peptides that selectively translocated into *C. albicans* and were able to quantify delivery of a biomolecular cargo. The 3-fold increase in translocation with MPG showed promising results and moving forward we would like to use the both simulations and experiments to design better peptides to enhance translocation. The knowledge gained from this study will enable the design of an alternate functional drug delivery vehicle to treat fungal infections. These results show that MPG can be used to deliver GFP. We need to understand if increasing the concentration of the fusion or modifying the residues of the CPPs can improve results. To understand how the peptide-cargo fusions are translocated and any intracellular effect of the cargo and the CPP, further studies will need to be done. Additionally, we believe similar studies with other CPPs or cargoes will help better understand the capabilities and limitations of CPP-cargo fusions in delivering cargo to fungal cells. Simulations have helped design new CPPs and

studying these altered CPPs and their fusions could help understand translocation and related mechanisms better.

3.5 References

1. Braun, B. R.; Johnson, A. D., Control of filament formation in Candida albicans by the transcriptional repressor TUP1. *Science* **1997,** *277* (5322), 105-9.
2. Peter G. Pappas; Carol A. Kauffman; David R. Andes; Cornelius J. Clancy; Kieren A. Marr; Luis Ostrosky-Zeichner; Annette C. Reboli; Mindy G. Schuster; Jose A. Vazquez; Thomas J. Walsh; and, T. E. Z.; Sobel, J. D., Clinical Practice Guideline for the Management of Candidiasis: 2016 Update by the Infectious Diseases Society of America. *Clinical Infectious Diseases* **2016,** *62*.
3. Ohkubo, Y. Z.; Pogorelov, T. V.; Arcario, M. J.; Christensen, G. A.; Tajkhorshid, E., Accelerating membrane insertion of peripheral proteins with a novel membrane mimetic model. *Biophys J* **2012,** *102* (9), 2130-9.
4. Adhikari, S.; Alahmadi, T. I.; Gong, Z.; Karlsson, A. J., Expression of Cell-Penetrating Peptides Fused to Protein Cargo. *J Mol Microbiol Biotechnol* **2018,** *28* (4), 159-168.
5. Sawaya, B. P.; Briggs, J. P.; Schnermann, J., Amphotericin B nephrotoxicity: The adverse consequences of altered membrane properties. *J Am Soc Nephrol* **1995,** *6* (2), 154-64.
6. Antibiotic resistance threats in the United States, 2019. **2019**.
7. Derossi, D.; Joliot, A. H.; Chassaing, G.; Prochiantz, A., The 3rd helix of the antennapedia homeodomain translocates through biological-membranes. *Journal of Biological Chemistry* **1994,** *269* (14), 10444-10450.
8. Frankel, A. D.; Pabo, C. O., Cellular uptake of the TAT protein from human immunodeficiency virus. *Cell* **1988,** *55* (6), 1189-93.
9. Ramaker, K.; Henkel, M.; Krause, T.; Rockendorf, N.; Frey, A., Cell penetrating peptides: a comparative transport analysis for 474 sequence motifs. *Drug Deliv* **2018,** *25* (1), 928-937.
10. Esposito, D.; Chatterjee, D. K., Enhancement of soluble protein expression through the use of fusion tags. *Curr Opin Biotechnol* **2006,** *17* (4), 353-8.
11. Green, M.; Loewenstein, P. M., Autonomous functional domains of chemically synthesized human immunodeficiency virus TAT trans-activator protein. *Cell* **1988,** *55* (6), 1179-88.
12. Morris, M. C.; Vidal, P.; Chaloin, L.; Heitz, F.; Divita, G., A new peptide vector for efficient delivery of oligonucleotides into mammalian cells. *Nucleic Acids Res* **1997,** *25* (14), 2730-2736.
13. Simeoni, F., Insight into the mechanism of the peptide-based gene delivery system MPG: implications for delivery of siRNA into mammalian cells. *Nucleic Acids Res* **2003,** *31* (11), 2717-2724.
14. Mochon, A. B.; Liu, H., The antimicrobial peptide histatin-5 causes a spatially restricted disruption on the *Candida albicans* surface, allowing rapid entry of the peptide into the cytoplasm. *PLoS Pathog* **2008,** *4* (10), e1000190.

15. Kwon, S. J.; Han, K.; Jung, S.; Lee, J. E.; Park, S.; Cheon, Y. P.; Lim, H. J., Transduction of the MPG-tagged fusion protein into mammalian cells and oocytes depends on amiloride-sensitive endocytic pathway. *BMC Biotechnol* **2009,** *9* (1), 73.
16. Morris, M. C.; Deshayes, S.; Heitz, F.; Divita, G., Cell-penetrating peptides: from molecular mechanisms to therapeutics. *Biol Cell* **2008,** *100* (4), 201-17.
17. Jang, W. S.; Bajwa, J. S.; Sun, J. N.; Edgerton, M., Salivary histatin 5 internalization by translocation, but not endocytosis, is required for fungicidal activity in Candida albicans. *Mol Microbiol* **2010,** *77* (2), 354-70.
18. Adhikari, S., Optimization of recombinant protein expression for cell-penetrating peptide fusions to protein cargo. **2017**.
19. Deshayes, S.; Decaffmeyer, M.; Brasseur, R.; Thomas, A., Structural polymorphism of two CPP: an important parameter of activity. *Biochim Biophys Acta* **2008,** *1778* (5), 1197-205.
20. Deshayes, S.; Gerbal-Chaloin, S.; Morris, M. C.; Aldrian-Herrada, G.; Charnet, P.; Divita, G.; Heitz, F., On the mechanism of non-endosomial peptide-mediated cellular delivery of nucleic acids. *Biochim Biophys Acta* **2004,** *1667* (2), 141-7.
21. Oppenheim, F. G.; Xu, T.; McMillian, F. M.; Levitz, S. M.; Diamond, R. D.; Offner, G. D.; Troxler, R. F., Histatins, a novel family of histidine-rich proteins in human parotid secretion. Isolation, characterization, primary structure, and fungistatic effects on Candida albicans. *J Biol Chem* **1988,** *263* (16), 7472-7.
22. Puri, S.; Edgerton, M., How does it kill?: understanding the candidacidal mechanism of salivary histatin 5. *Eukaryot Cell* **2014,** *13* (8), 958-64.
23. Du, H.; Puri, S.; McCall, A.; Norris, H. L.; Russo, T.; Edgerton, M., Human salivary protein histatin 5 has potent bactericidal activity against ESKAPE pathogens. *Front Cell Infect Microbiol* **2017,** *7*, 41.
24. Khan, S. A.; Fidel, P. L., Jr.; Thunayyan, A. A.; Varlotta, S.; Meiller, T. F.; Jabra-Rizk, M. A., Impaired Histatin-5 Levels and Salivary Antimicrobial Activity against C. albicans in HIV Infected Individuals. *J AIDS Clin Res* **2013,** *4* (193).
25. Jang, W. S.; Li, X. S.; Sun, J. N.; Edgerton, M., The P-113 fragment of histatin 5 requires a specific peptide sequence for intracellular translocation in Candida albicans, which is independent of cell wall binding. *Antimicrob Agents Chemother* **2008,** *52* (2), 497-504.
26. Dong, J.; Vylkova, S.; Li, X. S.; Edgerton, M., Calcium blocks fungicidal activity of human salivary histatin 5 through disruption of binding with Candida albicans. *J Dent Res* **2003,** *82* (9), 748-52.
27. Helmerhorst, E. J.; Breeuwer, P.; van't Hof, W.; Walgreen-Weterings, E.; Oomen, L. C.; Veerman, E. C.; Amerongen, A. V.; Abee, T., The cellular target of histatin 5 on *Candida albicans* is the energized mitochondrion. *J Biol Chem* **1999,** *274* (11), 7286-91.
28. Kristensen, M.; Birch, D.; Morck Nielsen, H., Applications and challenges for use of cell-penetrating peptides as delivery vectors for peptide and protein cargos. *Int J Mol Sci* **2016,** *17* (2).

29. Shin, M. C.; Zhang, J.; Min, K. A.; Lee, K.; Byun, Y.; David, A. E.; He, H.; Yang, V. C., Cell-penetrating peptides: achievements and challenges in application for cancer treatment. *Journal of biomedical materials research. Part A* **2014,** *102* (2), 575-587.
30. Dom, G.; Shaw-Jackson, C.; Matis, C.; Bouffioux, O.; Picard, J. J.; Prochiantz, A.; Mingeot-Leclercq, M. P.; Brasseur, R.; Rezsohazy, R., Cellular uptake of Antennapedia Penetratin peptides is a two-step process in which phase transfer precedes a tryptophan-dependent translocation. *Nucleic Acids Res* **2003,** *31* (2), 556-561.
31. Gariépy, J.; Kawamura, K., Vectorial delivery of macromolecules into cells using peptide-based vehicles. *Trends in Biotechnology* **2001,** *19* (1), 21-28.
32. Schwarze, S. R.; Ho, A.; Vocero-Akbani, A.; Dowdy, S. F., In vivo protein transduction: delivery of a biologically active protein into the mouse. *Science* **1999,** *285* (5433), 1569-72.
33. Koppelhus, U.; Nielsen, P. E., Antisense properties of peptide nucleic acid In *Antisense Drug Technology*
*(*Crooke, S. T., ed, Marcel Dekker, New York: 2001; pp 359–374.
34. Milech, N.; Longville, B. A.; Cunningham, P. T.; Scobie, M. N.; Bogdawa, H. M.; Winslow, S.; Anastasas, M.; Connor, T.; Ong, F.; Stone, S. R.; Kerfoot, M.; Heinrich, T.; Kroeger, K. M.; Tan, Y. F.; Hoffmann, K.; Thomas, W. R.; Watt, P. M.; Hopkins, R. M., GFP-complementation assay to detect functional CPP and protein delivery into living cells. *Sci Rep* **2015,** *5*, 18329.
35. Gong, Z.; Walls, M. T.; Karley, A. N.; Karlsson, A. J., Effect of a flexible linker on recombinant expression of cell-penetrating peptide fusion proteins and their translocation into fungal cells. *Mol Biotechnol* **2016,** *58* (12), 838-849.
36. Richard, J. P.; Melikov, K.; Vives, E.; Ramos, C.; Verbeure; B.; Gait, M. J.; Chernomordik, L. V., and; Lebleu, B., Cell-penetrating peptides: a re-evaluation of the mechanism of cellular uptake. *The Journal Of Biological Chemistry* **2003,** *278* (1), 585–590.
37. Smith, D. B.; Johnson, K. S., Single-Step Purification of Polypeptides Expressed in Escherichia-Coli as Fusions with Glutathione S-Transferase. *Gene* **1988,** *67* (1), 31-40.
38. Smith, D. B., Generating fusions to glutathione S-transferase for protein studies. *Methods Enzymol* **2000,** *326*, 254-70.
39. Ormo, M.; Cubitt, A. B.; Kallio, K.; Gross, L. A.; Tsien, R. Y.; Remington, S. J., Crystal structure of the *Aequorea victoria* green fluorescent protein. *Science* **1996,** *273* (5280), 1392-5.
40. Tsien, R. Y., The green fluorescent protein. *Annu Rev Biochem* **1998,** *67*, 509-44.
41. Nicoletti, I.; Migliorati, G.; Pagliacci, M. C.; Grignani, F.; Riccardi, C., A rapid and simple method for measuring thymocyte apoptosis by propidium iodide staining and flow cytometry. *Journal of Immunological Methods* **1991,** *139* (2), 271-279.

42. Riccardi, C.; Nicoletti, I., Analysis of apoptosis by propidium iodide staining and flow cytometry. *Nat Protoc* **2006,** *1* (3), 1458-61.
43. Richard, J. P.; Melikov, K.; Vives, E.; Ramos, C.; Verbeure, B.; Gait, M. J.; Chernomordik, L. V.; Lebleu, B., Cell-penetrating Peptides: A reevaluation of the mechanism of cellular uptake. *Journal of Biological Chemistry* **2003,** *278* (1), 585-590.
44. Shen, Y.; Maupetit, J.; Derreumaux, P.; Tufféry, P., Improved PEP-FOLD Approach for Peptide and Miniprotein Structure Prediction. *Journal of Chemical Theory and Computation* **2014,** *10* (10), 4745-4758.
45. Gong, Z.; Doolin, M. T.; Adhikari, S.; Stroka, K. M.; Karlsson, A. J., Role of charge and hydrophobicity in translocation of cell-penetrating peptides into Candida albicans cells. *AIChE Journal* **2019,** *65* (12).
46. Avitabile, C.; D'Andrea, L. D.; Romanelli, A., Circular Dichroism studies on the interactions of antimicrobial peptides with bacterial cells. *Scientific reports* **2014,** *4*, 4293-4293.
47. Malgieri, G.; Avitabile, C.; Palmieri, M.; D'Andrea, L. D.; Isernia, C.; Romanelli, A.; Fattorusso, R., Structural Basis of a Temporin 1b Analogue Antimicrobial Activity against Gram Negative Bacteria Determined by CD and NMR Techniques in Cellular Environment. *ACS Chem Biol* **2015,** *10* (4), 965-969.
48. Gong, Z.; Ikonomova, S. P.; Karlsson, A. J., Secondary structure of cell-penetrating peptides during interaction with fungal cells. *Protein Sci* **2018,** *27* (3), 702-713.

Chapter 4: Design CPP variants for translocation of CPP-cargo protein fusions into *Candida albicans* cells

In the previous chapter, we were successfully able to deliver a biomolecular cargo in *C. albicans cells*. Simulations and experiments were able to help us study and explain the translocation mechanism of the peptides. We were further able to use simulations as a tool to help design CPPs that could help improve translocation. The utility of using interaction energies of the MPG and how each residue contributes to translocation of the peptide was examined. In this chapter, MPG variants have been designed and discussed to study the delivery of GFP, inside *C. albicans.*

4.1 Introduction

In Chapter 3, CPPs were studied that can deliver a protein biomolecular cargo into the fungal pathogen, *Candida albicans*. MPG successfully delivered protein cargo to *C. albicans*, but the levels of translocation could be improved. MPG is a short amphipathic peptide that comprises different domains and the separate domains are responsible for interaction with nucleic acids and cellular uptake, intracellular trafficking of cargo and solubility of the peptide[1-3]; hydrophobic domain is responsible for membrane anchoring and for complex formation with hydrophobic cargoes[4], and the hydrophilic domain is

necessary to target a subcellular compartment, to increase solubility of the vector and for the complex formation with hydrophilic negatively-charged molecules[4-6].

Design of CPPs for improved translocation involves major considerations including the interaction of the CPPs with the membrane. Charge and hydrophobicity are important properties to consider for improving translocation efficacy of a peptide and a mechanistic understanding of translocation using modeling will further help in designing peptides. Experimental and simulation studies in the previous chapter, showed that MPG enters through the N-terminus and these results provide information to help design variants to better understand translocation. To explore the structure–function relationships of CPPs and their interaction with *C. albicans*, our lab has previously worked with translocation of another peptide, SynB, into *C. albicans*[7]. Increase in net charge and decrease in hydrophobicity of native SynB, led to designing of SynB variants that provided a better understanding of the role of specific properties in translocation. The derivatives of SynB, SynB-1, and SynB-2, were designed with higher charges, and showed the presence of a higher amount of peptide in the cytosol at a lower concentration of peptide. On reducing the hydrophobicity of native SynB, SynB-7, there was a reduction in vacuolar lysis, that was consistent with vacuolar localization but maintained the energy-dependent endocytosis translocation mechanism observed in SynB[7]. These SynB variants will be interesting to study for translocation of biomolecular cargo into *Candida* as they have not been studied for carrying cargo into fungal cells. The results support the extension of the study towards

peptide residue substitutions to improve translocation. In this chapter, we will study the translocation of GFP with variants of MPG.

As has been seen from previous work[8-10], charge and hydrophobicity play important role in transportation of CPPs into cells. Higher net charge affects cell viability significantly more than other properties[9-11]. Net charge of peptides, in general, affects membrane association and could enable the deeper membrane insertion and contact of hydrophobic residues[11].

To understand the behavior of the peptide residues and their role in translocation, we collaborated with Dr. Jeffery Klauda and his lab and determined the interaction energy of each of the residues of the wild-type MPG with the membrane and also the distance of each residue from the top membrane plane of a HMMM model[12] (Figure 3.9).

To design better CPPs, identifying the mode of action of CPPs and interpreting the type of interaction that they have with membrane components for example, the phospholipids is important. At the same time, it is essential to identify a peptide's primary and secondary structures. As discussed in Chapter 1, CPPs use three main mechanisms to enter the cells - direct penetration, translocation by forming a temporary structure and an endocytosis-mediated cell entry. CPPs interact with the plasma membrane, mostly by direct electrostatic interactions with the phospholipid headgroups in the membrane, but the interactions differ based on the CPP. For example, penetratin interacts specifically with negatively charged membranes while transportan does not[4, 13]. Other peptides like amphipathic peptides (for example, MPG) interact with the

membranes with their hydrophobic ends and have been known to form pore-like structures by forming a β-barrel structure[4, 14], whereas Pep-1 interacts with the membrane using an α-helical structure[4, 15]. SynB, a CPP which is part of the antimicrobial peptide (AMP) protegrin 1 (PG-1)[16] is known to translocate by energy-dependent endocytosis mechanisms[16, 17]. SynB shows a β-sheet structure in a partial hydrophobic environment and assumed a more dominant helical conformation in a pure hydrophobic environment[8]. To study the interaction of the peptide and *C. albicans*, circular dichroism was done and the results showed that SynB assumed a β-sheet conformation.

Based on previous work in the Karlsson lab[7] and results in Chapter 3, we studied variants of MPG that were rationally designed to enhance translocation. We worked on modifying the residues of MPG to try to enhance translocation. CPPs with higher net charges tend to enter cells via direct translocation and traffic to the cytosol, supported by a close interaction with the membrane. The hydrophobicity does not directly affect the translocation efficiency; however, it alters the membrane association pattern and affects the translocation mechanisms[18]. Translocation efficiency depends on the sequence, length and location of the positive charges in a sequence[14, 16], and thus adding Lys or Arg residues can help alter translocation. The guanidinium group in arginine can form two hydrogen bonds with phosphate headgroups in the membrane[19] replacement with arginine can help translocation. Hydrophobicity on the other hand can be altered by adding aromatic amino acids Trp, Phe and Tyr to peptide sequence. MD simulations have been used to complement experimental studies on CPPs and can

give important information on peptide residue interaction with membrane and the peptide's structural and conformational behavior in the presence of lipids. For example, Ulmschneider *et al.* used simulation to study interaction of melittin with a phosphatidylcholine (POPC) bilayer and its translocation[20]. The peptide residues below the phosphate head groups adopted a helical conformation while the residues out of the bilayer remain unfolded[20].

Simulations studies helped design MPG variants based on interaction energies that were calculated using a full membrane model. MPG variants were designed based on the charge and hydrophobicity of the peptide (Table 4.1). These variants were intended to study if translocation efficiency was changed by the net charge of the peptides and in turn the antifungal activity.

The SynB variants were designed previously in the Karlsson lab[7, 18] out of which SynB-2 has been shown to have higher translocation and toxicity compared to native SynB. On reducing the hydrophobicity of SynB (SynB-7), there was no increase in translocation or toxicity. We have chosen these two mutations along with the native SynB to compare translocation efficiency. These along with SynB + (combined properties of SynB-2 and SynB-7) would provide us with knowledge that could further help us in translocation studies. In this chapter, we will study translocation of GFP with variants of MPG. This study would provide us with knowledge how fusion of the peptides to GFP would affect the translocation and if peptide or cargo has a greater effect on translocation.

We will produce these fusions recombinantly and purify them to study their translocation using experimental and if feasible, will compare our results with simulations done in the Klauda Lab. The fusions of these new mutated peptides will be compared with the wild-type MPG-GFP and GFP only using analogous techniques outlined in Chapter 3.

With these new modified CPPs, we expect to see higher translocation of the fusions into *C. albicans*. Issues might arise with production of these fusions as each new peptide and cargo fusion expresses differently, though we do have shown previously that most constructs express well at a standard temperature and induction time.

4.2 Methods for introducing design changes to peptides

4.2.1 Cloning of plasmids

The expression plasmid for or study was constructed using pET-21(a) (Novagen, Madison, WI, USA). This plasmid comprises a C-terminal 6XHis tag. The oligonucleotides sequences for our constructs are given in Table 4.2.

4.2.2 Construction of CPP-cargo protein fusion constructs

Peptides were inserted into the pGST(-) plasmid for production by means of pairs of annealed oligonucleotides (Table 4.2) that were produced commercially (IDT, Skokie, IL, USA). These pairs contained the coding sequence for CPPs. The pairs of oligonucleotides were annealed to form double-stranded DNA inserts to code for the CPPs with EcoRI and SacI sticky ends for insertion into pGST(-) (Table 4.1). For example, the pairs EcoRI-T14K-Top1 and EcoRI-T14K-btm1 and the pairs SacI-T14K-Top2 and SacI-T14K-btm2 were annealed to form two dimers that combined to encode for T14K. These dimers were inserted between the EcoRI and SacI sites of pGST(-).

The DNA encoding the cargo, GFP, was PCR-amplified from a template plasmid in our lab stock that used the primers SacI-(Cargo)-F and (Cargo)-NotI-R (Table 5.2), where (Cargo) denotes GFP. The subsequent products were introduced between the SacI and NotI sites of pGST(-).

Table 4.1 Oligonucleotide sequences used in this study

Oligonucleotide sequence name	Sequence (5′ to 3′)	CPP/cargo/expression partner
SacI-ATG-GFP-F	GCGATGGAGCTCAGTAAAGGAGAAGAACTTTTC	GFP
GFP-NotI-R	AATAAAGCGGCCGCTTTGTATAGTTCATCCATGC	
MPG-Top1	aattcatgGGTGCTTTGTTTTTGGGCTTCTTGGGTGCAGCCGGAAGTACGATGGG	MPG
MPG-Bottom1	TCGTACTTCCGGCTGCACCCAAGAAGCCCAAAAACAAAGCACCcatg	

MPG-Top2	GGCGTGGAGCCAACCGAAAAA GAAGCGTAAAGTGgagct	
MPG-Bottom2	cCACTTTACGCTTCTTTTTCGGTT GGCTCCACGCCCCCA	
EcorI-S13K-Top1	aattcGGTGCTTTGTTTTTGGGCTT CTTGGGTGCAGCCGGAAAG	MPG variants
EcorI-S13K-btm1	CCCCATCGTCTTTCCGGCTGCAC CCAAGAAGCCCAAAAACAAAG CACCg	
SacI-S13K-Top2	ACGATGGGGGCGTGGAGCCAAC CGAAAAAGAAGCGTAAAGTGga gct	
SacI-S13K-btm2	cCACTTTACGCTTCTTTTTCGGTT GGCTCCACGC	
EcorI-T14K-Top1	aattcGGTGCTTTGTTTTTGGGCTT CTTGGGTGCAGCCGGAAGT	MPG variants
EcorI-T14K-btm1	CCCCATCTTACTTCCGGCTGCAC CCAAGAAGCCCAAAAACAAAG CACCg	
SacI-T14K-Top2	AAGATGGGGGCGTGGAGCCAAC CGAAAAAGAAGCGTAAAGTGga gct	
SacI-T14K-btm2	cCACTTTACGCTTCTTTTTCGGTT GGCTCCACGC	
BamHI-GST-F	GCGATGGGATCCATGTCCCCTA TACTAGGTTATTG	GST
GST-EcoRI-R	AATAAAGAATTCACCAGAACCA CTAGTTGAAC	

4.2.3 Bacterial strains, expression conditions and purification

Subsequent to plasmid construction, all plasmids were transformed into *E. coli* DH5α (Novagen) and sequenced. Following successful plasmid construction, the plasmids were transformed into *E. coli* BL21 (DE3; Novagen) for expression studies. 25 mL of over-night culture for each construct was subcultured into 1000 mL of fresh Luria-Bertani broth (10 mg/mL tryptone, 5 mg/mL yeast extract, and 5 mg/mL NaCl) at an optical density of OD_{600} = 0.05 and grown at 37°C for 2 h. The fusion protein expression was then induced by adding isopropyl β-D-1-thiogalactopyranoside (IPTG)

to each culture aliquot at a final concentration of 0.1 mM. The cultures were then incubated at 37 °C for 6 h.

After harvesting the cells by centrifugation, the cells were resuspended in the buffer for purification (125 mM Tris, 150 mM NaCl, 1 mM ethylenediaminetetraacetic acid (EDTA) (pH 7.5). The cells were then lysed using a homogenizer cell disruption system (Avestin). After lysis of each sample, the whole-cell lysates were pelleted by centrifugation at 11,419 × g for 50 min at 4 °C, and the supernatants containing the soluble fraction of the cell lysates were collected. The soluble fraction of each lysate was passed through a 0.45 μm filter and applied to an IMAC Profinity Ni-NTA resin column (Bio-Rad). After thoroughly washing the column, the flow-through and washes were collected. The proteins were eluted in a buffer containing 20 mM sodium phosphate, 0.5 M potassium chloride (KCl), and 500 mM imidazole (pH 7.4).

4.2.4 *C. albicans* strain and culture conditions

C. albicans strain SC5314 (American Type Culture Collection, Manassas, VA). *Candida* cells were inoculated from yeast-peptone-dextrose (YPD) agar plates (1% w/v yeast extract, 2% w/v peptone, 2% w/v glucose, 2% w/v agar) into 5 mL of liquid YPD medium (1% w/v yeast extract, 2% w/v peptone, and 2% w/v glucose) and were grown at 30 °C and 230 rpm, overnight. The overnight culture was introduced to 5mL of fresh YPD medium at OD_{600} = 0.1 (~ $2x10^6$ colony forming unit /mL). The culture was then

grown at 30 °C to OD_{600} = 0.5 (~ $1x10^7$ CFU/mL) at 225 rpm. Cells were harvested by centrifugation at 4,300 × g for 10 min and washed twice with 10 mM sodium phosphate (Na_2HPO_4) buffer to use in downstream assays.

4.2.5 Quantification of translocation into *C. albicans*

For each protein fusion, 100 µL of solution (100 µM) was prepared in 10 mM Na_2HPO_4 buffer, and was mixed with 100 µL of cell suspension containing 5 x 10^5 cells in 10 mM Na_2HPO_4. This mixture was then incubated at 30 °C for 1 h and 24 h. Cells were collected by centrifugation at 5000 × g for 10 min at 4 °C and washed once with 10 mM Na_2HPO_4. The cell pellets were further incubated with 200 µL of 0.025% trypsin (Invitrogen, Waltham, MA) at 37 °C for 30 min to remove surface-bound peptides or proteins[21]. Cells were then collected by centrifugation at 5000 × g for 10 min at 4 °C and washed with 10 mM Na_2HPO_4. Propidium iodide (PI, 1 mg/ml; Invitrogen) was added at 0.2 mg/ml right before flow cytometry. Cell suspensions were analyzed for GFP and PI fluorescence using a BD FACSCanto II flow cytometer (BD Biosciences, San Jose, CA). Only single cells were selected for analysis, and the analysis was performed using FlowJo software (FlowJo, LLC, Ashland, OR).

4.3 Results and discussion

The goal of this study was to produce mutated CPPs and their fusions to cargo, recombinantly, and to explore the translocation of the purified CPP-cargo into *C. albicans* and compare their translocation with wild-type CPPs. The CPPs chosen for this study were MPG and its variants (Table 4.2).

4.3.1 Design of MPG modifications

MPG-GFP can be translocated into *C. albicans* with very little killing (section 3.2). These translocation results logically support the idea of peptide residue substitutions. To understand the characteristics of the residues and their effect on translocation, Dr. Jeffery Klauda and his lab ran simulations and calculated the interaction energy of each residue of wild-type MPG with the membrane. The residue and their distance from the top membrane plane of the model membrane was also calculated (Figure 3.13).

Based on the experimental and simulation results presented in Chapter 3, we designed variants of MPG to evaluate for improved translocation. The residues S13 and T14 are both hydrophilic uncharged residues and do not contribute to translocation, as is seen from the computed interaction energies. We changed these residues to charged hydrophilic groups like lysine (K) and arginine (R), and having these residues' in the

mid-region will help with binding of the peptide to the membrane and when the peptide moves into the membrane the charged residues will help transport it to the other side. CPPs have been known to have charges in the mid-region of the sequences[22, 23], and, thus, modifying these residues (Table 4.3) would help increase translocation. Arginine and/or lysine will help conserve the hydrophilic nature at the particular sites and this will help us to identify the precise changes that affect translocation.

Table 4.2. CPP variants used in this study

Peptide	Sequence	Length (a.a.)	Charge*	Difference from parent peptide
	1 2 3 4 5 6 7 8 9 10 11 12 13 14 15 16 17 18 19 20 21 22 23 24 25 26 27			
MPG	G A L F L G F L G A A G S T M G A W S Q P K K K R K V	27	+5	Native
MPG-S13K	G A L F L G F L G A A G **K** T M G A W S Q P K K K R K V	27	+6	Increase in charge
MPG-T14K	G A L F L G F L G A A G S K M G A W S Q P K K K R K V	27	+6	Increase in charge

*Includes charge due to amino acid side chains

As is evident from Figure 3.13, the charged residues at the C-terminus of the wild-type MPG (MPG only for simulation studies) stick to the membrane and do not go into the membrane whereas the hydrophobic residues at N-terminus help translocation. Though these charges help with the peptide's attachment to the membrane, we have to make sure that the MPG-GFP (GFP is at attached at the C-terminus of MPG in our experimental studies) fusion can translocate into the cells. We believe that altering some of the charged residues to hydrophobic residues is likely to help and introducing W19 in place of S19 to see the effect of this mutation on

translocation. We expect that a hydrophobic residue would help translocation of MPG-GFP into the cells.

4.3.2 Expression and purification of MPG variants

The designed MPG variants were fused with GFP and produced recombinantly in *E. coli*. The variants were then purified with IMAC. There were some challenges with the expression and purification of S13K-GFP. Expression at 6 h and 37 °C were comparatively lower than other proteins. This could be attributed to the higher charge of the constructs and possible killing of *E. coli* cells thereby leading to lower production. This construct could possibly be induced for a longer time to enhance production. At the same time, the protein could be part of the insoluble portion. This could be due to protein misfolding, and re-solubilizing the insoluble portion could improve protein extraction. On the other hand, T14K-GFP could be produced well and we were able to produce purified protein sample at 100 μM (Figure 4.1).

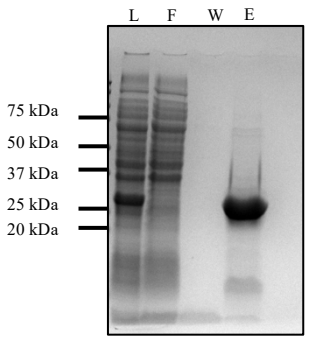

Figure 4.1. Purification of T14K-GFP. CPP fused to GFP and were expressed in BL21 (DE3) cells at 37 °C for 6 h with 0.01 mM IPTG. Coomassie stain was used to estimate the purity of fusion proteins. Crude soluble lysates (L), flowthrough (FT), washes (W) and elution (E) from immobilized metal affinity chromatography are shown. Purification of T14K-GFP. The crude soluble lysate contains the whole construct; flow-through does not bind to the column and so flows through; elutes are obtained using a buffer that contains 50% imidazole. Molecular weight: CPP-GFP = 30.5 kDa.

4.3.3 Translocation of MPG variants into *C. albicans* cells

The purified proteins were incubated with *C. albicans* for 1 h and 24 h hours at 30 °C in sodium phosphate buffer (NaPB). Translocation of the peptide fusions were evaluated using flow cytometry and was compared with the translocation of native MPG-GFP fusion to analyze the effect of peptide mutations on translocation. We compared the translocation of the of GFP, MPG-GFP and T14K-GFP at 100 μM (Table 4.3).

Table 4.3 Translocation of proteins into *C. albicans* measured at 24 h

Protein fusion	GFP positive (%)	PI positive (%)
GFP only	2.14	0.2
MPG-GFP	7.2	0.526
T14K-GFP	0.2	35

Though T14K-GFP does not show higher GFP positive (%) cells, we were able to observe a higher percentage of PI positive (%) cells. As we know, cells are normally impermeable to PI, but PI fluorescence can be detected inside cells with destabilized membranes. Destabilization can occur with cell death or with pore formation on the membrane. On comparison with the cells, GFP and MPG-GFP, we could see cells at the same condition, we can argue that the cells died due to translocation of our T14K-GFP fusion. But it should be noted that though there was higher PI positive uptake, GFP uptake was really low in case of T14K-GFP. The peptide might be interacting with the cells and permeabilizing the membrane without actually entering the cell. This could be beneficial if we can confirm that there is no toxicity to host cells, but the peptide-cargo fusion has antifungal properties. These data represent one replicate only and further experiments will need to be run to confirm our findings.

4.4 Discussion and conclusion

We are using CPPs as delivery systems to deliver macromolecular cargo into the fungal pathogen *C. albicans.* We have successfully delivered protein cargo inside fungal cells. These experiments begin to explore the effect of CPP modifications on translocation of cargo and more work on evaluating more peptides and their variants will provide an improved understanding of properties of peptides that affect translocation.

Further evaluation of the interaction of CPPs with *Candida* cells would provide insight into the biophysical properties that affect translocation, the mechanisms of translocation, and the toxicity of the peptides. Our initial data suggest that net charge of the peptides play a role in translocation, and further studies would help us in understanding the effect on translocation. Since, the phosphate heads of the membranes are negatively charged, it can be assumed that positive charged residues in peptides will lead to electrostatic interactions that would bring the residues in close contact with the cell membrane and affect translocation.

Further studies of the peptides and the mammalian cells are necessary to understand the effect of the peptides on these cells. In the initial sets of data for T14K-GFP, we observed a strong toxicity toward fungal cells which suggests that this peptide would be promising as antifungal agents. Future studies, could include just the peptide and compare its translocation efficacy with that of the peptide-cargo fusion. The concentration of the fusions should be increased to 200 μM (or higher) to compare with the translocation studies done in Chapter 3.

We have recognized CPPs that are able to translocate into *C. albicans* and deliver active biomolecular cargo. Our work explored the intracellular delivery of a macromolecular cargo into fungal cells. Our results suggest that biophysical properties of peptides play a role in translocation of CPPs into fungal cells and apply mechanisms that might lead to the toxicity to the cells. Further work could explore the translocation mechanisms of CPP-cargo fusions to improve their translocation efficacy into cells and study their toxicity profiles that can make CPPs viable therapeutic delivery agents. Improving the translocation of biomolecular functional cargo using CPPs, will ensure the usefulness of CPPs antifungal agents.

4.5 References

1. Morris, M. C.; Deshayes, S.; Heitz, F.; Divita, G., Cell-penetrating peptides: from molecular mechanisms to therapeutics. *Biol Cell* **2008,** *100* (4), 201-17.
2. Adhikari, S., Optimization of recombinant protein expression for cell-penetrating peptide fusions to protein cargo. **2017**.
3. Deshayes, S.; Decaffmeyer, M.; Brasseur, R.; Thomas, A., Structural polymorphism of two CPP: an important parameter of activity. *Biochim Biophys Acta* **2008,** *1778* (5), 1197-205.
4. Deshayes, S.; Morris, M. C.; Divita, G.; Heitz, F., Interactions of amphipathic CPPs with model membranes. *Biochim Biophys Acta* **2006,** *1758* (3), 328-35.
5. Walrant, A.; Bechara, C.; Alves, I. D.; Sagan, S., Molecular partners for interaction and cell internalization of cell-penetrating peptides: how identical are they? *Nanomedicine (Lond)* **2012,** *7* (1), 133-43.
6. L Chaloin, M. M., N Van Mau, J Mery, Synthetic primary amphipathic peptides as tools for the cellular import of drugs and nucleic acids. **2001**.
7. Gong, Z.; Doolin, M. T.; Adhikari, S.; Stroka, K. M.; Karlsson, A. J., Role of charge and hydrophobicity in translocation of cell-penetrating peptides into Candida albicans cells. *AIChE Journal* **2019,** *65* (12).
8. Gong, Z. Engineering Cell-Penetrating Peptides For Translocation And Intracellular Cargo Delivery In Candida Species. University of Maryland, College Park, College Park, Maryland, 2017.
9. Karlsson, A. J.; Pomerantz, W. C.; Weisblum, B.; Gellman, S. H.; Palecek, S. P., Antifungal activity from 14-helical beta-peptides. *J Am Chem Soc* **2006,** *128* (39), 12630-1.
10. Karlsson, A. J.; Pomerantz, W. C.; Neilsen, K. J.; Gellman, S. H.; Palecek, S. P., Effect of Sequence and Structural Properties on 14-Helical β-Peptide Activity against Candida albicans Planktonic Cells and Biofilms. *ACS Chem Biol* **2009,** *4* (7), 567-579.
11. Karagiannis, E. D.; Urbanska, A. M.; Sahay, G.; Pelet, J. M.; Jhunjhunwala, S.; Langer, R.; Anderson, D. G., Rational Design of a Biomimetic Cell Penetrating Peptide Library. *ACS Nano* **2013,** *7* (10), 8616-8626.
12. Ohkubo, Y. Z.; Pogorelov, T. V.; Arcario, M. J.; Christensen, G. A.; Tajkhorshid, E., Accelerating membrane insertion of peripheral proteins with a novel membrane mimetic model. *Biophys J* **2012,** *102* (9), 2130-9.
13. Magzoub, M.; Kilk, K.; Eriksson, L. E.; Langel, U.; Graslund, A., Interaction and structure induction of cell-penetrating peptides in the presence of phospholipid vesicles. *Biochim Biophys Acta* **2001,** *1512* (1), 77-89.
14. Deshayes, S.; Gerbal-Chaloin, S.; Morris, M. C.; Aldrian-Herrada, G.; Charnet, P.; Divita, G.; Heitz, F., On the mechanism of non-endosomial peptide-

mediated cellular delivery of nucleic acids. *Biochim Biophys Acta* **2004,** *1667* (2), 141-7.
15. Deshayes, S.; Heitz, A.; Morris, M. C.; Charnet, P.; Divita, G.; Heitz, F., Insight into the mechanism of internalization of the cell-penetrating carrier peptide Pep-1 through conformational analysis. *Biochemistry* **2004,** *43* (6), 1449-57.
16. Drin, G.; Cottin, S.; Blanc, E.; Rees, A. R.; Temsamani, J., Studies on the Internalization Mechanism of Cationic Cell-penetrating Peptides. *Journal of Biological Chemistry* **2003,** *278* (33), 31192-31201.
17. Jamal Temsamani; Laruelle, C., SynB peptide vectors: A new approach to drug delivery. *Chimica Oggi / Chemistry Today* **2010,** *28*.
18. Gong, Z.; Karlsson, A. J., Translocation of cell-penetrating peptides into Candida fungal pathogens. *Protein Sci* **2017,** *26* (9), 1714-1725.
19. Mishra, A.; Lai, G. H.; Schmidt, N. W.; Sun, V. Z.; Rodriguez, A. R.; Tong, R.; Tang, L.; Cheng, J.; Deming, T. J.; Kamei, D. T.; Wong, G. C., Translocation of HIV TAT peptide and analogues induced by multiplexed membrane and cytoskeletal interactions. *Proc Natl Acad Sci U S A* **2011,** *108* (41), 16883-8.
20. Chen, C. H.; Wiedman, G.; Khan, A.; Ulmschneider, M. B., Absorption and folding of melittin onto lipid bilayer membranes via unbiased atomic detail microsecond molecular dynamics simulation. *Biochim Biophys Acta* **2014,** *1838* (9), 2243-9.
21. Richard, J. P.; Melikov, K.; Vives, E.; Ramos, C.; Verbeure; B.; Gait, M. J.; Chernomordik, L. V., and; Lebleu, B., Cell-penetrating peptides: a re-evaluation of the mechanism of cellular uptake. *The Journal Of Biological Chemistry* **2003,** *278* (1), 585–590.
22. Esposito, D.; Chatterjee, D. K., Enhancement of soluble protein expression through the use of fusion tags. *Curr Opin Biotechnol* **2006,** *17* (4), 353-8.
23. Ramaker, K.; Henkel, M.; Krause, T.; Rockendorf, N.; Frey, A., Cell penetrating peptides: a comparative transport analysis for 474 sequence motifs. *Drug Deliv* **2018,** *25* (1), 928-937.

Chapter 5: Aggregation of fusion proteins

In the previous chapters, we have been able to successfully deliver a biomolecular cargo in *C. albicans cells* and have been able to use simulations as a tool to introduce changes into the peptides. Both simulations and experiments helped us study and explain the translocation mechanism of the peptides. In this chapter, we investigate factors like aggregation of fusions, that might affect translocation and list ways to mitigate the same.

5.1 Introduction

As discussed in chapter 3, for our translocation studies, we have been using concentrations of proteins as high as 200 μM and even on concentrating the proteins further, I was not able to increase translocation of the fusions into *Candida albicans*. One possible cause of the lack of improvement would be that the CPPs are inactivated due to aggregation. In this chapter, we explore the aggregation of CPP-cargo fusions. This work was performed in collaboration with Shakiba Nikfarjam and Dr. Taylor Woehl. I probed the reasons why translocation did not increase with increasing concentration above 200 μM. This led us to look into other factors that might be

affecting translocation at higher concentrations. The hypothesis here is that aggregation of the fusions could be inhibiting translocation.

Aggregation of proteins includes a variety of interactions that occur due to different mechanisms and can be classified as soluble or insoluble, covalent or noncovalent, reversible or irreversible, and native or denatured[2]. Soluble aggregates can be defined as those that are not visible as distinct particles and may not be removed by a 0.22 μm filter[2]. Insoluble aggregates, on the other hand, might be removed by filtration and are often observable to the naked eye[2]. Protein aggregates can be divided into three sub-categories based on their size and solubility. Soluble aggregates consist of protein oligomers and aggregates that range from 10 nm to 100 nm; subvisible particles range from 100 nm to 100 μm; 100 nm to 1 μm particles are submicron; and particles over 100 μm in size can be classified as visible particles[1, 3, 4].

The challenges to overcome protein aggregation is one of the main problems in commercialization of drug products[5]. Native oligomers are highly stable and have possibly higher solubility than their monomers, and insulin in the presence of zinc ions is an example of a stable protein pharmaceutical product[6]. In most cases though, aggregation affects product quality. There are increasing concerns that patients can develop immune responses to the drug when they are partially folded, irreversible aggregates that remain in the blood stream[7]. Aggregates are not only responsible for drug product quality but can also cause many diseases.

Proteins have a propensity to aggregate due to a variety of reasons[8]. Degree of aggregation can depend on intrinsic factors such as primary, secondary, tertiary or

quaternary structure or extrinsic environmental factors and processing conditions[8]. Protein aggregates can lead to reduced or a lack of biological activity that can lead to immunogenic response or other side effects[8]. This inherent tendency of proteins to aggregate makes their use in biological applications[9-11]. When proteins aggregate, they can sometimes form unwanted deposits[9-11]. In some diseases, for example, in Alzheimer's, proteins which are usually soluble, form deposits[10, 12]. Protein aggregation have been known to cause a variety of other diseases like Parkinson's and Huntington's disease[13].

Aggregation has been studied using a number of optical methods. Microscopy methodologies have been used for imaging purposes and for quantification of particles. In fact, researchers have used fluorescence microscopy methods like confocal microscopy and total internal reflection fluorescence to image subvisible particles[1, 14-16]. For pure optical scattering, scattering intensity (I) varies with particle radius (r) as $I \propto r^6$, which is a limitation to established optical methods as they cannot determine the weak scattering particles that have with sizes > ~1 μm[1, 17]. This is where interferometric scattering microscopy can help. Interferometric scattering microscopy is an optical microscopy method that works on collecting light scattered by an object jointly with a reference light, specified by the reflection at an interface[18]. This method is a highly sensitive imaging method for detection of nanoscopic objects.

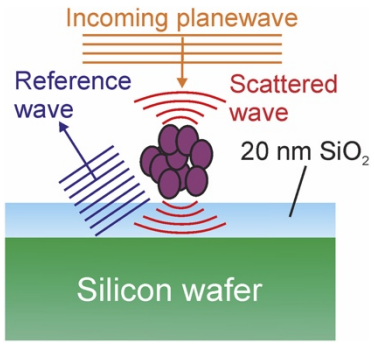

Figure 5.1. Schematic representation of multilayered interferometric scattering microscopy sensor to describe optical scattering and interference. A planewave (orange horizontal lines) disperses off of a protein aggregate (purple) and a silicon-silicon oxide interface that produces a reference wave (blue) which affects the scattered wave. This interference pattern is detected on a CMOS camera on a customized optical microscope. Figure directly taken from Figure 1 of Wong et al.[4] Reproduced with permission

Using interferometric scattering microscopy, the proportionality is modified to $I \propto r^3$ that interferes with particle scattering when a reference wave is formed by using layered sensor chips[17, 19]. This method introduces a phase shift in the particle scattering which leads to increase in sensitivity to minute, low contrast particles. These images obtained from the optical microscope are easy to understand as there is a dependence of particle size and the scattering intensity and Dr. Taylor Woehl's lab has been successful in using non-complex modeling techniques to process the images and extract information on particle size[1, 20]. This method has the capability to conserve high imaging contrast that does not depend on the exposure time or the scattering cross section of the object[18].

Another method that has been widely used to study aggregates dynamic light scattering (DLS). When a monochromatic beam of light points at any solution that contains macromolecules, the light disperses in all directions. This light scatters as a

function of the size and shape of the macromolecule[21]. The scattered light can either be mutually destructive that cancel out, or mutually constructive and generates a detectable signal[22]. Intensity fluctuations of the scattered light, caused by Brownian motion of macromolecules in solution, are studied, and information on diffusion coefficient (*D*) and hydrodynamic size of macromolecules can be acquired[21] (equations can be found in Section 5.4). Dynamic light scattering, measures the Brownian motion of macromolecules in solution, which happens due to the light hitting on the solvent molecules, and relates particle size to the diffusion coefficient. Motion of these macromolecules depends on the size, temperature, and solvent viscosity[21, 22]. Therefore, knowledge of precise temperature is crucial for DLS measurements[22]. Particle movement over a range of time is recorded and information on the size of macromolecules can be gained; large particles diffuse slowly, that results in analogous positions at different times as compared to small particles that move comparatively faster and do not assume a precise position[22]. A digital autocorrelator, correlates intensity fluctuations of scattered light to time to resolve intensity fluctuation, that can further be related to the diffusion of macromolecules[22].

5.2 Methods to study aggregation

5.2.1 Purification of proteins

25 mL of over-night culture for each construct was subcultured into 1000 mL of fresh Luria-Bertani broth (10 mg/mL tryptone, 5 mg/mL yeast extract, and 5 mg/mL NaCl)

at an optical density of OD_{600} = 0.05 and grown at 37°C for 2.5 h. The fusion protein expression was then induced by adding isopropyl β-D-1-thiogalactopyranoside (IPTG) to each culture aliquot at a final concentration of 0.1 mM. The cultures were then incubated at 37°C for 6 h.

After 6 h, cells were harvested by centrifugation, and the cells were resuspended in the buffer for purification (125 mM Tris (pH 7.5), 150 mM NaCl, 1 mM EDTA). The cells were then lysed using a homogenizer cell disruption system (Avestin). After lysis of each sample, the whole-cell lysates were pelleted by centrifugation at 11,419 × g for 50 min at 4 °C, and the supernatants containing the soluble fraction of the cell lysates were collected. The soluble fraction of each lysate was passed through a 0.45 μm filter and applied to an IMAC Profinity Ni-NTA resin column (Bio-Rad). After thoroughly washing the column, the flowthrough and washes were collected. The proteins were eluted in a buffer containing 20 mM sodium phosphate (pH 7.4), 0.5 M potassium chloride (KCl), and 500 mM imidazole. After collecting the elutes, protein concentration was measured using Nanodrop (Thermo Scientific, USA) and the protein was concentrated using vivaspin 6 molecular weight cut-off (MWCO) columns at 4,000 × g using a swinging bucket rotor (Beckman Coulter, Brea, CA).

5.2.2 Dynamic light scattering (DLS) to study aggregation

Protein samples were expressed *E. coli* and were purified using affinity chromatography. They were concentrated to 200 μM to match our translocation experiments. Protein samples were filtered with 0.20 μm filter before loading them into

cuvettes. They were illuminated by a laser beam and the fluctuations of the scattered light were identified at a known scattering angle θ using a fast photon detector. Scattering of light by particles imprints information about their motion. The fluctuation of scattered light is analyzed and this yields information about particles. We experimentally characterized the intensity fluctuations by calculating the intensity correlation function $g_2(t)$[23]:

$$g_2(q,\tau) = \frac{\langle I_s(q,t)\, I_s(q,t+\tau)\rangle}{\langle |I_s(q,t)|^2\rangle} \qquad \text{(Equation 5.1)}$$

where I is the intensity as function of time, t, and q is wave vector. This analysis compares the diffusion coefficient of the particle intensity $I(t)$ of the scattered light at a time t with that at some later time $(t+\tau)$, [24, 25] where τ is the lag time between the two time points.

For spherical monodisperse particles in a fluid, the autocorrelation function has a single characteristic decay time τ:

$$g_2(\tau) = \langle 1 + exp(-2\,\Gamma\tau\rangle \qquad \text{(Equation 5.2)}$$

The decay rate depends on the wave vector and thus the scattering angle. Γ is proportional to the diffusion coefficient of the particles and is the inverse of the decay time, τ_c, as:

$$\Gamma = Dq^2 \qquad \text{(Equation 5.3)}$$

where $q = (4\pi n/\lambda)\sin(\theta/2)$ is the wave vector, n is refractive index, λ is the laser wavelength, and θ is the scattering angle. For spherical non-interacting particles, the particle size can be determined by converting the diffusion coefficient to hydrodynamic radius R_h by using the Stokes-Einstein equation for the diffusion coefficient (D)[26]:

$$R_h = \frac{k_B T}{6\pi\eta D} \quad \text{(Equation 5.4)}$$

where k_B is Boltzmann's constant, T is the temperature, and η is the viscosity of the solvent. A fixed scattering angle of 60° was chosen and the experiments were performed at room temperature. Viscosity was set to 0.89 cP with a refractive index of 1.33.

5.2.3 Interferometry to study aggregation

The method for interferometry scattering microscopy is based on the method of Wong et al. 2019[1]. The samples were made on multilayered sensors that consisted of a silicon wafer piece coated with a 20 nm thick layer of silicon oxide (SiO_2). The starting material for the sensors was polished 100 mm silicon wafers that had a net thickness variation of <5 µm (Silicon Materials, Pittsburg, PA). A 110 nm thick SiO_2 layer was added first, by a wet thermal oxidation process and then imprinted with a hydrofluoric acid wet etch to attain the preferred thickness. An SiO_2 thickness of 20 nm was selected. Further, interferometric microscopy sensors were made by cutting the surface oxidized silicon wafer into 1 x 1 inch pieces. These sensor chips were then dried with filtered

air and cleaned with plasma for 5 min in air plasma (Harrick Plasma, PDC32G) for removal of remaining solvent and surfactant. 10 µl of liquid protein aggregate sample was put onto the sensor surface, which was then dried at room temperature, followed by rinsing with deionized water. Drying of the sensor was done to ensure that the large refractive index difference between air and SiO_2 intensifies the sensitivity of interferometry scattering microscopy[1, 19].

The interferometry scattering microscopy experiments were done on an altered upright optical microscope (Zeiss Axioscope) that was used in reflection mode. The modified design of the microscope incorporated a collimated 530 nm LED epi-illumination source (Thorlabs, Newton, NJ, 150 mW)[1]. To guarantee plane wave illumination and uniform light intensity across the complete imaging field, Kohler illumination was used. The images were obtained using a 20X dry objective lens with a numerical aperture of 0.45. This was then projected onto a monochrome 1900 × 1200 pixel CMOS camera with an exposure time of 1 ms (FLIR Grasshopper G3)[1]. To reduce the numerical aperture of the objective lens, a 1 mm diameter pinhole was introduced into the back focal plane. This adjustment increased the interferometry scattering microscopy image contrast by brightening the sample at low angles of incidence, which directed the scattered light directly onto the objective lens and not to wide angles, thereby reducing the background of the image[1, 27]. In the process of imaging the protein aggregates, they might dry which may make them change their size/shape but latest measurements of protein aggregate density have shown that density is related to the theoretical density of a protein exponentially, and is equal to 1.3g/cm^3 for submicron

protein aggregates[1, 28]. This hints at the fact that submicron protein aggregates have very little porosity and thus their size is not affected due to drying[1, 28].Results and Discussion

5.2.4 Study of aggregation using dynamic light scattering

To explore the presence of aggregates in GFP, MPG-GFP and Hst5-GFP, DLS was used to determine the presence of aggregates in our protein solutions at 200 μM in NaPB (Figure 5.1). The proteins were expressed in *E. coli* and purified by affinity chromatography. The proteins were then concentrated to 200 μM. DLS measurements were done at room temperature. The measurements of the hydrodynamic radius of the proteins are listed in Table 5.1.

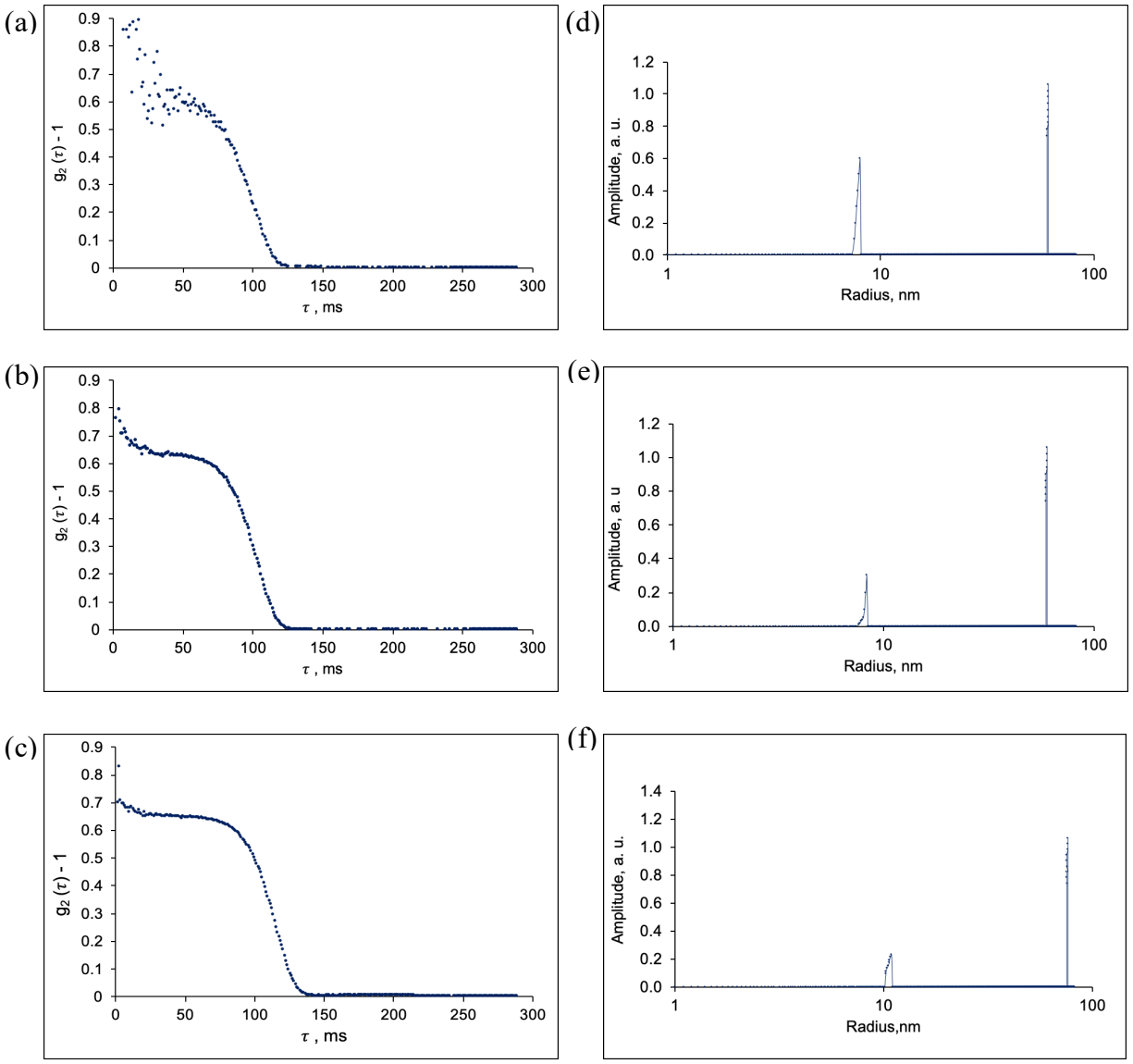

Figure 5.2. DLS analysis for correlation function and hydrodynamic radius. DLS correlation function (g_2) obtained for (a) GFP, (b) MPG-GFP and (c) Hst5-GFP at 200 μM and intensity distribution for (d) GFP, (e) MPG-GFP and (f) Hst5-GFP.

Table 5.1 Hydrodynamic radius analysis at protein concentrations of 200 µM in NaPB

Protein	Peak number	Hydrodynamic radius (nm)	Standard deviation
GFP	1	7.683	0.861
	2	59.92	12.79
MPG-GFP	1	8.058	1.975
	2	59.55	20.90
Hst5-GFP	1	10.48	2.308
	2	82.75	29.40

Hydrodynamic radius, is the radius of a comparable hard sphere that diffuses at the same rate as the molecule under study. Protein solutions and their complexes do not actually exist as hard spheres, and, therefore, the hydrodynamic radius is the apparent size assumed by the protein molecule. As can be seen from Figure 5.2 and Table 5.1, the size of GFP and MPG-GFP are ~8 nm and that for Hst5-GFP monomers is ~10 nm. Erickson et al. have determined the size and shape of protein molecules by use of different techniques[29]. Sedimentation and gel filtration techniques can be used to better determine the size of our aggregates. Much bigger aggregates were found and the correlation function is a single exponential, which means that the protein solutions were dominated by the aggregates, that is there were more aggregates than smaller particles. The concentration of proteins used in this experiment is comparatively lower for DLS measurements than those normally measured in DLS studies, and the aggregates contributed the most for the recorded intensities detected here. One interesting fact to note here is that, the standard deviation of peak number 2 (peak for aggregates) for each protein was large, thus leading us to believe that an array of polydisperse aggregates were present (Table 5.1). Although the sizes of the aggregates

for GFP and MPG-GFP are comparable (<100 nm), the relative population of aggregates for Hst5-GFP were quite different. There were more aggregates compared to monomers for Hst5-GFP.

These analyses identify the presence of aggregates in our protein samples and suggest future experiments to gain additional information on the aggregates and aggregation process. Though scattering angle might not have any dependence on aggregation, it will be worthwhile to measure the hydrodynamic radius at different scattering angles and see the effect of scattering angle on the samples. Temperature is another parameter that can be varied and experiments can be performed at both higher temperatures (for example, 37 °C and 50 °C) and lower (for example, 4 °C) to see the effect of temperature on aggregate formation. Our samples were filtered with 0.20 μm filters but further studies with 0.02 μm filters might help in removing aggregates from the solution. These would remove the smaller aggregates and we can have a stronger monomer peak. Experiments should be performed using these monomers to see their effect on translocation. These same experiments should also be done for a range of concentration, to understand the dependence of aggregation on concentration of proteins. Doing the DLS in parallel with the translocation experiments (experiments with flow cytometry as explained in chapter 3 and 4) could lead to an understanding of whether aggregation limits translocation.

5.2.5 Study of aggregation using interferometric scattering microscopy

To further study the presence of aggregates, initial studies with interferometric scattering microscopy were done with purified Hst5-GFP and MPG-GFP at a concentration of 200 µM. Dr. Woehl and his lab performed the experiments to identify aggregates in our samples. 10 µl of each of these proteins were applied on the chips and dried for 10 mins or higher depending on the time taken for drying. These were then observed under the microscope to determine the formation of aggregates, if any (Figure 5.3).

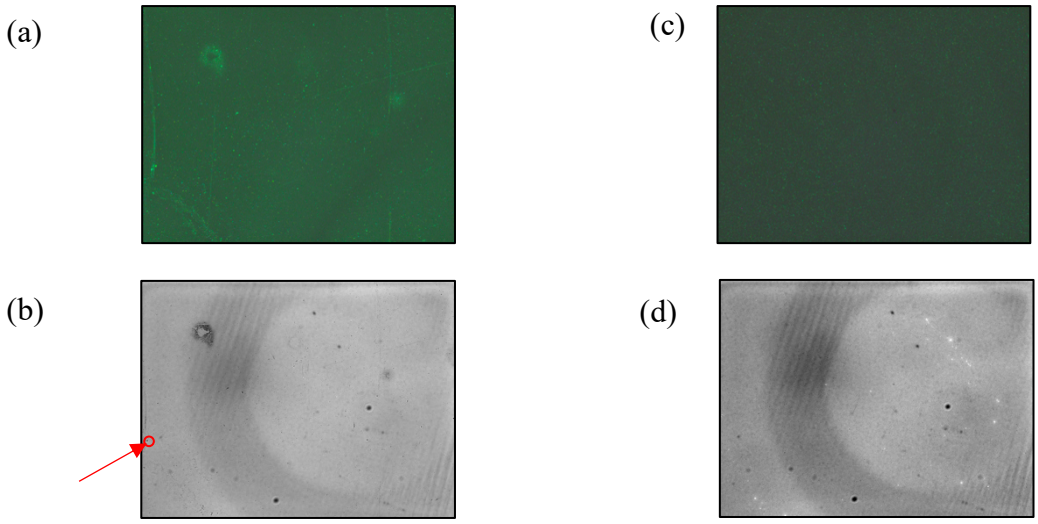

Figure 5.3. Interferometry images of Hst5-GFP and MPG-GFP. 10 µl of each protein was added to the chip, dried and washed with deionized water. Fluorescence and interferometric scattering images were captured. (a) fluorescence microscopy image of Hst5-GFP (b) interferometric scattering microscopy image of Hst5-GFP (c) fluorescence microscopy image of MPG-GFP (d) interferometric scattering microscopy image of MPG-GFP. The arrow points to a protein aggregate in the Hst5-GFP sample analyzed by interferometric scattering microscopy.

Fluorescent images of the proteins were taken and then analyzed for the presence of aggregates. Protein aggregates can be detected as small black spots in the image (Figure 5.3 (b), (d)). Protein aggregates are seen to immobilize on the surface of the sensor. Ultimately, the liquid layer got thinner than the protein aggregates and fixed them to the sensor surface. Additional buffer was washed away after cleansing with deionized water, and this process leaves the protein aggregates permanently attached to the sensor surface. Rinsing with deionized water remove the attached aggregates from the surface of the sensor and this could be attributed to electrostatic attraction between the positively charged aggregates and the negatively charged SiO_2 surface with

silanol groups. This makes sure that the aggregates remain attached to the sensor surface and can be observed under the microscope.

"Coffee ring" effects were observed which leads us to believe that aggregates concentrate near the edges of the droplets. In general, it has been seen that for like-charged particle/surfactant mixtures, the particles form a ring-shaped deposit, called "coffee-ring effect"[30]. During dropcasting, coffee-ring effect is a common occurrence. This happens due to solvent evaporation during film assembly that is stimulated by capillary flows in the drop which displace particles to the three-phase contact line, which results in particle accumulation at the dry film boundaries and thus the formation of coffee-ring like structure[31].

This initial study shows that our proteins aggregate and indicates the utility of interferometric scattering microscopy in studying CPP-cargo fusions. Additional experiments will identify optimal solution conditions to better image and quantify aggregates and study the effect of different concentrations of the proteins. We could also use image analysis to quantify the maximum scattering intensity for each particle on a 16-bit scale. These experiments would also allow us to quantify the particle size distribution along with data from measurements using DLS.

5.2.6 Possible ways of mitigating aggregation

DLS and interferometric scattering microscopy show that the protein fusions are aggregating and, in addition to studying the aggregation, it will also be important to control it. This study presents a representative set of data to show which factors among many can affect translocation of proteins fusions into cells. Further characterization using analytical techniques like sedimentation velocity using an analytical centrifuge should be done to measure the size of the aggregates and gel filtration can be used to separate the different aggregate sizes.

In this chapter, I have outlined various factors that during our experimental process could be contributing to aggregation of our proteins. For our future experiments we could focus on the various parameters like pH of a buffer solution, temperature, various stresses and shears that lead to aggregation and take measures and necessary steps to control them.

Cell culture is the first stage in protein expression. For expression of proteins, *E. coli* is commonly used cell system and expression is done under a variety of conditions and proteins have been known to aggregate into inclusion bodies during expression in bacterial systems[8, 32]. Factors like temperature, protein concentration, type and concentration of denaturant, pH, ionic strength, refolding catalysts, thiol/disulfide agents, and miscellaneous additives[8, 33-35] affect aggregation of proteins during refolding. Protein aggregation can be inhibited during expression and can be

modulated by process conditions like temperature, use of surfactants, and other additives[8, 36, 37].

To prepare proteins for purification after expression, we lyse the cells using a homogenizer in which we apply pressure to break open the cells to extract the protein lysate, and this process can induce aggregation. High pressure can cause protein unfolding and enable protein aggregation due to higher hydrophobic interactions[2, 38, 39]. Processes like shaking and shearing can induce aggregation but the aggregation depends on the time and intensity of exposure. If protein purification conditions are too harsh like pH of buffer, it can induce aggregation[8, 40]. Careful monitoring of process conditions during purification can help reduce aggregation. In our study, the purification of Hst5-GFP involved additional steps during purification. Factor Xa was used for off-column cleavage of GST, followed by introduction of the lysate to the chromatography column. While concentrating the proteins to the required concentration, the number of centrifugation cycles for each protein was different (for example, it needed much less time to concentrate GFP to 200 μM as compared to both MPG-GFP and Hst5-GFP) , and that could be a contributing factor too. Aggregates that are formed during cell culture or in any of the processing steps, might be removed during the purification procedure by manipulating the differences in various properties of the monomers and aggregates, that includes surface charge, hydrophobicity, and size[2].

Protein concentration has been attributed as a key factor that promotes protein aggregation and has been studied considerably. Increase in protein concentration could

result in the following: (1) decrease in aggregation due to overcrowding; (2) increase in aggregation due to increased association; and (3) precipitation due to limit of solubility[8]. Crowding favors formation of compact conformations that has the tendency to reduce aggregation[8]. However, increasing protein concentrations increases protein association that accelerates aggregation. Protein have a solubility limit, that depends on the solution. When protein concentration exceeds this solubility limit proteins have a tendency to aggregate and crash[8, 41]. In our experiments, we use a concentration of 200 μM which is high enough to observe aggregation via various experimental methods.

Protein aggregation can be varied by numerous solution conditions that play a critical role. pH of a solution is one of the most important factors that can alter protein aggregation. The surface charge of proteins in solution depends on the solution pH, and it affects both intramolecular folding interactions and intermolecular protein–protein interactions[8]. Altering the solution pH might change the aggregation rate-limiting steps and the mechanisms and pathways of formation of aggregates and thus, the morphology of protein aggregates[42]. A buffering agent can be used to preserve the optimum pH for stability. Filtration of the proteins might also help to take out insoluble aggregates. Size exclusion chromatography and gel electroporation could be used in conjunction to identify larger aggregates and their removal.

Translocation studies should be attempted with just the protein monomer or lower-order oligomers and see their effect on translocation. Protein concentration is one of the biggest factors that contributes to aggregation and once we can single out

the other factors which are greatly responsible for aggregation of our proteins, we would be able to have control measures to avoid aggregation, even at higher concentration. It would also be worthwhile to check if the aggregation is reversible i.e., if diluting the protein back to a lower concentration ensures that there are no more aggregates.

5.3 Conclusion

The purpose of this study was to determine if our protein samples at higher concentrations (concentrations at which translocation studies in chapter 3 were done) formed aggregates. Using both DLS and interferometry we were able to identify aggregates at concentration of 200 μM. These techniques are reliable methods to observe and quantify aggregation, and further studies are warranted to expand on our findings and relate them to translocation. Additionally, we outline potential ways to reduce aggregation in future experiments with CPP-GFP fusions. To reduce protein aggregation, we can choose an array of experiments and modulate the temperature, concentrations of proteins, pH of our buffers and monitor the conditions. With this study, we gain knowledge and understanding on aggregation and factors affecting aggregation that can be related to protein fusions.

5.4 References

1. Wong, N. A.; Uchida, N. V.; Dissanayake, T. U.; Patel, M.; Iqbal, M.; Woehl, T. J., Detection and Sizing of Submicron Particles in Biologics With Interferometric Scattering Microscopy. *Journal of Pharmaceutical Sciences* **2020,** *109* (1), 881-890.
2. Cromwell, M. E. M.; Hilario, E.; Jacobson, F., Protein aggregation and bioprocessing. *The AAPS journal* **2006,** *8* (3), E572-E579.
3. Singh, S. K.; Afonina, N.; Awwad, M.; Bechtold-Peters, K.; Blue, J. T.; Chou, D.; Cromwell, M.; Krause, H.-J.; Mahler, H.-C.; Meyer, B. K.; Narhi, L.; Nesta, D. P.; Spitznagel, T., An Industry Perspective on the Monitoring of Subvisible Particles as a Quality Attribute for Protein Therapeutics. *Journal of Pharmaceutical Sciences* **2010,** *99* (8), 3302-3321.
4. Joubert, M. K.; Luo, Q.; Nashed-Samuel, Y.; Wypych, J.; Narhi, L. O., Classification and Characterization of Therapeutic Antibody Aggregates. *Journal of Biological Chemistry* **2011,** *286* (28), 25118-25133.
5. Roberts, C. J., Protein aggregation and its impact on product quality. *Current Opinion in Biotechnology* **2014,** *30*, 211-217.
6. Brange, J.; Andersen, L.; Laursen, E. D.; Meyn, G.; Rasmussen, E., Toward understanding insulin fibrillation. *Journal of Pharmaceutical Sciences* **1997,** *86* (5), 517-525.
7. Jiskoot, W.; Randolph, T. W.; Volkin, D. B.; Russell Middaugh, C.; Schöneich, C.; Winter, G.; Friess, W.; Crommelin, D. J. A.; Carpenter, J. F., Protein Instability and Immunogenicity: Roadblocks to Clinical Application of Injectable Protein Delivery Systems for Sustained Release. *Journal of Pharmaceutical Sciences* **2012,** *101* (3), 946-954.
8. Wang, W.; Nema, S.; Teagarden, D., Protein aggregation—Pathways and influencing factors. *International Journal of Pharmaceutics* **2010,** *390* (2), 89-99.
9. Kopito, R. R., Aggresomes, inclusion bodies and protein aggregation. *Trends in Cell Biology* **2000,** *10* (12), 524-530.
10. Kelly, J. W., The alternative conformations of amyloidogenic proteins and their multi-step assembly pathways. *Current Opinion in Structural Biology* **1998,** *8* (1), 101-106.
11. Chiti, F.; Stefani, M.; Taddei, N.; Ramponi, G.; Dobson, C. M., Rationalization of the effects of mutations on peptide and protein aggregation rates. *Nature* **2003,** *424* (6950), 805-8.
12. Rochet, J.-C.; Lansbury, P. T., Amyloid fibrillogenesis: themes and variations. *Current Opinion in Structural Biology* **2000,** *10* (1), 60-68.
13. Scheibel, T.; Buchner, J., Protein Aggregation as a Cause for Disease. In *Molecular Chaperones in Health and Disease*, Starke, K.; Gaestel, M., Eds. Springer Berlin Heidelberg: Berlin, Heidelberg, 2006; pp 199-219.

14. Filipe, V.; Poole, R.; Kutscher, M.; Forier, K.; Braeckmans, K.; Jiskoot, W., Fluorescence Single Particle Tracking for the Characterization of Submicron Protein Aggregates in Biological Fluids and Complex Formulations. *Pharmaceutical Research* **2011,** *28* (5), 1112-1120.
15. Filipe, V.; Que, I.; Carpenter, J. F.; Löwik, C.; Jiskoot, W., In Vivo Fluorescence Imaging of IgG1 Aggregates After Subcutaneous and Intravenous Injection in Mice. *Pharmaceutical Research* **2014,** *31* (1), 216-227.
16. Walder, R.; Schwartz, D. K., Dynamics of protein aggregation at the oil–water interface characterized by single molecule TIRF microscopy. *Soft Matter* **2011,** *7* (17), 7616-7622.
17. Daaboul, G. G.; Yurt, A.; Zhang, X.; Hwang, G. M.; Goldberg, B. B.; Ünlü, M. S., High-Throughput Detection and Sizing of Individual Low-Index Nanoparticles and Viruses for Pathogen Identification. *Nano Letters* **2010,** *10* (11), 4727-4731.
18. Young, G.; Kukura, P., Interferometric Scattering Microscopy. *Annual Review of Physical Chemistry* **2019,** *70* (1), 301-322.
19. Scherr, S. M.; Daaboul, G. G.; Trueb, J.; Sevenler, D.; Fawcett, H.; Goldberg, B.; Connor, J. H.; Ünlü, M. S., Real-Time Capture and Visualization of Individual Viruses in Complex Media. *ACS Nano* **2016,** *10* (2), 2827-2833.
20. Young, G.; Hundt, N.; Cole, D.; Fineberg, A.; Andrecka, J.; Tyler, A.; Olerinyova, A.; Ansari, A.; Marklund, E. G.; Collier, M. P.; Chandler, S. A.; Tkachenko, O.; Allen, J.; Crispin, M.; Billington, N.; Takagi, Y.; Sellers, J. R.; Eichmann, C.; Selenko, P.; Frey, L.; Riek, R.; Galpin, M. R.; Struwe, W. B.; Benesch, J. L. P.; Kukura, P., Quantitative mass imaging of single biological macromolecules. *Science* **2018,** *360* (6387), 423.
21. Stetefeld, J.; McKenna, S. A.; Patel, T. R., Dynamic light scattering: a practical guide and applications in biomedical sciences. *Biophysical reviews* **2016,** *8* (4), 409-427.
22. Harding, S. E.; Jumel, K., Light Scattering. *Current Protocols in Protein Science* **1998,** *11* (1), 7.8.1-7.8.14.
23. Stetefeld, J.; McKenna, S. A.; Patel, T. R., Dynamic light scattering: a practical guide and applications in biomedical sciences. *Biophys Rev* **2016,** *8* (4), 409-427.
24. Van Holde, K. E.; Johnson, W. C.; Ho, P. S., *Principles of Physical Biochemistry*. Upper Saddle River: Pear son Education: 2006.
25. Berne, B. J.; Pecora, R., Dynamic Light Scattering: with Applications to Chemistry, Biology, and Physics. **2000**.
26. Russel, W. B.; Saville, D. A.; Schowalter, W. R., *Colloidal Dispersions*. New York: Cambridge Univ. Press: 1991.
27. Oguzhan Avci; Maria I. Campana; Celalettin Yurdakul; Ünlü, M. S., Pupil function engineering for enhanced nanoparticle visibility in wide-field interferometric microscopy. *Optica* **2017,** *4*, 247-254.
28. Cavicchi, R. E.; King, J.; Ripple, D. C., Measurement of Average Aggregate Density by Sedimentation and Brownian Motion Analysis. *Journal of Pharmaceutical Sciences* **2018,** *107* (5), 1304-1312.

29. Erickson, H. P., Size and shape of protein molecules at the nanometer level determined by sedimentation, gel filtration, and electron microscopy. *Biol Proced Online* **2009,** *11*, 32-51.
30. Anyfantakis, M.; Geng, Z.; Morel, M.; Rudiuk, S.; Baigl, D., Modulation of the Coffee-Ring Effect in Particle/Surfactant Mixtures: the Importance of Particle–Interface Interactions. *Langmuir* **2015**.
31. li, H.; Buesen, D.; Williams, R.; Henig, J.; Stapf, S.; Mukherjee, K.; Freier, E.; Lubitz, W.; Winkler, M.; Happe, T.; Plumeré, N., Preventing the Coffee-Ring Effect and Aggregate Sedimentation by in-Situ Gelation of Monodisperse Materials. *Chemical Science* **2018,** *9*.
32. Espargaró, A.; Castillo, V.; de Groot, N. S.; Ventura, S., The in Vivo and in Vitro Aggregation Properties of Globular Proteins Correlate With Their Conformational Stability: The SH3 Case. *Journal of Molecular Biology* **2008,** *378* (5), 1116-1131.
33. Jungbauer, A.; Kaar, W., Current status of technical protein refolding. *Journal of Biotechnology* **2007,** *128* (3), 587-596.
34. Mannall, G. J.; Titchener-Hooker, N. J.; Dalby, P. A., Factors affecting protein refolding yields in a fed-batch and batch-refolding system. *Biotechnology and Bioengineering* **2007,** *97* (6), 1523-1534.
35. Burgess, R. R., Chapter 17 Refolding Solubilized Inclusion Body Proteins. In *Methods in Enzymology*, Burgess, R. R.; Deutscher, M. P., Eds. Academic Press: 2009; Vol. 463, pp 259-282.
36. Hao, Y.; Chu, J.; Wang, Y.; Zhuang, Y.; Zhang, S., The inhibition of aggregation of recombinant human consensus interferon-α mutant during Pichia pastoris fermentation. *Applied Microbiology and Biotechnology* **2007,** *74* (3), 578-584.
37. Bahrami, A.; Shojaosadati, Seyed A.; Khalilzadeh, R.; Mohammadian, J.; Farahani, Ebrahim V.; Masoumian, Mohammad R., Prevention of human granulocyte colony-stimulating factor protein aggregation in recombinant Pichia pastoris fed-batch fermentation using additives. *Biotechnology and Applied Biochemistry* **2009,** *52* (2), 141-148.
38. Seefeldt, M. B.; Kim, Y.-S.; Tolley, K. P.; Seely, J.; Carpenter, J. F.; Randolph, T. W., High-pressure studies of aggregation of recombinant human interleukin-1 receptor antagonist: thermodynamics, kinetics, and application to accelerated formulation studies. *Protein science : a publication of the Protein Society* **2005,** *14* (9), 2258-2266.
39. Considine, T.; Patel, H. A.; Singh, H.; Creamer, L. K., Influence of binding conjugated linoleic acid and myristic acid on the heat- and high-pressure-induced unfolding and aggregation of β-lactoglobulin B. *Food Chemistry* **2007,** *102* (4), 1270-1280.
40. Shukla, A. A.; Gupta, P.; Han, X., Protein aggregation kinetics during Protein A chromatography: Case study for an Fc fusion protein. *Journal of Chromatography A* **2007,** *1171* (1), 22-28.

41. Adachi, K.; Ding, M.; Asakura, T.; Surrey, S., Relationship between beta4 hydrogen bond and beta6 hydrophobic interactions during aggregate, fiber or crystal formation in oversaturated solutions of hemoglobin A and S. *Archives of biochemistry and biophysics* **2009,** *481* (2), 137-144.
42. Olsen, S. N.; Andersen, K. B.; Randolph, T. W.; Carpenter, J. F.; Westh, P., Role of electrostatic repulsion on colloidal stability of Bacillus halmapalus alpha-amylase. *Biochimica et Biophysica Acta (BBA) - Proteins and Proteomics* **2009,** *1794* (7), 1058-1065.

Chapter 6: Conclusion and future work

In this thesis, we have improved the understanding of CPP-cargo fusions and how they interact with *Candida albicans*. In Chapters 3 and 4, we established that CPPs can be used to deliver functional larger cargo into *Candida* cells. Some initial studies show that the cargo has a more pronounced effect on the secondary structure of the fusion than the peptide. Preliminary simulation studies, have enabled us to rationally design CPPs to study translocation and help understand the structure-function relationship. In Chapter 5, we show that our fusion proteins aggregate at our concentrations of 200 μM and further studies could help relate this to translocation. Our work has substantial impact for understanding CPP-mediated delivery of biomolecular cargo fusions in fungal pathogens that provides the motivation for additional work to further explore the limitations of cargo delivery into fungal pathogens and ways to make it better. In this chapter, we discuss suggestions for future studies for detection of non-fluorescent cargo. We have described how Western blot and split-protein assays can be used to detect non-fluorescent cargos. Additionally, we have outlined design strategies to enhance properties of peptides and proteins by the use of protein engineering techniques like directed evolution and rational design.

6.1 Detection of fusions inside Candida albicans *cells for non-fluorescent cargo*

So far, we have studied translocation into *Candida* using GFP as our cargo, using flow cytometry, but such translocation assays cannot be used for non-fluorescent cargo. Techniques like flow cytometry, fluorescent microscopy and other fluorescent techniques use fluorescent molecules to quantitatively detect the translocation into cells. Fluorescent techniques involve the use of either fluorescently labeled peptides or cargo. The labeled peptides are expensive to synthesize and site-specific conjugation of the peptide to the cargo might not be specific[2]. Also, a large number of cargoes are non-fluorescent, and approaches need to be developed to detect them inside cells. This motivated us to use Western blot as an alternate detection method.

6.1.1 Detection of fusions inside *Candida albicans* cells for non-fluorescent cargo using Western blot

Preliminary studies to detect fusions using Western blot have been done, with GFP using HRP-conjugated anti-GFP by Western blot (Figure 6.1), and validate our results obtained from flow cytometry. Samples for Western blot were prepared similar to the procedure outlined in Chapter 3 for quantification using flow cytometry (Section 3.2.5).

Protein samples were mixed with cell suspension and incubated at 30 °C for 24 h. After 24 h, the cells were washed with NaPB, and then incubated with 200 µL of 0.025 % trypsin (Invitrogen) at 37 °C for 30 mins to remove surface-bound proteins. Next, cells were washed and re-suspended in 250 µL of 10 mM NaPB and were then pelleted by centrifugation. Cells were then, resuspended in a required amount of Y-PER Reagent (ThermoFisher Scientific), according to the manufacturer's protocol. Y-PER is a chemical lysis agent to that helps to separate the proteins from the cells. Proteins in the soluble cell lysate were then recovered and separated by sodium dodecyl sulfate polyacrylamide gel electrophoresis (SDS-PAGE). The separated proteins were transferred to a polyvinyl difluoride (PVDF) membrane using a transblot (BioRad) and stained with horseradish peroxidase (HRP)-conjugated anti-GFP antibody (Abcam) to identify the proteins inside the cell. Densitometry analysis was done on the Western blot, using ImageLab software (Version 5.2; Bio-Rad) to evaluate the relative translocation level based on the signal of the detected bands. A one-way ANOVA analysis (GraphPad Prism 7.03) was used for statistical analysis to measure the

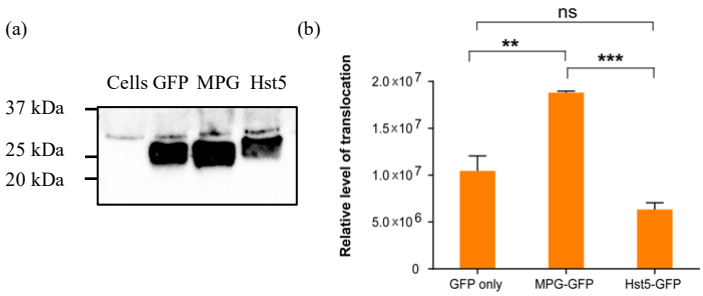

Figure 6.1. Detection of proteins inside *C. albicans* using anti-GFP. The protein fusions were expressed in E. coli BL21(DE3). Soluble cell lysates were prepared using Y-PER reagent and analyzed by Western blot. The samples were normalized by culture volume. Proteins were detected using an HRP-conjugated anti-GFP antibody. The relative translocation level confirmed that MPG-GFP translocation was significantly better than Hst5-GFP ($p \leq 0.001$). Molecular weights: GFP = 27 kDa, Hst5-GFP = 30.010 kDa, MPG-GFP = 30.500 kDa. Densitometry analysis done on 3 separate biological replicates.

statistical significance of each construct. The relative translocation level confirmed that MPG-GFP translocation was significantly better than Hst5-GFP ($p \leq 0.001$).

Though we have successfully detected the fusions inside *C. albicans* using Western blot, we are limited in evaluation of translocation and cannot evaluate function of the translocated protein. Another limitation is that we only get the average translocation for cells as a group, and individual cell data is not available and Western blot is not particularly quantitative. It is crucial to demonstrate that the internalized peptide-cargo fusions are capable of mediating biological functions once they are inside the cells. We do not have much evidence on cytosolic delivery and appropriate biological availability of the cargo delivered by the CPP, except that GFP remains fluorescent. While Western blot is cheap, easy to use, and produces quick results, there is no information available on localization data. We require a way to visualize any cargo, both fluorescent and non-fluorescent by a common technique to be able to compare between translocation and a split protein complementation assay is a promising alternative.

6.1.2 Split complementation assay for assessment of functional delivery of cargo

Our suggested approach is to use a split-protein complementation assay. In a split protein complementation assay, a protein (e.g., GFP) is split into two separate parts and become functional only when they come together (Figure 6.1)[1].

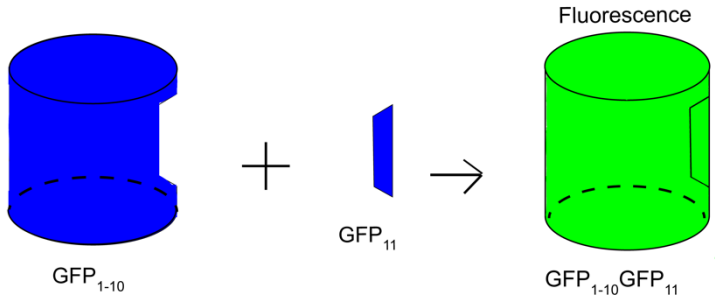

Figure 6.2. Representation of GFP complementation. Fluorescence is detected when the fragments GFP_{11} GFP_{1-10} protein come together.

Two fragments of GFP would work well for this approach. We would fuse CPP to the smaller fragment of GFP, and this fusion would be produced in *E. coli*., and the other fragment will be produced in our target organism. When these two fragments come together inside the target cells (Figure 6.2) they exhibit fluorescence. By fusing our cargo protein to the CPP-smaller fragment, we could identify delivery of any non-fluorescent cargo by measuring GFP fluorescence. This method will allow future studies more dedicated to the localization and function of any delivered cargo.

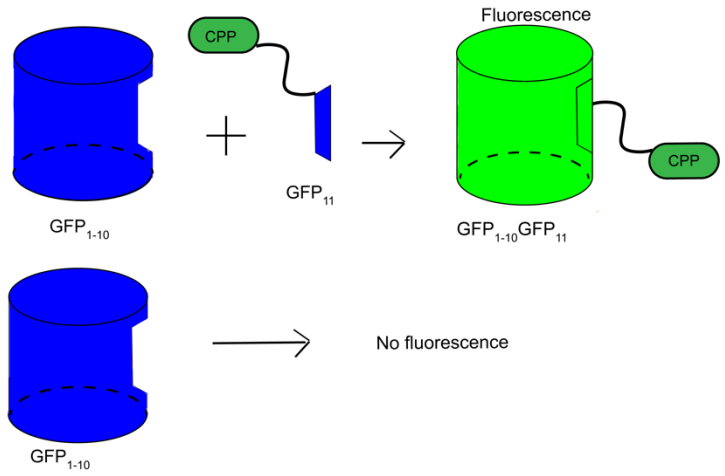

Figure 6.3. Protein-protein interactions. Fragment GFP_{1-10} and GFP_{11} are separately produced and are non-fluorescent but when they come together and they exhibit the classic fluorescence of a GFP molecule. (Adapted from www.picswe.com)

To design our system, we will use the template used by Cabantous et al. to detect uptake of our proteins[3, 4]. The self-assembling split-GFP protein-solubility assay[3, 4] will be designed as follows, using the GFP fragments designed by Cabantous et al.: GFP_{1-10}, the larger protein fragment, will be expressed in the cytosol of the target cells while the smaller GFP_{11} protein fragment will be fused to a CPP-cargo comprising moiety. The CPP fusion to a fragment of GFP, will guarantee that the complementation will happen if the fusion goes across the cell membrane and enters the cytoplasm to self-assemble into fluorescent GFP molecules (Figure 6.3).

I recommend starting with experiments for translocation in *Saccharomyces cerevisiae*, since it is a well-studied genetic model[5], before moving into *C. albicans* where heterologous protein expression will be more challenging[6]. We will produce the larger GFP_{1-10} fragment in *S. cerevisiae.* We will investigate the complementation signals made in the cells with the different fragments GFP_{1-10} and CPP-GFP_{11}

constructs and quantify GFP complementation with a fluorescence plate reader, flow cytometry and fluorescence microscopy.

Figure 6.4. Illustration of GFP complementation assay**.** Fluorescence is detected when CPP-protein fused to S11-peptide penetrates the cell membrane to complement cytosolic GFP_{1-10} protein[1]. [Source: Milech *et al.*, Scientific reports, *Copyright © 2015*, used with permission].

With $GFP_{1–10}$ being expressed in the cytoplasm, fluorescence will only appear when the CPP-GFP_{11} fusion penetrates and enters the cytoplasm and combines with GFP_{1-10}, to form the fluorescent molecule (Figure 6.3). This has the added advantage of confirming the delivery of the cargo protein to a location in the cell, and exert its biological function, rather than being trapped in the endosome. The split-GFP-based assay will be suitable for studying the translocation of a smaller sized cargo, and a non-fluorescent cargo that can be converted to into something that will be fluorescent inside the cell.

6.2 Use of Directed evolution to design CPPs for enhanced translocation

In chapter 2, I outlined protein engineering techniques that can be used to enhance peptide properties. Once such technique is the use of directed evolution. It imitates natural selection, and a large library can be generated by creating random or targeted mutations into the gene for any peptide. This library can then be exposed to multiple screening rounds and mutagenesis, and favorable mutants can be isolated from the first round and these mutants can be used as the basis for the next round and so on[7, 8]. These rounds of selection can continue until desired mutants with desired fitness have been achieved[8-10]. With directed evolution you have the flexibility of choosing the characteristic(s) you want to design for and iterating the screening until you achieve the required accuracy. Directed evolution has the advantage that is that there is no need to understand the mechanism of the desired activity or how mutations affect this activity[11]. But choosing the right screening technique is of utmost importance. Only a single variant is in each well, and, thus, genotype-to-phenotype linkage can be maintained. Display techniques like cell-surface display and in vitro display bring provide the ability to screen large numbers of variants to directed evolution, but reducing the library size can help to screen a library with less resources. Saturation mutagenesis would help us to use the combination of rational design and directed evolution. In site-saturation mutagenesis, peptides are screened for desirable fitness with all 20 canonical amino being sampled at the residue(s) of importance[12, 13]. We will identify important amino acids and subject them to site-saturation mutagenesis. The

resulting library can be screened for the best mutant. The best mutants can then be subjected to another round of mutagenesis. The peptides can be fluorescently labeled and we can use a fluorescent plate reader, incubate our labeled peptides with our cells and study their uptake (follow similar experimental procedure as for translocation studies in Chapters 3 and 4). For the mutants that translocated more into our cells, a second round of mutagenesis can lead to better peptides and so on.

6.3 Use of machine learning as a tool to design new and better CPPs to target fungal pathogens

Machine learning can be used to improve characteristics of peptides. A database of peptides can be used to train a model by finding patterns in a given set of peptides. The trained model can then generate new peptides with the preferred criteria. Machine-learning imitates directed evolution and helps selection of peptide with desirable fitness[14-17]. This section talks about the use of machine to design new peptides to target fungal pathogens. The ideas in this section were developed in collaboration with Mahdi Ghorbani.

With the growing research in the field of CPPs, predictive models can differentiate between whether a sequence of peptide is antifungal or antimicrobial in general, and this in turn reduces the cost of commercial synthesis and the experimental time for testing every peptide sequence in antimicrobial peptide studies. Machine

learning (ML) models like support vector machines (SVM), and random forest (RF) have received a lot of attention in recent years due to their ability to distinguish between positive and negative examples with improved precision[14, 18-20]. We would use ML methods to predict the antifungal activity of peptides, and also generate peptide sequences that are not degradable by enzymatic degradation and distinguish peptides that have synergy with current antifungal drugs. Herein, the following features will be used to characterize our peptides and differentiate them from non-CPPs: hydrophobicity, charge, amino acid frequency, amino acid repeats, number of arginine residues, size, hydrophilicity, sequence length, dipeptide frequencies, amino acid length, and tripeptide.

We would need to first generate a library based on experimental results. We would screen peptides for their activity as CPPs in *C. albicans* cells using experimental techniques like flow cytometry and fluorescence microscopy. Once we have a general data set of positive and negative examples, we will use ML to test antimicrobial peptides and classify them as CPPs vs. non-CPPs based on their translocation into mammalian cells, and fungal cells with the potential to function as peptide permeable into fungal cells without any toxicity to mammalian cells. This aim will help identify CPPs that can translocate into fungal cells and will warrant the development of preliminary structure-functional relationships for translocation into fungal cells. We will use known CPPs and known non-CPPs from the literature to serve as our library of positive and negative data-sets and use a variety of features to list and find potential CPPs[21]. The dataset for different sets can be obtained from repository for antifungal

peptides - DRAMP[22], toxic peptides – ToxinPred[23], non-toxic or random peptides from SwissProt and TrEMBL[23]. Gupta et al., saw that residues such as Cys, His, Asn, and Pro were abundantly present and favored at different locations in toxic peptides[23]. We will further use BLAST to find regions of similarity between biological sequences[24]. The Basic Local Alignment Search Tool (BLAST) finds regions of local similarity between sequences[24]. The program compares nucleotide or protein sequences to sequence databases and calculates the statistical significance of matches. BLAST can be used to infer functional and evolutionary relationships between sequences as well as help identify members of gene families[24]. We will use SVM and RF, and use the models on the datasets listed above and on the basis of the features mentioned before, we will predict the model with the best accuracy. This will help us to recognize features that make a peptide sequence antifungal and non-toxic to human cells and it can be used as a design criterion for CPPs. To exert antifungal activity, these peptides need to cross the cell barrier and thus behave as cell-penetrating peptides. To help generate better CPPs we can apply machine learning and determine features that make peptides antifungal and utilize it to cause random mutations to increase translocation into fungal cells without causing harm to mammalian cells.

6.4 *Evaluation of CPP-mediated translocation with C-terminal attachment of cargo*

Our experiments and simulations result in Chapter 3 have shown that MPG can enter *C. albicans* cells and deliver functional cargo inside the cells. In our preliminary experiments, we have studied the delivery of GFP into *C. albicans* cells. We recombinantly produced the proteins at 37 °C for 6 h based on my previous study[25], and purified the CPP-cargo constructs to study their translocation into *Candida* using flow cytometry. In our studies with the different CPPs, MPG preferentially delivered GFP but Hst5 was not able to. At the same time, simulation studies in Chapter 3 (Section 3.3.1) show that MPG entered the model yeast membrane but Hst5 remained attached to the membrane and did not go in. The simulation studies hinted on the fact that MPGs amphipathic structure, with N-terminal hydrophobicity made the transfer possible[26]. All our current constructs have a C-terminal attachment of cargo (Figure 6.5) but Gong et al.[27] has shown higher translocation with a smaller cargo but a N-terminal attachment. To understand the factors affecting the translocation, for example, CPP structure, sequence, placement of cargo, further studies need to be done to decide on the right placement of cargo in a CPP-cargo fusion construct. Thus, one proposed idea would be to design constructs with GFP attached on the N-terminus, followed by a flexible linker (glycine serine linker, G_4S) which in turn is fused to either MPG, pVEC or Hst5.

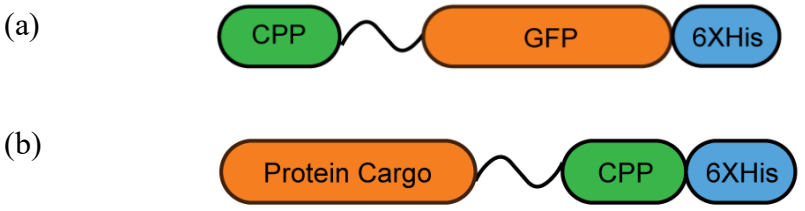

Figure 6.5. Construct design for translocation into *C. albicans*. (a) Design of current constructs with a C-terminal cargo attachment (b) Proposed design of constructs with a N-terminal cargo attachment.

This study will help us in understanding whether the placement of cargo has any implications on the translocation into fungal cells. This study can further shed light on to mechanism of transport as a function of CPP structure and sequence.

6.5 References

1. Milech, N.; Longville, B. A.; Cunningham, P. T.; Scobie, M. N.; Bogdawa, H. M.; Winslow, S.; Anastasas, M.; Connor, T.; Ong, F.; Stone, S. R.; Kerfoot, M.; Heinrich, T.; Kroeger, K. M.; Tan, Y. F.; Hoffmann, K.; Thomas, W. R.; Watt, P. M.; Hopkins, R. M., GFP-complementation assay to detect functional CPP and protein delivery into living cells. *Sci Rep* **2015,** *5*, 18329.
2. Hermanson, G. T., Functional targets. In *Bioconjugate Techniques*, Second ed.; Academic Press: Rockford, Illinois, 2008; p 1233.
3. Cabantous, S.; Terwilliger, T. C.; Waldo, G. S., Protein tagging and detection with engineered self-assembling fragments of green fluorescent protein. *Nat Biotechnol* **2005,** *23* (1), 102-7.
4. Cabantous, S.; Waldo, G. S., In vivo and in vitro protein solubility assays using split GFP. *Nature Methods* **2006,** *3*, 845.
5. Strausberg, R. L.; Strausberg, S. L., Overview of protein expression in Saccharomyces cerevisiae. *Curr Protoc Protein Sci* **2001,** *Chapter 5* (1), Unit5 6.
6. Sánchez-Martínez, C.; Pérez-Martín, J., Dimorphism in fungal pathogens: Candida albicans and Ustilago maydis—similar inputs, different outputs. *Current Opinion in Microbiology* **2001,** *4* (2), 214-221.
7. Lehmann, M.; Wyss, M., Engineering proteins for thermostability: the use of sequence alignments versus rational design and directed evolution. *Current Opinion in Biotechnology* **2001,** *12* (4), 371-375.
8. Adhikari, S.; Leissa, J. A.; Karlsson, A. J., Beyond function: Engineering improved peptides for therapeutic applications. *AIChE Journal* **2020,** *66* (3), e16776.
9. Song, J. K.; Rhee, J. S., Simultaneous Enhancement of Thermostability and Catalytic Activity of Phospholipase A1 by Evolutionary Molecular Engineering. *Applied and Environmental Microbiology* **2000,** *66* (3), 890-894.
10. Yokobayashi, Y.; Weiss, R.; Arnold, F. H., Directed evolution of a genetic circuit. *Proc Natl Acad Sci U S A* **2002,** *99* (26), 16587-91.
11. Giger, L.; Caner, S.; Obexer, R.; Kast, P.; Baker, D.; Ban, N.; Hilvert, D., Evolution of a designed retro-aldolase leads to complete active site remodeling. *Nat Chem Biol* **2013,** *9* (8), 494-498.
12. Reetz, M. T.; Carballeira, J. D.; Vogel, A., Iterative saturation mutagenesis on the basis of B factors as a strategy for increasing protein thermostability. *Angew Chem Int Ed Engl* **2006,** *45* (46), 7745-51.
13. Reetz, M. T.; Carballeira, J. D., Iterative saturation mutagenesis (ISM) for rapid directed evolution of functional enzymes. *Nat Protoc* **2007,** *2* (4), 891-903.
14. Fjell, C. D.; Jenssen, H.; Hilpert, K.; Cheung, W. A.; Pante, N.; Hancock, R. E.; Cherkasov, A., Identification of novel antibacterial peptides by chemoinformatics and machine learning. *J Med Chem* **2009,** *52* (7), 2006-15.

15. Khosravian, M.; Faramarzi, F. K.; Beigi, M. M.; Behbahani, M.; Mohabatkar, H., Predicting antibacterial peptides by the concept of Chou's pseudo-amino acid composition and machine learning methods. *Protein Pept Lett* **2013,** *20* (2), 180-6.
16. Sanders, W. S.; Johnston, C. I.; Bridges, S. M.; Burgess, S. C.; Willeford, K. O., Prediction of cell penetrating peptides by support vector machines. *PLoS Comput Biol* **2011,** *7* (7), e1002101.
17. Nielsen, H.; Brunak, S.; von Heijne, G., Machine learning approaches for the prediction of signal peptides and other protein sorting signals. *Protein Eng* **1999,** *12* (1), 3-9.
18. Khosravian, M. K. F., Fateme; Mohammad Beigi, Majid; Behbahani, Mandana; Mohabatkar, Hassan, Predicting Antibacterial Peptides by the Concept of Chou's Pseudo-amino Acid Composition and Machine Learning Methods. *Protein and Peptide Letters* **2013,** *20*, 180-186(7).
19. Lee, E. Y.; Lee, M. W.; Fulan, B. M.; Ferguson, A. L.; Wong, G. C. L., What can machine learning do for antimicrobial peptides, and what can antimicrobial peptides do for machine learning? *Interface focus* **2017,** *7* (6), 20160153-20160153.
20. Agrawal, P.; Bhalla, S.; Chaudhary, K.; Kumar, R.; Sharma, M.; Raghava, G. P. S. In silico approach for prediction of antifungal peptides *Frontiers in microbiology* [Online], 2018, p. 323. PubMed. http://europepmc.org/abstract/MED/29535692 https://doi.org/10.3389/fmicb.2018.00323 https://europepmc.org/articles/PMC5834480 https://europepmc.org/articles/PMC5834480?pdf=render (accessed 2018).
21. King, M. D.; Long, T.; Andersen, T.; McDougal, O. M., Genetic Algorithm Managed Peptide Mutant Screening: Optimizing Peptide Ligands for Targeted Receptor Binding. *Journal of Chemical Information and Modeling* **2016,** *56* (12), 2378-2387.
22. Fan, L.; Sun, J.; Zhou, M.; Zhou, J.; Lao, X.; Zheng, H.; Xu, H., DRAMP: a comprehensive data repository of antimicrobial peptides. *Scientific reports* **2016,** *6*, 24482-24482.
23. Gupta, S.; Kapoor, P.; Chaudhary, K.; Gautam, A.; Kumar, R.; Open Source Drug Discovery, C.; Raghava, G. P. S., In silico approach for predicting toxicity of peptides and proteins. *PloS one* **2013,** *8* (9), e73957-e73957.
24. Altschul, S. F.; Gish, W.; Miller, W.; Myers, E. W.; Lipman, D. J., Basic local alignment search tool. *Journal of Molecular Biology* **1990,** *215* (3), 403-410.
25. Adhikari, S.; Alahmadi, T. I.; Gong, Z.; Karlsson, A. J., Expression of Cell-Penetrating Peptides Fused to Protein Cargo. *J Mol Microbiol Biotechnol* **2018,** *28* (4), 159-168.
26. Simeoni, F., Insight into the mechanism of the peptide-based gene delivery system MPG: implications for delivery of siRNA into mammalian cells. *Nucleic Acids Res* **2003,** *31* (11), 2717-2724.

27. Gong, Z.; Ikonomova, S. P.; Karlsson, A. J., Secondary structure of cell-penetrating peptides during interaction with fungal cells. *Protein Sci* **2018,** *27* (3), 702-713.
28. Gong, Z.; Doolin, M. T.; Adhikari, S.; Stroka, K. M.; Karlsson, A. J., Role of charge and hydrophobicity in translocation of cell-penetrating peptides into Candida albicans cells. *AIChE Journal* **2019,** *65* (12).

Appendix A

Table A1 - Statistical analysis of Measurement of relative fluorescence unit (RFU)

Tukey's multiple comparisons test	Mean Difference.	95% CI of diff.	Significance	Summary
450 (nm)				
GFP vs. MPG-GFP	-10.7	-11289 to 11268	No	ns
GFP vs. Hst5-GFP	-1.738	-11280 to 11277	No	ns
MPG-GFP vs. Hst5-GFP	8.958	-11269 to 11287	No	ns
460 (nm)				
GFP vs. MPG-GFP	-45.09	-11323 to 11233	No	ns
GFP vs. Hst5-GFP	-26.06	-11304 to 11252	No	ns
MPG-GFP vs. Hst5-GFP	19.03	-11259 to 11297	No	ns
470 (nm)				
GFP vs. MPG-GFP	-1449	-12727 to 9830	No	ns
GFP vs. Hst5-GFP	-929.8	-12208 to 10349	No	ns
MPG-GFP vs. Hst5-GFP	519.1	-10759 to 11797	No	ns
480 (nm)				
GFP vs. MPG-GFP	-9846	-21124 to 1432	No	ns
GFP vs. Hst5-GFP	-5313	-16592 to 5965	No	ns
MPG-GFP vs. Hst5-GFP	4533	-6746 to 15811	No	ns
490 (nm)				
GFP vs. MPG-GFP	-4890	-16168 to 6388	No	ns
GFP vs. Hst5-GFP	-89.46	-11368 to 11189	No	ns
MPG-GFP vs. Hst5-GFP	4801	-6478 to 16079	No	ns
500				
GFP vs. MPG-GFP	-2962	-14241 to 8316	No	ns
GFP vs. Hst5-GFP	-5155	-16433 to 6124	No	ns
MPG-GFP vs. Hst5-GFP	-2192	-13471 to 9086	No	ns

510 (nm)				
GFP vs. MPG-GFP	-2136	-13415 to 9142	No	ns
GFP vs. Hst5-GFP	-7951	-19230 to 3327	No	ns
MPG-GFP vs. Hst5-GFP	-5815	-17093 to 5463	No	ns
520 (nm)				
GFP vs. MPG-GFP	21762	10484 to 33040	Yes	****
GFP vs. Hst5-GFP	15819	4540 to 27097	Yes	**
MPG-GFP vs. Hst5-GFP	-5943	-17222 to 5335	No	ns
530 (nm)				
GFP vs. MPG-GFP	17105	5826 to 28383	Yes	**
GFP vs. Hst5-GFP	12659	1380 to 23937	Yes	*
MPG-GFP vs. Hst5-GFP	-4446	-15725 to 6832	No	ns
540 (nm)				
GFP vs. MPG-GFP	13283	2005 to 24562	Yes	*
GFP vs. Hst5-GFP	9167	-2111 to 20445	No	ns
MPG-GFP vs. Hst5-GFP	-4116	-15395 to 7162	No	ns
550 (nm)				
GFP vs. MPG-GFP	9289	-1989 to 20567	No	ns
GFP vs. Hst5-GFP	7056	-4223 to 18334	No	ns
MPG-GFP vs. Hst5-GFP	-2233	-13511 to 9045	No	ns
560 (nm)				
GFP vs. MPG-GFP	5649	-5629 to 16928	No	ns
GFP vs. Hst5-GFP	4400	-6879 to 15678	No	ns
MPG-GFP vs. Hst5-GFP	-1250	-12528 to 10029	No	ns
570 (nm)				
GFP vs. MPG-GFP	3441	-7838 to 14719	No	ns
GFP vs. Hst5-GFP	2707	-8571 to 13985	No	ns
MPG-GFP vs. Hst5-GFP	-733.6	-12012 to 10545	No	ns
580 (nm)				
GFP vs. MPG-GFP	2002	-9277 to 13280	No	ns
GFP vs. Hst5-GFP	1576	-9703 to 12854	No	ns
MPG-GFP vs. Hst5-GFP	-426	-11704 to 10852	No	ns

Table A2 - Statistical analysis of Relative translocation – comparison between samples

Tukey's multiple comparisons test	Mean Difference	95% CI of diff.	Significant	Summary
cells only				
1 h vs. 4 h	-0.5144	-3.265 to 2.237	No	ns
1 h vs. 18 h	4.005	1.254 to 6.756	Yes	**
1 h vs. 24 h	2.801	0.05048 to 5.552	Yes	*
4 h vs. 18 h	4.519	1.768 to 7.270	Yes	***
4 h vs. 24 h	3.316	0.5649 to 6.067	Yes	*
18 h vs. 24 h	-1.203	-3.954 to 1.548	No	ns
cells +methanol				
1 h vs. 4 h	0.669	-2.082 to 3.420	No	ns
1 h vs. 18 h	2.12	-0.6310 to 4.871	No	ns
1 h vs. 24 h	1.973	-0.7776 to 4.724	No	ns
4 h vs. 18 h	1.451	-1.300 to 4.202	No	ns
4 h vs. 24 h	1.304	-1.447 to 4.055	No	ns
18 h vs. 24 h	-0.1467	-2.898 to 2.604	No	ns
cells + GFP				
1 h vs. 4 h	-1.315	-4.066 to 1.436	No	ns
1 h vs. 18 h	1.308	-1.443 to 4.059	No	ns
1 h vs. 24 h	1.74	-1.011 to 4.491	No	ns
4 h vs. 18 h	2.623	-0.1280 to 5.374	No	ns
4 h vs. 24 h	3.055	0.3040 to 5.806	Yes	*
18 h vs. 24 h	0.432	-2.319 to 3.183	No	ns
cells + MPG-GFP				
1 h vs. 4 h	-1.272	-4.023 to 1.479	No	ns
1 h vs. 18 h	1.4	-1.351 to 4.151	No	ns
1 h vs. 24 h	0.8547	-1.896 to 3.606	No	ns
4 h vs. 18 h	2.672	-0.07932 to 5.423	No	ns
4 h vs. 24 h	2.126	-0.6246 to 4.877	No	ns
18 h vs. 24 h	-0.5453	-3.296 to 2.206	No	ns

cells + Hst5-GFP				
1 h vs. 4 h	-0.3413	-3.092 to 2.410	No	ns
1 h vs. 18 h	1.545	-1.206 to 4.296	No	ns
1 h vs. 24 h	1.469	-1.282 to 4.220	No	ns
4 h vs. 18 h	1.887	-0.8643 to 4.638	No	ns
4 h vs. 24 h	1.81	-0.9410 to 4.561	No	ns
18 h vs. 24 h	-0.07667	-2.828 to 2.674	No	ns

Table A3 - Statistical analysis of Relative translocation – comparison between time points

Tukey's multiple comparisons test	Mean Difference	95% CI of diff.	Significant	Summary
1 h				
cells only vs. cells +methanol	-94.61	-99.11 to -90.11	Yes	****
cells only vs. cells + GFP	2.462	-2.040 to 6.964	No	ns
cells only vs. cells + MPG-GFP	2.411	-2.091 to 6.913	No	ns
cells only vs. cells + Hst5-GFP	2.234	-2.268 to 6.736	No	ns
cells +methanol vs. cells + GFP	97.07	92.57 to 101.6	Yes	****
cells +methanol vs. cells + MPG-GFP	97.02	92.52 to 101.5	Yes	****
cells +methanol vs. cells + Hst5-GFP	96.84	92.34 to 101.3	Yes	****
cells + GFP vs. cells + MPG-GFP	-0.05133	-4.553 to 4.451	No	ns
cells + GFP vs. cells + Hst5-GFP	-0.2287	-4.731 to 4.273	No	ns
cells + MPG-GFP vs. cells + Hst5-GFP	-0.1773	-4.679 to 4.325	No	ns
4 h				
cells only vs. cells +methanol	-93.42	-97.93 to -88.92	Yes	****
cells only vs. cells + GFP	1.662	-2.840 to 6.164	No	ns
cells only vs. cells + MPG-GFP	1.654	-2.848 to 6.156	No	ns
cells only vs. cells + Hst5-GFP	2.407	-2.095 to 6.909	No	ns
cells +methanol vs. cells + GFP	95.09	90.58 to 99.59	Yes	****
cells +methanol vs. cells + MPG-GFP	95.08	90.58 to 99.58	Yes	****
cells +methanol vs. cells + Hst5-GFP	95.83	91.33 to 100.3	Yes	****
cells + GFP vs. cells + MPG-GFP	-0.008	-4.510 to 4.494	No	ns
cells + GFP vs. cells + Hst5-GFP	0.745	-3.757 to 5.247	No	ns
cells + MPG-GFP vs. cells + Hst5-GFP	0.753	-3.749 to 5.255	No	ns
18 h				
cells only vs. cells +methanol	-96.49	-101.0 to -91.99	Yes	****
cells only vs. cells + GFP	-0.2346	-4.737 to 4.267	No	ns
cells only vs. cells + MPG-GFP	-0.1939	-4.696 to 4.308	No	ns
cells only vs. cells + Hst5-GFP	-0.2259	-4.728 to 4.276	No	ns
cells +methanol vs. cells + GFP	96.26	91.76 to 100.8	Yes	****

cells +methanol vs. cells + MPG-GFP	96.3	91.80 to 100.8	Yes	****
cells +methanol vs. cells + Hst5-GFP	96.27	91.76 to 100.8	Yes	****
cells + GFP vs. cells + MPG-GFP	0.04067	-4.461 to 4.543	No	ns
cells + GFP vs. cells + Hst5-GFP	0.008667	-4.493 to 4.511	No	ns
cells + MPG-GFP vs. cells + Hst5-GFP	-0.032	-4.534 to 4.470	No	ns
24 h				
cells only vs. cells +methanol	-95.44	-99.94 to -90.93	Yes	****
cells only vs. cells + GFP	1.401	-3.101 to 5.903	No	ns
cells only vs. cells + MPG-GFP	0.4642	-4.038 to 4.966	No	ns
cells only vs. cells + Hst5-GFP	0.9009	-3.601 to 5.403	No	ns
cells +methanol vs. cells + GFP	96.84	92.33 to 101.3	Yes	****
cells +methanol vs. cells + MPG-GFP	95.9	91.40 to 100.4	Yes	****
cells +methanol vs. cells + Hst5-GFP	96.34	91.83 to 100.8	Yes	****
cells + GFP vs. cells + MPG-GFP	-0.9367	-5.439 to 3.565	No	ns
cells + GFP vs. cells + Hst5-GFP	-0.5	-5.002 to 4.002	No	ns
cells + MPG-GFP vs. cells + Hst5-GFP	0.4367	-4.065 to 4.939	No	ns

Table A4 - Statistical analysis of Measurement of relative fluorescence unit (RFU)

Tukey's multiple comparisons test	Mean Difference	95% CI of diff.	Significant	Summary	Adjusted P Value
GFP only vs. MPG-GFP	-8347000	-1.272e+007 to -3.970e+006	Yes	**	0.0027
GFP only vs. Hst5-GFP	4124000	-252305 to 8.501e+006	No	ns	0.0623
MPG-GFP vs. Hst5-GFP	12470000	8.094e+006 to 1.685e+007	Yes	***	0.0003

References for Chapter 1

1. Ghannoum, M. A.; Rice, L. B., Antifungal agents: mode of action, mechanisms of resistance, and correlation of these mechanisms with bacterial resistance. *Clin Microbiol Rev* **1999,** *12* (4), 501-17.
2. Database, N. C. f. B. I. P., Amphotericin b, CID=1972. In *https://pubchem.ncbi.nlm.nih.gov/compound/Amphotericin-b (accessed on May 4, 2020)*, Pubchem: Vol. 500 x 500 pixels.
3. Database, N. C. f. B. I. P., Fluconazole, CID=3365. In *https://pubchem.ncbi.nlm.nih.gov/compound/Fluconazole (accessed on May 4, 2020)*, Pubchem.
4. Singh, T.; Murthy, A. S. N.; Yang, H. J.; Im, J., Versatility of cell-penetrating peptides for intracellular delivery of siRNA. *Drug Deliv* **2018,** *25* (1), 1996-2006.
5. Braun, K. P.; Gant, N. F.; Olson, C. M.; Parisi, V.; Forrest, K. A.; Peterson, C. M., A discriminant function for preeclampsia: case-control study of minor hemoglobins, red cell enzymes, and clinical laboratory values. *Am J Perinatol* **1997,** *14* (5), 297-302.
6. Richardson, J. P.; Moyes, D. L., Adaptive immune responses to Candida albicans infection. *Virulence* **2015,** *6* (4), 327-37.
7. Peter G. Pappas; Carol A. Kauffman; David R. Andes; Cornelius J. Clancy; Kieren A. Marr; Luis Ostrosky-Zeichner; Annette C. Reboli; Mindy G. Schuster; Jose A. Vazquez; Thomas J. Walsh; and, T. E. Z.; Sobel, J. D., Clinical Practice Guideline for the Management of Candidiasis: 2016 Update by the Infectious Diseases Society of America. *Clinical Infectious Diseases* **2016,** *62*.
8. Sánchez-Martínez, C.; Pérez-Martín, J., Dimorphism in fungal pathogens: Candida albicans and Ustilago maydis—similar inputs, different outputs. *Curr Opin Microbiol* **2001,** *4* (2), 214-221.
9. Moran, C.; Grussemeyer, C. A.; Spalding, J. R.; Benjamin, D. K., Jr.; Reed, S. D., Candida albicans and non-albicans bloodstream infections in adult and pediatric patients: comparison of mortality and costs. *Pediatr Infect Dis J* **2009,** *28* (5), 433-435.
10. Cannon, R. D.; Lamping, E.; Holmes, A. R.; Niimi, K.; Tanabe, K.; Niimi, M.; Monk, B. C., Candida albicans drug resistance another way to cope with stress. *Microbiology* **2007,** *153* (Pt 10), 3211-7.

11. White, T. C.; Marr, K. A.; Bowden, R. A., Clinical, cellular, and molecular factors that contribute to antifungal drug resistance. *Clin Microbiol Rev* **1998,** *11* (2), 382-402.
12. Pappas, P. G.; Rex, J. H.; Sobel, J. D.; Filler, S. G.; Dismukes, W. E.; Walsh, T. J.; Edwards, J. E.; Infectious Diseases Society of, A., Guidelines for treatment of candidiasis. *Clin Infect Dis* **2004,** *38* (2), 161-89.
13. Holz, R. W., The effects of the polyene antibiotics nystatin and amphotericin B on thin lipid membranes. *Ann N Y Acad Sci* **1974,** *235* (0), 469-79.
14. De Kruijff, B.; Demel, R. A., Polyene antibiotic-sterol interactions in membranes of Acholeplasma laidlawii cells and lecithin liposomes. III. Molecular structure of the polyene antibiotic-cholesterol complexes. *Biochim Biophys Acta, Biomembr* **1974,** *339* (1), 57-70.
15. D., K., The plasma membrane of C*andida albicans* and its role in the action of antifungal drugs. *The eukaryotic microbial cell* **1980**.
16. D., K., The protoplast membrane and antifungal drugs. *Fungal protoplasts: applications in biochemistry and genetics* **1985**.
17. Titsworth, E.; Grunberg, E., Chemotherapeutic activity of 5-fluorocytosine and amphotericin B against Candida albicans in mice. *Antimicrob Agents Chemother* **1973,** *4* (3), 306-8.
18. Weete, J. D.; Abril, M.; Blackwell, M., Phylogenetic distribution of fungal sterols. *PLoS One* **2010,** *5* (5), e10899.
19. Hitchcock, C. A.; Dickinson, K.; Brown, S. B.; Evans, E. G.; Adams, D. J., Interaction of azole antifungal antibiotics with cytochrome P-450-dependent 14 alpha-sterol demethylase purified from Candida albicans. *Biochem J* **1990,** *266* (2), 475-80.
20. Sanati, H.; Belanger, P.; Fratti, R.; Ghannoum, M., A new triazole, voriconazole (UK-109,496), blocks sterol biosynthesis in Candida albicans and Candida krusei. *Antimicrob Agents Chemother* **1997,** *41* (11), 2492-6.
21. Antibiotic resistance threats in the United States, 2019. **2019**.
22. Reissmann, S., Cell penetration: scope and limitations by the application of cell-penetrating peptides. *J Pept Sci* **2014,** *20* (10), 760-84.
23. Ruseska, I.; Zimmer, A., Internalization mechanisms of cell-penetrating peptides. *Beilstein J Nanotechnol* **2020,** *11*, 101-123.
24. Zhang, D.; Wang, J.; Xu, D., Cell-penetrating peptides as noninvasive transmembrane vectors for the development of novel multifunctional drug-delivery systems. *J Control Release* **2016,** *229*, 130-139.
25. Hudecz, F.; Banoczi, Z.; Csik, G., Medium-sized peptides as built in carriers for biologically active compounds. *Med Res Rev* **2005,** *25* (6), 679-736.

26. Fischer, R.; Fotin-Mleczek, M.; Hufnagel, H.; Brock, R., Break on through to the Other Side—Biophysics and Cell Biology Shed Light on Cell-Penetrating Peptides. *ChemBioChem* **2005,** *6* (12), 2126-2142.
27. Koren, E.; Torchilin, V. P., Cell-penetrating peptides:Breaking through to the other side. *Trends Mol Med* **2012,** *18* (7), 385-93.
28. Copolovici, D. M.; Langel, K.; Eriste, E.; Langel, U., Cell-penetrating peptides: design, synthesis, and applications. *ACS Nano* **2014,** *8* (3), 1972-94.
29. Mae, M.; Langel, U., Cell-penetrating peptides as vectors for peptide, protein and oligonucleotide delivery. *Curr Opin Pharmacol* **2006,** *6* (5), 509-14.
30. Madani, F.; Lindberg, S.; Langel, U.; Futaki, S.; Graslund, A., Mechanisms of cellular uptake of cell-penetrating peptides. *J Biophys* **2011,** *2011*, 414729.
31. Rousselle, C.; Clair, P.; Lefauconnier, J. M.; Kaczorek, M.; Scherrmann, J. M.; Temsamani, J., New advances in the transport of doxorubicin through the blood-brain barrier by a peptide vector-mediated strategy. *Mol Pharmacol* **2000,** *57* (4), 679-86.
32. Muratovska, A.; Eccles, M. R., Conjugate for efficient delivery of short interfering RNA (siRNA) into mammalian cells. *FEBS Lett* **2004,** *558* (1-3), 63-68.
33. Morris, M. C.; Vidal, P.; Chaloin, L.; Heitz, F.; Divita, G., A new peptide vector for efficient delivery of oligonucleotides into mammalian cells. *Nucleic Acids Res* **1997,** *25* (14), 2730-2736.
34. Morris, M. C.; Deshayes, S.; Heitz, F.; Divita, G., Cell-penetrating peptides: from molecular mechanisms to therapeutics. *Biol Cell* **2008,** *100* (4), 201-17.
35. Stetsenko, D. A.; Gait, M. J., Efficient conjugation of peptides to oligonucleotides by "native ligation". *J Org Chem* **2000,** *65* (16), 4900-8.
36. Fisher, L.; Soomets, U.; Cortes Toro, V.; Chilton, L.; Jiang, Y.; Langel, U.; Iverfeldt, K., Cellular delivery of a double-stranded oligonucleotide NFkappaB decoy by hybridization to complementary PNA linked to a cell-penetrating peptide. *Gene Ther* **2004,** *11* (16), 1264-72.
37. Shokolenko, I. N.; Alexeyev, M. F.; LeDoux, S. P.; Wilson, G. L., TAT-mediated protein transduction and targeted delivery of fusion proteins into mitochondria of breast cancer cells. *DNA Repair (Amst)* **2005,** *4* (4), 511-8.
38. Wadia, J. S.; Stan, R. V.; Dowdy, S. F., Transducible TAT-HA fusogenic peptide enhances escape of TAT-fusion proteins after lipid raft macropinocytosis. *Nat Med* **2004,** *10* (3), 310-5.
39. Olson, E. S.; Jiang, T.; Aguilera, T. A.; Nguyen, Q. T.; Ellies, L. G.; Scadeng, M.; Tsien, R. Y., Activatable cell penetrating peptides linked to nanoparticles as dual probes for in vivo fluorescence and MR imaging of proteases. *Proc Natl Acad Sci U S A* **2010,** *107* (9), 4311-6.

40. Masuda, R.; Yamamoto, K.; Koide, T., Cellular Uptake of IgG Using Collagen-Like Cell-Penetrating Peptides. *Biol Pharm Bull* **2016,** *39* (1), 130-4.
41. Lim, K. J.; Sung, B. H.; Shin, J. R.; Lee, Y. W.; Kim, D. J.; Yang, K. S.; Kim, S. C., A cancer specific cell-penetrating peptide, BR2, for the efficient delivery of an scFv into cancer cells. *PLoS One* **2013,** *8* (6), e66084.
42. Rajarao, G. K.; Nekhotiaeva, N.; Good, L., Peptide-mediated delivery of green fluorescent protein into yeasts and bacteria. *FEMS Microbiol Lett* **2002,** *215* (2), 267-72.
43. Jain, M.; Chauhan, S. C.; Singh, A. P.; Venkatraman, G.; Colcher, D.; Batra, S. K., Penetratin improves tumor retention of single-chain antibodies: a novel step toward optimization of radioimmunotherapy of solid tumors. *Cancer Res* **2005,** *65* (17), 7840-6.
44. Pooga, M.; Langel, Ü., Classes of Cell-Penetrating Peptides. In *Cell-Penetrating Peptides: Methods and Protocols*, Langel, Ü., Ed. Springer New York: New York, NY, 2015; pp 3-28.
45. Ziegler, A., Thermodynamic studies and binding mechanisms of cell-penetrating peptides with lipids and glycosaminoglycans. *Adv Drug Deliv Rev* **2008,** *60* (4-5), 580-97.
46. Mitchell, D. J.; Kim, D. T.; Steinman, L.; Fathman, C. G.; Rothbard, J. B., Polyarginine enters cells more efficiently than other polycationic homopolymers. *J Pept Res* **2000,** *56* (5), 318-25.
47. Drin, G.; Cottin, S.; Blanc, E.; Rees, A. R.; Temsamani, J., Studies on the Internalization Mechanism of Cationic Cell-penetrating Peptides. *Journal of Biological Chemistry* **2003,** *278* (33), 31192-31201.
48. Unnamalai, N.; Kang, B. G.; Lee, W. S., Cationic oligopeptide-mediated delivery of dsRNA for post-transcriptional gene silencing in plant cells. *FEBS Lett* **2004,** *566* (1-3), 307-10.
49. Gurnev, P. A.; Yang, S. T.; Melikov, K. C.; Chernomordik, L. V.; Bezrukov, S. M., Cationic cell-penetrating peptide binds to planar lipid bilayers containing negatively charged lipids but does not induce conductive pores. *Biophys J* **2013,** *104* (9), 1933-9.
50. Beloor, J.; Zeller, S.; Choi, C. S.; Lee, S. K.; Kumar, P., Cationic cell-penetrating peptides as vehicles for siRNA delivery. *Ther Deliv* **2015,** *6* (4), 491-507.
51. Kalafatovic, D.; Giralt, E., Cell-Penetrating Peptides: Design Strategies beyond Primary Structure and Amphipathicity. *Molecules* **2017,** *22* (11), 1929.
52. Derossi, D.; Joliot, A. H.; Chassaing, G.; Prochiantz, A., The 3rd helix of the antennapedia homeodomain translocates through biological-membranes. *Journal of Biological Chemistry* **1994,** *269* (14), 10444-10450.

53. Samad Mussa Farkhani, A. V., Hadi Karami, Samane Mohammadi, Nasrin Sohrabi, Fariba Badrzadeh, Cell penetrating peptides: Efficient vectors for delivery of nanoparticles, nanocarriers, therapeutic and diagnostic molecules. *Peptides* **2014** *Volume 57* 78–94
54. Mueller, N. H.; Ammar, D. A.; Petrash, J. M., Cell penetration peptides for enhanced entry of alphaB-crystallin into lens cells. *Invest Ophthalmol Vis Sci* **2013,** *54* (1), 2-8.
55. He, H.; Ye, J.; Wang, Y.; Liu, Q.; Chung, H. S.; Kwon, Y. M.; Shin, M. C.; Lee, K.; Yang, V. C., Cell-penetrating peptides meditated encapsulation of protein therapeutics into intact red blood cells and its application. *J Control Release* **2014,** *176*, 123-132.
56. Lorents, A.; Kodavali, P. K.; Oskolkov, N.; Langel, U.; Hallbrink, M.; Pooga, M., Cell-penetrating peptides split into two groups based on modulation of intracellular calcium concentration. *J Biol Chem* **2012,** *287* (20), 16880-9.
57. Palm-Apergi, C.; Lorents, A.; Padari, K.; Pooga, M.; Hallbrink, M., The membrane repair response masks membrane disturbances caused by cell-penetrating peptide uptake. *FASEB J* **2009,** *23* (1), 214-23.
58. Vives, E.; Brodin, P.; Lebleu, B., A truncated HIV-1 Tat protein basic domain rapidly translocates through the plasma membrane and accumulates in the cell nucleus. *J Biol Chem* **1997,** *272* (25), 16010-7.
59. Futaki, S.; Suzuki, T.; Ohashi, W.; Yagami, T.; Tanaka, S.; Ueda, K.; Sugiura, Y., Arginine-rich peptides. An abundant source of membrane-permeable peptides having potential as carriers for intracellular protein delivery. *J Biol Chem* **2001,** *276* (8), 5836-40.
60. Nakase, I.; Hirose, H.; Tanaka, G.; Tadokoro, A.; Kobayashi, S.; Takeuchi, T.; Futaki, S., Cell-surface accumulation of flock house virus-derived peptide leads to efficient internalization via macropinocytosis. *Mol Ther* **2009,** *17* (11), 1868-76.
61. Elmquist, A.; Lindgren, M.; Bartfai, T.; Langel, U., VE-cadherin-derived cell-penetrating peptide, pVEC, with carrier functions. *Exp Cell Res* **2001,** *269* (2), 237-44.
62. Trehin, R.; Krauss, U.; Beck-Sickinger, A. G.; Merkle, H. P.; Nielsen, H. M., Cellular uptake but low permeation of human calcitonin-derived cell penetrating peptides and Tat(47-57) through well-differentiated epithelial models. *Pharm Res* **2004,** *21* (7), 1248-56.
63. Morris, M. C.; Depollier, J.; Mery, J.; Heitz, F.; Divita, G., A peptide carrier for the delivery of biologically active proteins into mammalian cells. *Nat Biotechnol* **2001,** *19* (12), 1173-6.
64. Pooga, M.; Hällbrink, M.; Zorko, M.; Uuml; Langel, l., Cell penetration by transportan. *The FASEB Journal* **1998,** *12* (1), 67-77.

65. Soomets, U.; Lindgren, M.; Gallet, X.; Hällbrink, M.; Elmquist, A.; Balaspiri, L.; Zorko, M.; Pooga, M.; Brasseur, R.; Langel, Ü., Deletion analogues of transportan. *Biochimica et Biophysica Acta (BBA) - Biomembranes* **2000,** *1467* (1), 165-176.
66. Oehlke, J., A. Scheller, B. Wiesner, E. Krause, M. Beyermann, E. Klauschenz, M. Melzig, and M. Bienert, , Cellular uptake of an alpha-helical amphipathic model peptide with the potential to deliver polar compounds into the cell interior non-endocytically. *Biochimica Et Biophysica Acta-Biomembranes,* **1998,** *1414*, 127-139.
67. Scheller, A.; Oehlke, J.; Wiesner, B.; Dathe, M.; Krause, E.; Beyermann, M.; Melzig, M.; Bienert, M., Structural requirements for cellular uptake of alpha-helical amphipathic peptides. *J Pept Sci* **1999,** *5* (4), 185-94.
68. Forsman, H.; Bylund, J.; Oprea, T. I.; Karlsson, A.; Boulay, F.; Rabiet, M. J.; Dahlgren, C., The leukocyte chemotactic receptor FPR2, but not the closely related FPR1, is sensitive to cell-penetrating pepducins with amino acid sequences descending from the third intracellular receptor loop. *Biochim Biophys Acta* **2013,** *1833* (8), 1914-23.
69. Lin, Y. Z.; Yao, S. Y.; Veach, R. A.; Torgerson, T. R.; Hawiger, J., Inhibition of nuclear translocation of transcription factor NF-kappa B by a synthetic peptide containing a cell membrane-permeable motif and nuclear localization sequence. *J Biol Chem* **1995,** *270* (24), 14255-8.
70. Rhee, M.; Davis, P., Mechanism of uptake of C105Y, a novel cell-penetrating peptide. *J Biol Chem* **2006,** *281* (2), 1233-40.
71. Gao, C.; Mao, S.; Ditzel, H. J.; Farnaes, L.; Wirsching, P.; Lerner, R. A.; Janda, K. D., A cell-penetrating peptide from a novel pVII-pIX phage-displayed random peptide library. *Bioorg Med Chem* **2002,** *10* (12), 4057-65.
72. Marks, J. R.; Placone, J.; Hristova, K.; Wimley, W. C., Spontaneous membrane-translocating peptides by orthogonal high-throughput screening. *J Am Chem Soc* **2011,** *133* (23), 8995-9004.
73. Oehlke, J.; Birth, P.; Klauschenz, E.; Wiesner, B.; Beyermann, M.; Oksche, A.; Bienert, M., Cellular uptake of antisense oligonucleotides after complexing or conjugation with cell-penetrating model peptides. *Eur J Biochem* **2002,** *269* (16), 4025-32.
74. Martin, I.; Teixido, M.; Giralt, E., Design, synthesis and characterization of a new anionic cell-penetrating peptide: SAP(E). *Chembiochem* **2011,** *12* (6), 896-903.
75. Herbig, M. E.; Weller, K.; Krauss, U.; Beck-Sickinger, A. G.; Merkle, H. P.; Zerbe, O., Membrane surface-associated helices promote lipid interactions and cellular uptake of human calcitonin-derived cell penetrating peptides. *Biophys J* **2005,** *89* (6), 4056-66.

76. Conner, S. D.; Schmid, S. L., Regulated portals of entry into the cell. *Nature* **2003,** *422* (6927), 37-44.
77. Rejman, J.; Oberle, V.; Zuhorn, I. S.; Hoekstra, D., Size-dependent internalization of particles via the pathways of clathrin- and caveolae-mediated endocytosis. *Biochem J* **2004,** *377* (Pt 1), 159-69.
78. Sorkin, A.; Puthenveedu, M. A., Clathrin-Mediated Endocytosis. In *Vesicle Trafficking in Cancer*, Yarden, Y.; Tarcic, G., Eds. Springer New York: New York, NY, 2013; pp 1-31.
79. Lim, J. P.; Gleeson, P. A., Macropinocytosis: an endocytic pathway for internalising large gulps. *Immunol Cell Biol* **2011,** *89* (8), 836-43.
80. Lee, M. T.; Hung, W. C.; Chen, F. Y.; Huang, H. W., Many-body effect of antimicrobial peptides: on the correlation between lipid's spontaneous curvature and pore formation. *Biophys J* **2005,** *89* (6), 4006-16.
81. Kristensen, M.; Birch, D.; Morck Nielsen, H., Applications and challenges for use of cell-penetrating peptides as delivery vectors for peptide and protein cargos. *Int J Mol Sci* **2016,** *17* (2).
82. Bechara, C.; Sagan, S., Cell-penetrating peptides: 20 years later, where do we stand? *FEBS Lett* **2013,** *587* (12), 1693-702.
83. Derossi, D.; Calvet, S.; Trembleau, A.; Brunissen, A.; Chassaing, G.; Prochiantz, A., Cell Internalization of the Third Helix of the Antennapedia Homeodomain Is Receptor-independent. *Journal of Biological Chemistry* **1996,** *271* (30), 18188-18193.
84. Mäger, I.; Eiríksdóttir, E.; Langel, K.; El Andaloussi, S.; Langel, Ü., Assessing the uptake kinetics and internalization mechanisms of cell-penetrating peptides using a quenched fluorescence assay. *Biochimica et Biophysica Acta (BBA) - Biomembranes* **2010,** *1798* (3), 338-343.
85. Muñoz, A.; Marcos, J. F.; Read, N. D., Concentration-dependent mechanisms of cell penetration and killing by the de novo designed antifungal hexapeptide PAF26. *Molecular Microbiology* **2012,** *85* (1), 89-106.
86. López-García, B.; Pérez-Payá, E.; Marcos, J. F., Identification of novel hexapeptides bioactive against phytopathogenic fungi through screening of a synthetic peptide combinatorial library. *Applied and environmental microbiology* **2002,** *68* (5), 2453-2460.
87. Elmquist, A.; Hansen, M.; Langel, U., Structure-activity relationship study of the cell-penetrating peptide pVEC. *Biochim Biophys Acta* **2006,** *1758* (6), 721-9.
88. Green, M.; Loewenstein, P. M., Autonomous functional domains of chemically synthesized human immunodeficiency virus TAT trans-activator protein. *Cell* **1988,** *55* (6), 1179-88.

89. Stewart, K. M.; Horton, K. L.; Kelley, S. O., Cell-penetrating peptides as delivery vehicles for biology and medicine. *Org Biomol Chem* **2008,** *6* (13), 2242-55.
90. Cosgrave, L.; Devocelle, M.; Forster, R. J.; Keyes, T. E., Multimodal cell imaging by ruthenium polypyridyl labelled cell penetrating peptides. *Chem Commun (Camb)* **2010,** *46* (1), 103-5.
91. Derivery, E.; Bartolami, E.; Matile, S.; Gonzalez-Gaitan, M., Efficient delivery of quantum dots into the cytosol of cells using cell-penetrating poly(disulfide)s. *J Am Chem Soc* **2017,** *139* (30), 10172-10175.
92. Kameyama, S.; Horie, M.; Kikuchi, T.; Omura, T.; Takeuchi, T.; Nakase, I.; Sugiura, Y.; Futaki, S., Effects of cell-permeating peptide binding on the distribution of 125I-labeled Fab fragment in rats. *Bioconjug Chem* **2006,** *17* (3), 597-602.
93. Massodi, I.; Bidwell, G. L., 3rd; Raucher, D., Evaluation of cell penetrating peptides fused to elastin-like polypeptide for drug delivery. *J Control Release* **2005,** *108* (2-3), 396-408.
94. Parenteau, J.; Klinck, R.; Good, L.; Langel, U.; Wellinger, R. J.; Elela, S. A., Free uptake of cell-penetrating peptides by fission yeast. *FEBS Lett* **2005,** *579* (21), 4873-8.
95. Gong, Z.; Walls, M. T.; Karley, A. N.; Karlsson, A. J., Effect of a flexible linker on recombinant expression of cell-penetrating peptide fusion proteins and their translocation into fungal cells. *Mol Biotechnol* **2016,** *58* (12), 838-849.
96. Khafagy, E. S.; Morishita, M.; Kamei, N.; Eda, Y.; Ikeno, Y.; Takayama, K., Efficiency of cell-penetrating peptides on the nasal and intestinal absorption of therapeutic peptides and proteins. *Int. J. Pharm.* **2009,** *381* 49–55
97. Dinca, A.; Chien, W. M.; Chin, M. T., Intracellular delivery of proteins with cell-penetrating peptides for therapeutic uses in human disease. *Int J Mol Sci* **2016,** *17* (2), 263.
98. Habault, J.; Poyet, J. L., Recent advances in cell penetrating peptide-based anticancer therapies. *Molecules* **2019,** *24* (5), 927.
99. Chinak, O.; Golubitskaya, E.; Pyshnaya, I.; Stepanov, G.; Zhuravlev, E.; Richter, V.; Koval, O., Nucleic acids delivery into the cells using pro-apoptotic protein lactaptin. *Front Pharmacol* **2019,** *10* (1043), 1043.
100. Yue-Wern Huang ; Han-Jung Lee; Larry M. Tolliver; Aronstam, R. S., Delivery of Nucleic Acids and Nanomaterials by Cell-Penetrating Peptides: Opportunities and Challenges. *BioMed Research International* **2015**.
101. Eguchi, A.; Dowdy, S. F., siRNA delivery using peptide transduction domains. *Trends Pharmacol Sci* **2009,** *30* (7), 341-5.

102. Chiu, Y. L.; Ali, A.; Chu, C. Y.; Cao, H.; Rana, T. M., Visualizing a correlation between siRNA localization, cellular uptake, and RNAi in living cells. *Chem Biol* **2004,** *11* (8), 1165-75.
103. Wang, Y. H.; Hou, Y. W.; Lee, H. J., An intracellular delivery method for siRNA by an arginine-rich peptide. *J Biochem Biophys Methods* **2007,** *70* (4), 579-86.
104. Turner, J. J.; Jones, S.; Fabani, M. M.; Ivanova, G.; Arzumanov, A. A.; Gait, M. J., RNA targeting with peptide conjugates of oligonucleotides, siRNA and PNA. *Blood Cells Mol Dis* **2007,** *38* (1), 1-7.
105. Simeoni, F., Insight into the mechanism of the peptide-based gene delivery system MPG: implications for delivery of siRNA into mammalian cells. *Nucleic Acids Res* **2003,** *31* (11), 2717-2724.
106. Lundberg, P.; El-Andaloussi, S.; Sutlu, T.; Johansson, H.; Langel, U., Delivery of short interfering RNA using endosomolytic cell-penetrating peptides. *FASEB J* **2007,** *21* (11), 2664-71.
107. Meng, S.; Wei, B.; Xu, R.; Zhang, K.; Wang, L.; Zhang, R.; Li, J., TAT peptides mediated small interfering RNA delivery to Huh-7 cells and efficiently inhibited hepatitis C virus RNA replication. *Intervirology* **2009,** *52* (3), 135-40.
108. Lakshmanan, M.; Yoshizumi, T.; Sudesh, K.; Kodama, Y.; Numata, K., Double-stranded DNA introduction into intact plants using peptide–DNA complexes. *Plant Biotechnol* **2015,** *32* (1), 39-45.
109. Veldhoen, S.; Laufer, S. D.; Trampe, A.; Restle, T., Cellular delivery of small interfering RNA by a non-covalently attached cell-penetrating peptide: quantitative analysis of uptake and biological effect. *Nucleic Acids Res* **2006,** *34* (22), 6561-73.
110. Wadia, J. S.; Dowdy, S. F., Protein transduction technology. *Curr Opin Biotechnol* **2002,** *13* (1), 52-6.
111. Gump, J. M.; Dowdy, S. F., TAT transduction: the molecular mechanism and therapeutic prospects. *Trends Mol Med* **2007,** *13* (10), 443-8.
112. Futaki, S.; Ohashi, W.; Suzuki, T.; Niwa, M.; Tanaka, S.; Ueda, K.; Harashima, H.; Sugiura, Y., Stearylated arginine-rich peptides: a new class of transfection systems. *Bioconjug Chem* **2001,** *12* (6), 1005-11.
113. Wang, H. Y.; Chen, J. X.; Sun, Y. X.; Deng, J. Z.; Li, C.; Zhang, X. Z.; Zhuo, R. X., Construction of cell penetrating peptide vectors with N-terminal stearylated nuclear localization signal for targeted delivery of DNA into the cell nuclei. *J Control Release* **2011,** *155* (1), 26-33.
114. Jeong, C.; Yoo, J.; Lee, D.; Kim, Y. C., A branched TAT cell-penetrating peptide as a novel delivery carrier for the efficient gene transfection. *Biomater Res* **2016,** *20* (1), 28.

115. Li, J.; Feng, L.; Fan, L.; Zha, Y.; Guo, L.; Zhang, Q.; Chen, J.; Pang, Z.; Wang, Y.; Jiang, X.; Yang, V. C.; Wen, L., Targeting the brain with PEG-PLGA nanoparticles modified with phage-displayed peptides. *Biomaterials* **2011,** *32* (21), 4943-50.
116. Zhu, L.; Wang, T.; Perche, F.; Taigind, A.; Torchilin, V. P., Enhanced anticancer activity of nanopreparation containing an MMP2-sensitive PEG-drug conjugate and cell-penetrating moiety. *Proc Natl Acad Sci U S A* **2013,** *110* (42), 17047-52.
117. Silva, S.; Almeida, A. J.; Vale, N., Combination of cell-penetrating peptides with nanoparticles for therapeutic application: A review. *Biomolecules* **2019,** *9* (1), 22.
118. Wang, H.; Xu, K.; Liu, L.; Tan, J. P.; Chen, Y.; Li, Y.; Fan, W.; Wei, Z.; Sheng, J.; Yang, Y. Y.; Li, L., The efficacy of self-assembled cationic antimicrobial peptide nanoparticles against Cryptococcus neoformans for the treatment of meningitis. *Biomaterials* **2010,** *31* (10), 2874-81.
119. Liu, B. R.; Li, J. F.; Lu, S. W.; Leel, H. J.; Huang, Y. W.; Shannon, K. B.; Aronstam, R. S., Cellular internalization of quantum dots noncovalently conjugated with arginine-rich cell-penetrating peptides. *J Nanosci Nanotechnol* **2010,** *10* (10), 6534-43.
120. Lindgren, M.; Rosenthal-Aizman, K.; Saar, K.; Eiriksdottir, E.; Jiang, Y.; Sassian, M.; Ostlund, P.; Hallbrink, M.; Langel, U., Overcoming methotrexate resistance in breast cancer tumour cells by the use of a new cell-penetrating peptide. *Biochem Pharmacol* **2006,** *71* (4), 416-25.
121. Goun, E. A.; Pillow, T. H.; Jones, L. R.; Rothbard, J. B.; Wender, P. A., Molecular transporters: synthesis of oligoguanidinium transporters and their application to drug delivery and real-time imaging. *Chembiochem* **2006,** *7* (10), 1497-515.
122. Kirschberg, T. A.; VanDeusen, C. L.; Rothbard, J. B.; Yang, M.; Wender, P. A., Arginine-based molecular transporters: the synthesis and chemical evaluation of releasable taxol-transporter conjugates. *Org Lett* **2003,** *5* (19), 3459-62.
123. Dixon, M. J.; Bourre, L.; MacRobert, A. J.; Eggleston, I. M., Novel prodrug approach to photodynamic therapy: Fmoc solid-phase synthesis of a cell permeable peptide incorporating 5-aminolaevulinic acid. *Bioorg Med Chem Lett* **2007,** *17* (16), 4518-22.
124. Rajarao G. K.; and, N. N.; Good, L., The signal peptide NPFSD fused to ricin A chain enhances cell uptake and cytotoxicity in Candida albicans. *Biochemical and Biophysical Research Communications* **2003,** *301*, 529–534.

125. Palm, C.; Netzereab, S.; Hallbrink, M., Quantitatively determined uptake of cell-penetrating peptides in non-mammalian cells with an evaluation of degradation and antimicrobial effects. *Peptides* **2006,** *27* (7), 1710-6.
126. Gong, Z.; Ikonomova, S. P.; Karlsson, A. J., Secondary structure of cell-penetrating peptides during interaction with fungal cells. *Protein Sci* **2018,** *27* (3), 702-713.
127. Gong, Z.; Doolin, M. T.; Adhikari, S.; Stroka, K. M.; Karlsson, A. J., Role of charge and hydrophobicity in translocation of cell-penetrating peptides into Candida albicans cells. *AIChE Journal* **2019,** *65* (12).

References for Chapter 2

1. Adhikari, S.; Leissa, J. A.; Karlsson, A. J., Beyond function: Engineering improved peptides for therapeutic applications. *AIChE Journal* **2019,** *66* (3), e16776.
2. Fosgerau, K.; Hoffmann, T., Peptide therapeutics: current status and future directions. *Drug Discov Today* **2015,** *20* (1), 122-8.
3. Uhlig, T.; Kyprianou, T.; Martinelli, F. G.; Oppici, C. A.; Heiligers, D.; Hills, D.; Calvo, X. R.; Verhaert, P., The emergence of peptides in the pharmaceutical business: From exploration to exploitation. *EuPA Open Proteomics* **2014,** *4*, 58-69.
4. Lau, J. L.; Dunn, M. K., Therapeutic peptides: Historical perspectives, current development trends, and future directions. *Bioorg Med Chem* **2018,** *26* (10), 2700-2707.
5. Otvos, L., Jr.; Wade, J. D., Current challenges in peptide-based drug discovery. *Front Chem* **2014,** *2*, 62.
6. Abbvie, Abbvie Inc. Form 10-K 2018. Retrieved from U.S. Securities and Exchange Commission EDGAR: https://www.sec.gov/edgar/searchedgar/companysearch.html. Filed 2019, February 27.
7. Sanofi, Sanofi. Form 20-F 2018. Retrieved from U.S. Securities and Exchange Commission EDGAR: https://www.sec.gov/edgar/searchedgar/companysearch.html. Filed 2019, March 8.
8. Gupta, S.; Jain, A.; Chakraborty, M.; Sahni, J. K.; Ali, J.; Dang, S., Oral delivery of therapeutic proteins and peptides: a review on recent developments. *Drug Deliv* **2013,** *20* (6), 237-46.
9. Qvit, N.; Rubin, S. J. S.; Urban, T. J.; Mochly-Rosen, D.; Gross, E. R., Peptidomimetic therapeutics: scientific approaches and opportunities. *Drug Discov Today* **2017,** *22* (2), 454-462.
10. Neumann-Staubitz, P.; Neumann, H., The use of unnatural amino acids to study and engineer protein function. *Curr Opin Struct Biol* **2016,** *38*, 119-28.
11. Joshi, S.; Chen, L.; Winter, M. B.; Lin, Y. L.; Yang, Y.; Shapovalova, M.; Smith, P. M.; Liu, C.; Li, F.; LeBeau, A. M., The rational design of therapeutic peptides for aminopeptidase n using a substrate-based approach. *Sci Rep* **2017,** *7* (1), 1424.
12. Lipovsek, D.; Mena, M.; Lippow, S. M.; Basu, S.; Baynes, B. M., Library construction for protein engineering. In *Protein engineering and design*, Park, S. J.; Cochran, J. R., Eds. CRC Press: 2010.
13. Lehmann, M.; Wyss, M., Engineering proteins for thermostability: The use of sequence alignments versus rational design and directed evolution. *Curr Opin Biotech* **2001,** *12* (4), 371-375.

14. Song, J. K.; Rhee, J. S., Simultaneous enhancement of thermostability and catalytic activity of phospholipase A(1) by evolutionary molecular engineering. *Appl Environ Microbiol* **2000,** *66* (3), 890-4.
15. Yokobayashi, Y.; Weiss, R.; Arnold, F. H., Directed evolution of a genetic circuit. *Proc Natl Acad Sci U S A* **2002,** *99* (26), 16587-91.
16. Zweigerdt, R.; Braun, T.; Arnold, H. H., Faithful expression of the Myf-5 gene during mouse myogenesis requires distant control regions: a transgene approach using yeast artificial chromosomes. *Dev Biol* **1997,** *192* (1), 172-80.
17. Wittrup, K. D., Protein engineering by cell-surface display. *Curr Opin Biotechnol* **2001,** *12* (4), 395-9.
18. Jenson, J. M.; Xue, V.; Stretz, L.; Mandal, T.; Reich, L. L.; Keating, A. E., Peptide design by optimization on a data-parameterized protein interaction landscape. *Proc Natl Acad Sci U S A* **2018,** *115* (44), E10342-E10351.
19. Lamla, T.; Erdmann, V. A., Searching sequence space for high-affinity binding peptides using ribosome display. *J Mol Biol* **2003,** *329* (2), 381-388.
20. Winter, G.; Griffiths, A. D.; Hawkins, R. E.; Hoogenboom, H. R., Making antibodies by phage display technology. *Annu Rev Immunol* **1994,** *12* (1), 433-55.
21. Smith, G. P., Filamentous fusion phage: novel expression vectors that display cloned antigens on the virion surface. *Science* **1985,** *228* (4705), 1315-7.
22. Pande, J.; Szewczyk, M. M.; Grover, A. K., Phage display: concept, innovations, applications and future. *Biotechnol Adv* **2010,** *28* (6), 849-58.
23. Cherf, G. M.; Cochran, J. R., Applications of yeast surface display for protein engineering. *Methods Mol Biol* **2015,** *1319*, 155-75.
24. Boder, E. T.; Wittrup, K. D., Yeast surface display for screening combinatorial polypeptide libraries. *Nat Biotechnol* **1997,** *15* (6), 553-7.
25. Simeon, R.; Chen, Z., In vitro-engineered non-antibody protein therapeutics. *Protein Cell* **2018,** *9* (1), 3-14.
26. Charbit, A.; Boulain, J. C.; Ryter, A.; Hofnung, M., Probing the topology of a bacterial membrane protein by genetic insertion of a foreign epitope; expression at the cell surface. *EMBO J* **1986,** *5* (11), 3029-37.
27. Daugherty, P. S., Protein engineering with bacterial display. *Curr Opin Struct Biol* **2007,** *17* (4), 474-80.
28. Freudl, R.; MacIntyre, S.; Degen, M.; Henning, U., Cell surface exposure of the outer membrane protein OmpA of Escherichia coli K-12. *J Mol Biol* **1986,** *188* (3), 491-4.
29. Nicolay, T.; Vanderleyden, J.; Spaepen, S., Autotransporter-based cell surface display in Gram-negative bacteria. *Crit Rev Microbiol* **2015,** *41* (1), 109-23.
30. Lu, Z.; Murray, K. S.; Van Cleave, V.; LaVallie, E. R.; Stahl, M. L.; McCoy, J. M., Expression of thioredoxin random peptide libraries on the Escherichia coli cell surface as functional fusions to flagellin: a system designed for exploring protein-protein interactions. *Biotechnology (N Y)* **1995,** *13* (4), 366-72.

31. Mishra, B.; Reiling, S.; Zarena, D.; Wang, G., Host defense antimicrobial peptides as antibiotics: design and application strategies. *Curr Opin Chem Biol* **2017,** *38*, 87-96.
32. Lee, S. Y.; Choi, J. H.; Xu, Z., Microbial cell-surface display. *Trends Biotechnol* **2003,** *21* (1), 45-52.
33. Hanes, J.; Pluckthun, A., In vitro selection and evolution of functional proteins by using ribosome display. *Proc Natl Acad Sci U S A* **1997,** *94* (10), 4937-42.
34. He, M.; Taussig, M. J., Ribosome display: cell-free protein display technology. *Brief Funct Genomic Proteomic* **2002,** *1* (2), 204-12.
35. Reetz, M. T.; Carballeira, J. D., Iterative saturation mutagenesis (ISM) for rapid directed evolution of functional enzymes. *Nat Protoc* **2007,** *2* (4), 891-903.
36. Reetz, M. T.; Carballeira, J. D.; Vogel, A., Iterative saturation mutagenesis on the basis of B factors as a strategy for increasing protein thermostability. *Angew Chem Int Ed Engl* **2006,** *45* (46), 7745-51.
37. Reetz, M. T.; Wang, L. W.; Bocola, M., Directed evolution of enantioselective enzymes: iterative cycles of CASTing for probing protein-sequence space. *Angew Chem Int Ed Engl* **2006,** *45* (8), 1236-41.
38. Bradley, L. H., High-quality combinatorial protein libraries using the binary patterning approach. In *Protein Design: Methods and Applications*, Köhler, V., Ed. Springer New York: New York, NY, 2014; pp 117-128.
39. Kamtekar, S.; Schiffer, J. M.; Xiong, H.; Babik, J. M.; Hecht, M. H., Protein design by binary patterning of polar and nonpolar amino acids. *Science* **1993,** *262* (5140), 1680-5.
40. Bradley, L. H.; Wei, Y.; Thumfort, P.; Wurth, C.; Hecht, M. H., Protein design by binary patterning of polar and nonpolar amino acids. In *Protein Engineering Protocols*, Arndt, K. M.; Müller, K. M., Eds. Humana Press: Totowa, NJ, 2007; pp 155-166.
41. West, M. W.; Wang, W.; Patterson, J.; Mancias, J. D.; Beasley, J. R.; Hecht, M. H., De novo amyloid proteins from designed combinatorial libraries. *Proc Natl Acad Sci U S A* **1999,** *96* (20), 11211-6.
42. Wilson, D. S.; Keefe, A. D.; Szostak, J. W., The use of mRNA display to select high-affinity protein-binding peptides. *Proc Natl Acad Sci U S A* **2001,** *98* (7), 3750-5.
43. Coluzza, I., Computational protein design: A review. *J Phys Condens Matter* **2017,** *29* (14), 143001.
44. Nikiforovich, G. V., Computational molecular modeling in peptide drug design. *Int J Pept Protein Res* **1994,** *44* (6), 513-31.
45. Musiani, F.; Rossetti, G.; Capece, L.; Gerger, T. M.; Micheletti, C.; Varani, G.; Carloni, P., Molecular Dynamics Simulations Identify Time Scale of Conformational Changes Responsible for Conformational Selection in Molecular Recognition of HIV-1 Transactivation Responsive RNA. *Journal of the American Chemical Society* **2014,** *136* (44), 15631-15637.

46. Klepeis, J. L.; Lindorff-Larsen, K.; Dror, R. O.; Shaw, D. E., Long-timescale molecular dynamics simulations of protein structure and function. *Current Opinion in Structural Biology* **2009,** *19* (2), 120-127.
47. Beck, D. A.; White, G. W.; Daggett, V., Exploring the energy landscape of protein folding using replica-exchange and conventional molecular dynamics simulations. *J Struct Biol* **2007,** *157* (3), 514-23.
48. Yesylevskyy, S.; Marrink, S. J.; Mark, A. E., Alternative mechanisms for the interaction of the cell-penetrating peptides penetratin and the TAT peptide with lipid bilayers. *Biophys J* **2009,** *97* (1), 40-9.
49. Nguyen, T. H.; Rao, N. Z.; Schroeder, W. M.; Moore, P. B., Coarse-grained molecular dynamics of tetrameric transmembrane peptide bundles within a lipid bilayer. *Chem Phys Lipids* **2010,** *163* (6), 530-7.
50. Shelley, M. Y.; Selvan, M. E.; Zhao, J.; Babin, V.; Liao, C.; Li, J.; Shelley, J. C., A new mixed all-atom/coarse-grained model: Application to melittin aggregation in aqueous solution. *J Chem Theory Comput* **2017,** *13* (8), 3881-3897.
51. Fjell, C. D.; Jenssen, H.; Hilpert, K.; Cheung, W. A.; Pante, N.; Hancock, R. E.; Cherkasov, A., Identification of novel antibacterial peptides by chemoinformatics and machine learning. *J Med Chem* **2009,** *52* (7), 2006-15.
52. Khosravian, M.; Faramarzi, F. K.; Beigi, M. M.; Behbahani, M.; Mohabatkar, H., Predicting antibacterial peptides by the concept of Chou's pseudo-amino acid composition and machine learning methods. *Protein Pept Lett* **2013,** *20* (2), 180-6.
53. Sanders, W. S.; Johnston, C. I.; Bridges, S. M.; Burgess, S. C.; Willeford, K. O., Prediction of cell penetrating peptides by support vector machines. *PLoS Comput Biol* **2011,** *7* (7), e1002101.
54. Nielsen, H.; Brunak, S.; von Heijne, G., Machine learning approaches for the prediction of signal peptides and other protein sorting signals. *Protein Eng* **1999,** *12* (1), 3-9.
55. Verma, R.; Schwaneberg, U.; Roccatano, D., Computer-aided protein directed evolution: A review of web servers, databases and other computational tools for protein engineering. *Comput Struct Biotechnol J* **2012,** *2*, e201209008.
56. Camacho, C. J.; Katsumata, Y.; Ascherman, D. P., Structural and thermodynamic approach to peptide immunogenicity. *PLoS Comput Biol* **2008,** *4* (11), e1000231.
57. Sani, M. A.; Separovic, F., How membrane-active peptides get into lipid membranes. *Acc Chem Res* **2016,** *49* (6), 1130-8.
58. Sommese, R. F.; Sivaramakrishnan, S.; Baldwin, R. L.; Spudich, J. A., Helicity of short E-R/K peptides. *Protein Sci* **2010,** *19* (10), 2001-5.
59. Swanson, C. J.; Sivaramakrishnan, S., Harnessing the unique structural properties of isolated alpha-helices. *J Biol Chem* **2014,** *289* (37), 25460-7.
60. Wolny, M.; Batchelor, M.; Bartlett, G. J.; Baker, E. G.; Kurzawa, M.; Knight, P. J.; Dougan, L.; Woolfson, D. N.; Paci, E.; Peckham, M., Characterization of long and stable de novo single alpha-helix domains provides novel insight into their stability. *Sci Rep* **2017,** *7*, 44341.

61. Chou, S.; Shao, C.; Wang, J.; Shan, A.; Xu, L.; Dong, N.; Li, Z., Short, multiple-stranded beta-hairpin peptides have antimicrobial potency with high selectivity and salt resistance. *Acta Biomater* **2016,** *30*, 78-93.
62. Bureau, H. R.; Hershkovits, E.; Quirk, S.; Hernandez, R., Determining the energetics of small beta-sheet peptides using adaptive steered molecular dynamics. *J Chem Theory Comput* **2016,** *12* (4), 2028-37.
63. Capelli, R.; Villemot, F.; Moroni, E.; Tiana, G.; van der Vaart, A.; Colombo, G., Assessment of mutational effects on peptide stability through confinement simulations. *J Phys Chem Lett* **2016,** *7* (1), 126-30.
64. Yakimov, A. P.; Afanaseva, A. S.; Khodorkovskiy, M. A.; Petukhov, M. G., Design of stable alpha-helical peptides and thermostable proteins in biotechnology and biomedicine. *Acta Naturae* **2016,** *8* (4), 70-81.
65. Eijsink, V. G.; Gaseidnes, S.; Borchert, T. V.; van den Burg, B., Directed evolution of enzyme stability. *Biomol Eng* **2005,** *22* (1-3), 21-30.
66. Giver, L.; Gershenson, A.; Freskgard, P. O.; Arnold, F. H., Directed evolution of a thermostable esterase. *Proc Natl Acad Sci U S A* **1998,** *95* (22), 12809-13.
67. Socha, R. D.; Tokuriki, N., Modulating protein stability - directed evolution strategies for improved protein function. *FEBS J* **2013,** *280* (22), 5582-95.
68. Traxlmayr, M. W.; Obinger, C., Directed evolution of proteins for increased stability and expression using yeast display. *Arch Biochem Biophys* **2012,** *526* (2), 174-80.
69. Bond, C. J.; Marsters, J. C.; Sidhu, S. S., Contributions of CDR3 to VHH Domain Stability and the Design of Monobody Scaffolds for Naive Antibody Libraries. *J Mol Biol* **2003,** *332* (3), 643-655.
70. Julian, M. C.; Lee, C. C.; Tiller, K. E.; Rabia, L. A.; Day, E. K.; Schick, A. J., 3rd; Tessier, P. M., Co-evolution of affinity and stability of grafted amyloid-motif domain antibodies. *Protein Eng Des Sel* **2015,** *28* (10), 339-50.
71. Gröschel, A. H.; Müller, A. H. E., Self-assembly concepts for multicompartment nanostructures. *Nanoscale* **2015,** *7* (28), 11841-11876.
72. Tian, X.; Sun, F.; Zhou, X. R.; Luo, S. Z.; Chen, L., Role of peptide self-assembly in antimicrobial peptides. *J Pept Sci* **2015,** *21* (7), 530-9.
73. Habibi, N.; Kamaly, N.; Memic, A.; Shafiee, H., Self-assembled peptide-based nanostructures: Smart nanomaterials toward targeted drug delivery. *Nano Today* **2016,** *11* (1), 41-60.
74. Deidda, G.; Jonnalagadda, S. V. R.; Spies, J. W.; Ranella, A.; Mossou, E.; Forsyth, V. T.; Mitchell, E. P.; Bowler, M. W.; Tamamis, P.; Mitraki, A., Self-assembled amyloid peptides with arg-gly-asp (rgd) motifs as scaffolds for tissue engineering. *ACS Biomater Sci Eng* **2016,** *3* (7), 1404-1416.
75. Zhou, X. R.; Cao, Y.; Zhang, Q.; Tian, X. B.; Dong, H.; Chen, L.; Luo, S. Z., Self-assembly nanostructure controlled sustained release, activity and stability of peptide drugs. *Int J Pharm* **2017,** *528* (1-2), 723-731.

76. Zhang, H.; Park, J.; Jiang, Y.; Woodrow, K. A., Rational design of charged peptides that self-assemble into robust nanofibers as immune-functional scaffolds. *Acta Biomater* **2017,** *55*, 183-193.
77. Frederix, P. W.; Scott, G. G.; Abul-Haija, Y. M.; Kalafatovic, D.; Pappas, C. G.; Javid, N.; Hunt, N. T.; Ulijn, R. V.; Tuttle, T., Exploring the sequence space for (tri-)peptide self-assembly to design and discover new hydrogels. *Nat Chem* **2015,** *7* (1), 30-7.
78. Wang, M.; Wang, J.; Zhou, P.; Deng, J.; Zhao, Y.; Sun, Y.; Yang, W.; Wang, D.; Li, Z.; Hu, X.; King, S. M.; Rogers, S. E.; Cox, H.; Waigh, T. A.; Yang, J.; Lu, J. R.; Xu, H., Nanoribbons self-assembled from short peptides demonstrate the formation of polar zippers between beta-sheets. *Nat Commun* **2018,** *9* (1), 5118.
79. Chen, Y.; Xing, Z.; Liao, D.; Qiu, F., Neglected hydrophobicity of dimethanediyl group in peptide self-assembly: A hint from amyloid-like peptide GNNQQNY and its derivatives. *J Phys Chem B* **2018,** *122* (46), 10470-10477.
80. Rad-Malekshahi, M.; Lempsink, L.; Amidi, M.; Hennink, W. E.; Mastrobattista, E., Biomedical applications of self-assembling peptides. *Bioconjug Chem* **2016,** *27* (1), 3-18.
81. Zhou, P.; Deng, L.; Wang, Y.; Lu, J. R.; Xu, H., Different nanostructures caused by competition of intra- and inter-beta-sheet interactions in hierarchical self-assembly of short peptides. *J Colloid Interface Sci* **2016,** *464*, 219-28.
82. Fowler, S. B.; Poon, S.; Muff, R.; Chiti, F.; Dobson, C. M.; Zurdo, J., Rational design of aggregation-resistant bioactive peptides: reengineering human calcitonin. *Proc Natl Acad Sci U S A* **2005,** *102* (29), 10105-10.
83. Schellekens, H., Bioequivalence and the immunogenicity of biopharmaceuticals. *Nat Rev Drug Discov* **2002,** *1* (6), 457-62.
84. Zapadka, K. L.; Becher, F. J.; Gomes Dos Santos, A. L.; Jackson, S. E., Factors affecting the physical stability (aggregation) of peptide therapeutics. *Interface Focus* **2017,** *7* (6), 20170030.
85. Chiti, F.; Stefani, M.; Taddei, N.; Ramponi, G.; Dobson, C. M., Rationalization of the effects of mutations on peptide and protein aggregation rates. *Nature* **2003,** *424* (6950), 805-8.
86. Zhou, P.; Hou, S.; Bai, Z.; Li, Z.; Wang, H.; Chen, Z.; Meng, Y., Disrupting the intramolecular interaction between proto-oncogene c-Src SH3 domain and its self-binding peptide PPII with rationally designed peptide ligands. *Artif Cells Nanomed Biotechnol* **2018,** *46* (6), 1122-1131.
87. Esler, W. P.; Stimson, E. R.; Ghilardi, J. R.; Lu, Y. A.; Felix, A. M.; Vinters, H. V.; Mantyh, P. W.; Lee, J. P.; Maggio, J. E., Point substitution in the central hydrophobic cluster of a human beta-amyloid congener disrupts peptide folding and abolishes plaque competence. *Biochemistry* **1996,** *35* (44), 13914-21.
88. Azriel, R.; Gazit, E., Analysis of the minimal amyloid-forming fragment of the islet amyloid polypeptide. An experimental support for the key role of the phenylalanine residue in amyloid formation. *J Biol Chem* **2001,** *276* (36), 34156-61.

89. Ashburn, T. T.; Lansbury, P. T., Interspecies sequence variations affect the kinetics and thermodynamics of amyloid formation: peptide models of pancreatic amyloid. *Journal of the American Chemical Society* **1993,** *115* (23), 11012-11013.
90. Gsponer, J.; Haberthur, U.; Caflisch, A., The role of side-chain interactions in the early steps of aggregation: Molecular dynamics simulations of an amyloid-forming peptide from the yeast prion Sup35. *Proc Natl Acad Sci U S A* **2003,** *100* (9), 5154-9.
91. Armstrong, A. H.; Chen, J.; McKoy, A. F.; Hecht, M. H., Mutations that replace aromatic side chains promote aggregation of the Alzheimer's Aβ peptide. *Biochemistry* **2011,** *50* (19), 4058-67.
92. Kim, W.; Hecht, M. H., Generic hydrophobic residues are sufficient to promote aggregation of the Alzheimer's Aβ42 peptide. *Proc Natl Acad Sci U S A* **2006,** *103* (43), 15824-9.
93. McGregor, D. P., Discovering and improving novel peptide therapeutics. *Curr Opin Pharmacol* **2008,** *8* (5), 616-9.
94. Fominaya, J.; Bravo, J.; Rebollo, A., Strategies to stabilize cell penetrating peptides for in vivo applications. *Ther Deliv* **2015,** *6* (10), 1171-94.
95. Ji, S.; Li, W.; Zhang, L.; Zhang, Y.; Cao, B., Cecropin A-melittin mutant with improved proteolytic stability and enhanced antimicrobial activity against bacteria and fungi associated with gastroenteritis in vitro. *Biochem Biophys Res Commun* **2014,** *451* (4), 650-5.
96. Sun, X.; Salih, E.; Oppenheim, F. G.; Helmerhorst, E. J., Activity-based mass spectrometric characterization of proteases and inhibitors in human saliva. *Proteomics Clin Appl* **2009,** *3* (7), 810-820.
97. Soder, P. O., Proteolytic activity in the oral cavity: proteolytic enzymes from human saliva and dental plaque material. *J Dent Res* **1972,** *51* (2), 389-93.
98. Nakamura, M.; Slots, J., Salivary enzymes. Origin and relationship to periodontal disease. *J Periodontal Res* **1983,** *18* (6), 559-69.
99. Naglik, J. R.; Challacombe, S. J.; Hube, B., Candida albicans secreted aspartyl proteinases in virulence and pathogenesis. *Microbiol Mol Biol Rev* **2003,** *67* (3), 400-28, table of contents.
100. Sriranganadane, D.; Waridel, P.; Salamin, K.; Reichard, U.; Grouzmann, E.; Neuhaus, J. M.; Quadroni, M.; Monod, M., Aspergillus protein degradation pathways with different secreted protease sets at neutral and acidic pH. *J Proteome Res* **2010,** *9* (7), 3511-9.
101. Molhoek, E. M.; van Dijk, A.; Veldhuizen, E. J. A.; Haagsman, H. P.; Bikker, F. J., Improved proteolytic stability of chicken cathelicidin-2 derived peptides by D-amino acid substitutions and cyclization. *Peptides* **2011,** *32* (5), 875-880.
102. Leisle, L.; Valiyaveetil, F.; Mehl, R. A.; Ahern, C. A., Incorporation of non-canonical amino acids. *Adv Exp Med Biol* **2015,** *869*, 119-51.
103. McGlinchey, R. P.; Lee, J. C., Cysteine cathepsins are essential in lysosomal degradation of alpha-synuclein. *Proc Natl Acad Sci U S A* **2015,** *112* (30), 9322-7.
104. Ikonomova, S. P.; Moghaddam-Taaheri, P.; Jabra-Rizk, M. A.; Wang, Y.; Karlsson, A. J., Engineering improved variants of the antifungal peptide histatin 5 with

reduced susceptibility to Candida albicans secreted aspartic proteases and enhanced antimicrobial potency. *FEBS J* **2018,** *285* (1), 146-159.
105. Wang, J.; Song, J.; Yang, Z.; He, S.; Yang, Y.; Feng, X.; Dou, X.; Shan, A., Antimicrobial peptides with high proteolytic resistance for combating gram-negative bacteria. *J Med Chem* **2019,** *62* (5), 2286-2304.
106. Howell, S. M.; Fiacco, S. V.; Takahashi, T. T.; Jalali-Yazdi, F.; Millward, S. W.; Hu, B.; Wang, P.; Roberts, R. W., Serum stable natural peptides designed by mRNA display. *Sci Rep* **2014,** *4*, 6008.
107. Sieber, V.; Pluckthun, A.; Schmid, F. X., Selecting proteins with improved stability by a phage-based method. *Nat Biotechnol* **1998,** *16* (10), 955-60.
108. Jiang, W.; Boder, E. T., High-throughput engineering and analysis of peptide binding to class II MHC. *Proc Natl Acad Sci U S A* **2010,** *107* (30), 13258-63.
109. Cieslewicz, M.; Tang, J.; Yu, J. L.; Cao, H.; Zavaljevski, M.; Motoyama, K.; Lieber, A.; Raines, E. W.; Pun, S. H., Targeted delivery of proapoptotic peptides to tumor-associated macrophages improves survival. *Proc Natl Acad Sci U S A* **2013,** *110* (40), 15919-24.
110. Leal, J.; Dong, T.; Taylor, A.; Siegrist, E.; Gao, F.; Smyth, H. D. C.; Ghosh, D., Mucus-penetrating phage-displayed peptides for improved transport across a mucus-like model. *Int J Pharm* **2018,** *553* (1-2), 57-64.
111. Reich, L. L.; Dutta, S.; Keating, A. E., Sortcery-a high-throughput method to affinity rank peptide ligands. *J Mol Biol* **2015,** *427* (11), 2135-50.
112. Manzo, G.; Scorciapino, M. A.; Wadhwani, P.; Burck, J.; Montaldo, N. P.; Pintus, M.; Sanna, R.; Casu, M.; Giuliani, A.; Pirri, G.; Luca, V.; Ulrich, A. S.; Rinaldi, A. C., Enhanced amphiphilic profile of a short beta-stranded peptide improves its antimicrobial activity. *PLoS One* **2015,** *10* (1), e0116379.
113. Gallo, M.; Defaus, S.; Andreu, D., 1988-2018: Thirty years of drug smuggling at the nano scale. Challenges and opportunities of cell-penetrating peptides in biomedical research. *Arch Biochem Biophys* **2019,** *661*, 74-86.
114. Derakhshankhah, H.; Jafari, S., Cell penetrating peptides: A concise review with emphasis on biomedical applications. *Biomed Pharmacother* **2018,** *108*, 1090-1096.
115. Gomes, B.; Augusto, M. T.; Felicio, M. R.; Hollmann, A.; Franco, O. L.; Goncalves, S.; Santos, N. C., Designing improved active peptides for therapeutic approaches against infectious diseases. *Biotechnol Adv* **2018,** *36* (2), 415-429.
116. Drin, G.; Cottin, S.; Blanc, E.; Rees, A. R.; Temsamani, J., Studies on the Internalization Mechanism of Cationic Cell-penetrating Peptides. *Journal of Biological Chemistry* **2003,** *278* (33), 31192-31201.
117. Thoren, P. E.; Persson, D.; Isakson, P.; Goksor, M.; Onfelt, A.; Norden, B., Uptake of analogs of penetratin, Tat(48-60) and oligoarginine in live cells. *Biochem Biophys Res Commun* **2003,** *307* (1), 100-7.
118. Wang, G.; Epand, R. F.; Mishra, B.; Lushnikova, T.; Thomas, V. C.; Bayles, K. W.; Epand, R. M., Decoding the functional roles of cationic side chains of the major

antimicrobial region of human cathelicidin LL-37. *Antimicrob Agents Chemother* **2012,** *56* (2), 845-56.
119. Gong, Z.; Karlsson, A. J., Translocation of cell-penetrating peptides into Candida fungal pathogens. *Protein Sci* **2017,** *26* (9), 1714-1725.
120. Kimura, S.; Kawano, T.; Iwasaki, T., Short polyhistidine peptides penetrate effectively into Nicotiana tabacum-cultured cells and Saccharomyces cerevisiae cells. *Biosci Biotechnol Biochem* **2017,** *81* (1), 112-118.
121. Wei, C.; Pohorille, A., Sequence-dependent interfacial adsorption and permeation of dipeptides across phospholipid membranes. *J Phys Chem B* **2017,** *121* (42), 9859-9867.
122. Kabelka, I.; Vacha, R., Optimal hydrophobicity and reorientation of amphiphilic peptides translocating through membrane. *Biophys J* **2018,** *115* (6), 1045-1054.
123. Tian, Y.; Zeng, X.; Li, J.; Jiang, Y.; Zhao, H.; Wang, D.; Huang, X.; Li, Z., Achieving enhanced cell penetration of short conformationally constrained peptides through amphiphilicity tuning. *Chem Sci* **2017,** *8* (11), 7576-7581.
124. Kim, S.; Hyun, S.; Lee, Y.; Lee, Y.; Yu, J., Nonhemolytic cell-penetrating peptides: Site specific introduction of glutamine and lysine residues into the alpha-helical peptide causes deletion of its direct membrane disrupting ability but retention of its cell penetrating ability. *Biomacromolecules* **2016,** *17* (9), 3007-15.

References for Chapter 3

1. Braun, B. R.; Johnson, A. D., Control of filament formation in Candida albicans by the transcriptional repressor TUP1. *Science* **1997,** *277* (5322), 105-9.
2. Peter G. Pappas; Carol A. Kauffman; David R. Andes; Cornelius J. Clancy; Kieren A. Marr; Luis Ostrosky-Zeichner; Annette C. Reboli; Mindy G. Schuster; Jose A. Vazquez; Thomas J. Walsh; and, T. E. Z.; Sobel, J. D., Clinical Practice Guideline for the Management of Candidiasis: 2016 Update by the Infectious Diseases Society of America. *Clinical Infectious Diseases* **2016,** *62*.
3. Ohkubo, Y. Z.; Pogorelov, T. V.; Arcario, M. J.; Christensen, G. A.; Tajkhorshid, E., Accelerating membrane insertion of peripheral proteins with a novel membrane mimetic model. *Biophys J* **2012,** *102* (9), 2130-9.
4. Adhikari, S.; Alahmadi, T. I.; Gong, Z.; Karlsson, A. J., Expression of Cell-Penetrating Peptides Fused to Protein Cargo. *J Mol Microbiol Biotechnol* **2018,** *28* (4), 159-168.
5. Sawaya, B. P.; Briggs, J. P.; Schnermann, J., Amphotericin B nephrotoxicity: The adverse consequences of altered membrane properties. *J Am Soc Nephrol* **1995,** *6* (2), 154-64.
6. Antibiotic resistance threats in the United States, 2019. **2019**.
7. Derossi, D.; Joliot, A. H.; Chassaing, G.; Prochiantz, A., The 3rd helix of the antennapedia homeodomain translocates through biological-membranes. *Journal of Biological Chemistry* **1994,** *269* (14), 10444-10450.
8. Frankel, A. D.; Pabo, C. O., Cellular uptake of the TAT protein from human immunodeficiency virus. *Cell* **1988,** *55* (6), 1189-93.
9. Ramaker, K.; Henkel, M.; Krause, T.; Rockendorf, N.; Frey, A., Cell penetrating peptides: a comparative transport analysis for 474 sequence motifs. *Drug Deliv* **2018,** *25* (1), 928-937.
10. Esposito, D.; Chatterjee, D. K., Enhancement of soluble protein expression through the use of fusion tags. *Curr Opin Biotechnol* **2006,** *17* (4), 353-8.
11. Green, M.; Loewenstein, P. M., Autonomous functional domains of chemically synthesized human immunodeficiency virus TAT trans-activator protein. *Cell* **1988,** *55* (6), 1179-88.
12. Morris, M. C.; Vidal, P.; Chaloin, L.; Heitz, F.; Divita, G., A new peptide vector for efficient delivery of oligonucleotides into mammalian cells. *Nucleic Acids Res* **1997,** *25* (14), 2730-2736.
13. Simeoni, F., Insight into the mechanism of the peptide-based gene delivery system MPG: implications for delivery of siRNA into mammalian cells. *Nucleic Acids Res* **2003,** *31* (11), 2717-2724.

14. Mochon, A. B.; Liu, H., The antimicrobial peptide histatin-5 causes a spatially restricted disruption on the *Candida albicans* surface, allowing rapid entry of the peptide into the cytoplasm. *PLoS Pathog* **2008,** *4* (10), e1000190.
15. Kwon, S. J.; Han, K.; Jung, S.; Lee, J. E.; Park, S.; Cheon, Y. P.; Lim, H. J., Transduction of the MPG-tagged fusion protein into mammalian cells and oocytes depends on amiloride-sensitive endocytic pathway. *BMC Biotechnol* **2009,** *9* (1), 73.
16. Morris, M. C.; Deshayes, S.; Heitz, F.; Divita, G., Cell-penetrating peptides: from molecular mechanisms to therapeutics. *Biol Cell* **2008,** *100* (4), 201-17.
17. Jang, W. S.; Bajwa, J. S.; Sun, J. N.; Edgerton, M., Salivary histatin 5 internalization by translocation, but not endocytosis, is required for fungicidal activity in Candida albicans. *Mol Microbiol* **2010,** *77* (2), 354-70.
18. Adhikari, S., Optimization of recombinant protein expression for cell-penetrating peptide fusions to protein cargo. **2017**.
19. Deshayes, S.; Decaffmeyer, M.; Brasseur, R.; Thomas, A., Structural polymorphism of two CPP: an important parameter of activity. *Biochim Biophys Acta* **2008,** *1778* (5), 1197-205.
20. Deshayes, S.; Gerbal-Chaloin, S.; Morris, M. C.; Aldrian-Herrada, G.; Charnet, P.; Divita, G.; Heitz, F., On the mechanism of non-endosomial peptide-mediated cellular delivery of nucleic acids. *Biochim Biophys Acta* **2004,** *1667* (2), 141-7.
21. Oppenheim, F. G.; Xu, T.; McMillian, F. M.; Levitz, S. M.; Diamond, R. D.; Offner, G. D.; Troxler, R. F., Histatins, a novel family of histidine-rich proteins in human parotid secretion. Isolation, characterization, primary structure, and fungistatic effects on Candida albicans. *J Biol Chem* **1988,** *263* (16), 7472-7.
22. Puri, S.; Edgerton, M., How does it kill?: understanding the candidacidal mechanism of salivary histatin 5. *Eukaryot Cell* **2014,** *13* (8), 958-64.
23. Du, H.; Puri, S.; McCall, A.; Norris, H. L.; Russo, T.; Edgerton, M., Human salivary protein histatin 5 has potent bactericidal activity against ESKAPE pathogens. *Front Cell Infect Microbiol* **2017,** *7*, 41.
24. Khan, S. A.; Fidel, P. L., Jr.; Thunayyan, A. A.; Varlotta, S.; Meiller, T. F.; Jabra-Rizk, M. A., Impaired Histatin-5 Levels and Salivary Antimicrobial Activity against C. albicans in HIV Infected Individuals. *J AIDS Clin Res* **2013,** *4* (193).
25. Jang, W. S.; Li, X. S.; Sun, J. N.; Edgerton, M., The P-113 fragment of histatin 5 requires a specific peptide sequence for intracellular translocation in Candida albicans, which is independent of cell wall binding. *Antimicrob Agents Chemother* **2008,** *52* (2), 497-504.
26. Dong, J.; Vylkova, S.; Li, X. S.; Edgerton, M., Calcium blocks fungicidal activity of human salivary histatin 5 through disruption of binding with Candida albicans. *J Dent Res* **2003,** *82* (9), 748-52.
27. Helmerhorst, E. J.; Breeuwer, P.; van't Hof, W.; Walgreen-Weterings, E.; Oomen, L. C.; Veerman, E. C.; Amerongen, A. V.; Abee, T., The cellular target of histatin 5 on *Candida albicans* is the energized mitochondrion. *J Biol Chem* **1999,** *274* (11), 7286-91.

28. Kristensen, M.; Birch, D.; Morck Nielsen, H., Applications and challenges for use of cell-penetrating peptides as delivery vectors for peptide and protein cargos. *Int J Mol Sci* **2016,** *17* (2).
29. Shin, M. C.; Zhang, J.; Min, K. A.; Lee, K.; Byun, Y.; David, A. E.; He, H.; Yang, V. C., Cell-penetrating peptides: achievements and challenges in application for cancer treatment. *Journal of biomedical materials research. Part A* **2014,** *102* (2), 575-587.
30. Dom, G.; Shaw-Jackson, C.; Matis, C.; Bouffioux, O.; Picard, J. J.; Prochiantz, A.; Mingeot-Leclercq, M. P.; Brasseur, R.; Rezsohazy, R., Cellular uptake of Antennapedia Penetratin peptides is a two-step process in which phase transfer precedes a tryptophan-dependent translocation. *Nucleic Acids Res* **2003,** *31* (2), 556-561.
31. Gariépy, J.; Kawamura, K., Vectorial delivery of macromolecules into cells using peptide-based vehicles. *Trends in Biotechnology* **2001,** *19* (1), 21-28.
32. Schwarze, S. R.; Ho, A.; Vocero-Akbani, A.; Dowdy, S. F., In vivo protein transduction: delivery of a biologically active protein into the mouse. *Science* **1999,** *285* (5433), 1569-72.
33. Koppelhus, U.; Nielsen, P. E., Antisense properties of peptide nucleic acid In *Antisense Drug Technology*
*(*Crooke, S. T., ed, Marcel Dekker, New York: 2001; pp 359–374.
34. Milech, N.; Longville, B. A.; Cunningham, P. T.; Scobie, M. N.; Bogdawa, H. M.; Winslow, S.; Anastasas, M.; Connor, T.; Ong, F.; Stone, S. R.; Kerfoot, M.; Heinrich, T.; Kroeger, K. M.; Tan, Y. F.; Hoffmann, K.; Thomas, W. R.; Watt, P. M.; Hopkins, R. M., GFP-complementation assay to detect functional CPP and protein delivery into living cells. *Sci Rep* **2015,** *5*, 18329.
35. Gong, Z.; Walls, M. T.; Karley, A. N.; Karlsson, A. J., Effect of a flexible linker on recombinant expression of cell-penetrating peptide fusion proteins and their translocation into fungal cells. *Mol Biotechnol* **2016,** *58* (12), 838-849.
36. Richard, J. P.; Melikov, K.; Vives, E.; Ramos, C.; Verbeure; B.; Gait, M. J.; Chernomordik, L. V., and; Lebleu, B., Cell-penetrating peptides: a re-evaluation of the mechanism of cellular uptake. *The Journal Of Biological Chemistry* **2003,** *278* (1), 585–590.
37. Smith, D. B.; Johnson, K. S., Single-Step Purification of Polypeptides Expressed in Escherichia-Coli as Fusions with Glutathione S-Transferase. *Gene* **1988,** *67* (1), 31-40.
38. Smith, D. B., Generating fusions to glutathione S-transferase for protein studies. *Methods Enzymol* **2000,** *326*, 254-70.
39. Ormo, M.; Cubitt, A. B.; Kallio, K.; Gross, L. A.; Tsien, R. Y.; Remington, S. J., Crystal structure of the *Aequorea victoria* green fluorescent protein. *Science* **1996,** *273* (5280), 1392-5.
40. Tsien, R. Y., The green fluorescent protein. *Annu Rev Biochem* **1998,** *67*, 509-44.

41. Nicoletti, I.; Migliorati, G.; Pagliacci, M. C.; Grignani, F.; Riccardi, C., A rapid and simple method for measuring thymocyte apoptosis by propidium iodide staining and flow cytometry. *Journal of Immunological Methods* **1991,** *139* (2), 271-279.
42. Riccardi, C.; Nicoletti, I., Analysis of apoptosis by propidium iodide staining and flow cytometry. *Nat Protoc* **2006,** *1* (3), 1458-61.
43. Richard, J. P.; Melikov, K.; Vives, E.; Ramos, C.; Verbeure, B.; Gait, M. J.; Chernomordik, L. V.; Lebleu, B., Cell-penetrating Peptides: A reevaluation of the mechanism of cellular uptake. *Journal of Biological Chemistry* **2003,** *278* (1), 585-590.
44. Shen, Y.; Maupetit, J.; Derreumaux, P.; Tufféry, P., Improved PEP-FOLD Approach for Peptide and Miniprotein Structure Prediction. *Journal of Chemical Theory and Computation* **2014,** *10* (10), 4745-4758.
45. Gong, Z.; Doolin, M. T.; Adhikari, S.; Stroka, K. M.; Karlsson, A. J., Role of charge and hydrophobicity in translocation of cell-penetrating peptides into Candida albicans cells. *AIChE Journal* **2019,** *65* (12).
46. Avitabile, C.; D'Andrea, L. D.; Romanelli, A., Circular Dichroism studies on the interactions of antimicrobial peptides with bacterial cells. *Scientific reports* **2014,** *4*, 4293-4293.
47. Malgieri, G.; Avitabile, C.; Palmieri, M.; D'Andrea, L. D.; Isernia, C.; Romanelli, A.; Fattorusso, R., Structural Basis of a Temporin 1b Analogue Antimicrobial Activity against Gram Negative Bacteria Determined by CD and NMR Techniques in Cellular Environment. *ACS Chem Biol* **2015,** *10* (4), 965-969.
48. Gong, Z.; Ikonomova, S. P.; Karlsson, A. J., Secondary structure of cell-penetrating peptides during interaction with fungal cells. *Protein Sci* **2018,** *27* (3), 702-713.

References for Chapter 4

1. Morris, M. C.; Deshayes, S.; Heitz, F.; Divita, G., Cell-penetrating peptides: from molecular mechanisms to therapeutics. *Biol Cell* **2008,** *100* (4), 201-17.
2. Adhikari, S., Optimization of recombinant protein expression for cell-penetrating peptide fusions to protein cargo. **2017**.
3. Deshayes, S.; Decaffmeyer, M.; Brasseur, R.; Thomas, A., Structural polymorphism of two CPP: an important parameter of activity. *Biochim Biophys Acta* **2008,** *1778* (5), 1197-205.
4. Deshayes, S.; Morris, M. C.; Divita, G.; Heitz, F., Interactions of amphipathic CPPs with model membranes. *Biochim Biophys Acta* **2006,** *1758* (3), 328-35.
5. Walrant, A.; Bechara, C.; Alves, I. D.; Sagan, S., Molecular partners for interaction and cell internalization of cell-penetrating peptides: how identical are they? *Nanomedicine (Lond)* **2012,** *7* (1), 133-43.
6. L Chaloin, M. M., N Van Mau, J Mery, Synthetic primary amphipathic peptides as tools for the cellular import of drugs and nucleic acids. **2001**.
7. Gong, Z.; Doolin, M. T.; Adhikari, S.; Stroka, K. M.; Karlsson, A. J., Role of charge and hydrophobicity in translocation of cell-penetrating peptides into Candida albicans cells. *AIChE Journal* **2019,** *65* (12).
8. Gong, Z. Engineering Cell-Penetrating Peptides For Translocation And Intracellular Cargo Delivery In Candida Species. University of Maryland, College Park, College Park, Maryland, 2017.
9. Karlsson, A. J.; Pomerantz, W. C.; Weisblum, B.; Gellman, S. H.; Palecek, S. P., Antifungal activity from 14-helical beta-peptides. *J Am Chem Soc* **2006,** *128* (39), 12630-1.
10. Karlsson, A. J.; Pomerantz, W. C.; Neilsen, K. J.; Gellman, S. H.; Palecek, S. P., Effect of Sequence and Structural Properties on 14-Helical β-Peptide Activity against Candida albicans Planktonic Cells and Biofilms. *ACS Chem Biol* **2009,** *4* (7), 567-579.
11. Karagiannis, E. D.; Urbanska, A. M.; Sahay, G.; Pelet, J. M.; Jhunjhunwala, S.; Langer, R.; Anderson, D. G., Rational Design of a Biomimetic Cell Penetrating Peptide Library. *ACS Nano* **2013,** *7* (10), 8616-8626.
12. Ohkubo, Y. Z.; Pogorelov, T. V.; Arcario, M. J.; Christensen, G. A.; Tajkhorshid, E., Accelerating membrane insertion of peripheral proteins with a novel membrane mimetic model. *Biophys J* **2012,** *102* (9), 2130-9.
13. Magzoub, M.; Kilk, K.; Eriksson, L. E.; Langel, U.; Graslund, A., Interaction and structure induction of cell-penetrating peptides in the presence of phospholipid vesicles. *Biochim Biophys Acta* **2001,** *1512* (1), 77-89.
14. Deshayes, S.; Gerbal-Chaloin, S.; Morris, M. C.; Aldrian-Herrada, G.; Charnet, P.; Divita, G.; Heitz, F., On the mechanism of non-endosomial peptide-mediated cellular delivery of nucleic acids. *Biochim Biophys Acta* **2004,** *1667* (2), 141-7.

15. Deshayes, S.; Heitz, A.; Morris, M. C.; Charnet, P.; Divita, G.; Heitz, F., Insight into the mechanism of internalization of the cell-penetrating carrier peptide Pep-1 through conformational analysis. *Biochemistry* **2004,** *43* (6), 1449-57.
16. Drin, G.; Cottin, S.; Blanc, E.; Rees, A. R.; Temsamani, J., Studies on the Internalization Mechanism of Cationic Cell-penetrating Peptides. *Journal of Biological Chemistry* **2003,** *278* (33), 31192-31201.
17. Jamal Temsamani; Laruelle, C., SynB peptide vectors: A new approach to drug delivery. *Chimica Oggi / Chemistry Today* **2010,** *28*.
18. Gong, Z.; Karlsson, A. J., Translocation of cell-penetrating peptides into Candida fungal pathogens. *Protein Sci* **2017,** *26* (9), 1714-1725.
19. Mishra, A.; Lai, G. H.; Schmidt, N. W.; Sun, V. Z.; Rodriguez, A. R.; Tong, R.; Tang, L.; Cheng, J.; Deming, T. J.; Kamei, D. T.; Wong, G. C., Translocation of HIV TAT peptide and analogues induced by multiplexed membrane and cytoskeletal interactions. *Proc Natl Acad Sci U S A* **2011,** *108* (41), 16883-8.
20. Chen, C. H.; Wiedman, G.; Khan, A.; Ulmschneider, M. B., Absorption and folding of melittin onto lipid bilayer membranes via unbiased atomic detail microsecond molecular dynamics simulation. *Biochim Biophys Acta* **2014,** *1838* (9), 2243-9.
21. Richard, J. P.; Melikov, K.; Vives, E.; Ramos, C.; Verbeure; B.; Gait, M. J.; Chernomordik, L. V., and; Lebleu, B., Cell-penetrating peptides: a re-evaluation of the mechanism of cellular uptake. *The Journal Of Biological Chemistry* **2003,** *278* (1), 585–590.
22. Esposito, D.; Chatterjee, D. K., Enhancement of soluble protein expression through the use of fusion tags. *Curr Opin Biotechnol* **2006,** *17* (4), 353-8.
23. Ramaker, K.; Henkel, M.; Krause, T.; Rockendorf, N.; Frey, A., Cell penetrating peptides: a comparative transport analysis for 474 sequence motifs. *Drug Deliv* **2018,** *25* (1), 928-937.

References for Chapter 5

1. Wong, N. A.; Uchida, N. V.; Dissanayake, T. U.; Patel, M.; Iqbal, M.; Woehl, T. J., Detection and Sizing of Submicron Particles in Biologics With Interferometric Scattering Microscopy. *Journal of Pharmaceutical Sciences* **2020,** *109* (1), 881-890.
2. Cromwell, M. E. M.; Hilario, E.; Jacobson, F., Protein aggregation and bioprocessing. *The AAPS journal* **2006,** *8* (3), E572-E579.
3. Singh, S. K.; Afonina, N.; Awwad, M.; Bechtold-Peters, K.; Blue, J. T.; Chou, D.; Cromwell, M.; Krause, H.-J.; Mahler, H.-C.; Meyer, B. K.; Narhi, L.; Nesta, D. P.; Spitznagel, T., An Industry Perspective on the Monitoring of Subvisible Particles as a Quality Attribute for Protein Therapeutics. *Journal of Pharmaceutical Sciences* **2010,** *99* (8), 3302-3321.
4. Joubert, M. K.; Luo, Q.; Nashed-Samuel, Y.; Wypych, J.; Narhi, L. O., Classification and Characterization of Therapeutic Antibody Aggregates. *Journal of Biological Chemistry* **2011,** *286* (28), 25118-25133.
5. Roberts, C. J., Protein aggregation and its impact on product quality. *Current Opinion in Biotechnology* **2014,** *30*, 211-217.
6. Brange, J.; Andersen, L.; Laursen, E. D.; Meyn, G.; Rasmussen, E., Toward understanding insulin fibrillation. *Journal of Pharmaceutical Sciences* **1997,** *86* (5), 517-525.
7. Jiskoot, W.; Randolph, T. W.; Volkin, D. B.; Russell Middaugh, C.; Schöneich, C.; Winter, G.; Friess, W.; Crommelin, D. J. A.; Carpenter, J. F., Protein Instability and Immunogenicity: Roadblocks to Clinical Application of Injectable Protein Delivery Systems for Sustained Release. *Journal of Pharmaceutical Sciences* **2012,** *101* (3), 946-954.
8. Wang, W.; Nema, S.; Teagarden, D., Protein aggregation—Pathways and influencing factors. *International Journal of Pharmaceutics* **2010,** *390* (2), 89-99.
9. Kopito, R. R., Aggresomes, inclusion bodies and protein aggregation. *Trends in Cell Biology* **2000,** *10* (12), 524-530.
10. Kelly, J. W., The alternative conformations of amyloidogenic proteins and their multi-step assembly pathways. *Current Opinion in Structural Biology* **1998,** *8* (1), 101-106.
11. Chiti, F.; Stefani, M.; Taddei, N.; Ramponi, G.; Dobson, C. M., Rationalization of the effects of mutations on peptide and protein aggregation rates. *Nature* **2003,** *424* (6950), 805-8.
12. Rochet, J.-C.; Lansbury, P. T., Amyloid fibrillogenesis: themes and variations. *Current Opinion in Structural Biology* **2000,** *10* (1), 60-68.
13. Scheibel, T.; Buchner, J., Protein Aggregation as a Cause for Disease. In *Molecular Chaperones in Health and Disease*, Starke, K.; Gaestel, M., Eds. Springer Berlin Heidelberg: Berlin, Heidelberg, 2006; pp 199-219.
14. Filipe, V.; Poole, R.; Kutscher, M.; Forier, K.; Braeckmans, K.; Jiskoot, W., Fluorescence Single Particle Tracking for the Characterization of Submicron Protein

Aggregates in Biological Fluids and Complex Formulations. *Pharmaceutical Research* **2011,** *28* (5), 1112-1120.
15. Filipe, V.; Que, I.; Carpenter, J. F.; Löwik, C.; Jiskoot, W., In Vivo Fluorescence Imaging of IgG1 Aggregates After Subcutaneous and Intravenous Injection in Mice. *Pharmaceutical Research* **2014,** *31* (1), 216-227.
16. Walder, R.; Schwartz, D. K., Dynamics of protein aggregation at the oil–water interface characterized by single molecule TIRF microscopy. *Soft Matter* **2011,** *7* (17), 7616-7622.
17. Daaboul, G. G.; Yurt, A.; Zhang, X.; Hwang, G. M.; Goldberg, B. B.; Ünlü, M. S., High-Throughput Detection and Sizing of Individual Low-Index Nanoparticles and Viruses for Pathogen Identification. *Nano Letters* **2010,** *10* (11), 4727-4731.
18. Young, G.; Kukura, P., Interferometric Scattering Microscopy. *Annual Review of Physical Chemistry* **2019,** *70* (1), 301-322.
19. Scherr, S. M.; Daaboul, G. G.; Trueb, J.; Sevenler, D.; Fawcett, H.; Goldberg, B.; Connor, J. H.; Ünlü, M. S., Real-Time Capture and Visualization of Individual Viruses in Complex Media. *ACS Nano* **2016,** *10* (2), 2827-2833.
20. Young, G.; Hundt, N.; Cole, D.; Fineberg, A.; Andrecka, J.; Tyler, A.; Olerinyova, A.; Ansari, A.; Marklund, E. G.; Collier, M. P.; Chandler, S. A.; Tkachenko, O.; Allen, J.; Crispin, M.; Billington, N.; Takagi, Y.; Sellers, J. R.; Eichmann, C.; Selenko, P.; Frey, L.; Riek, R.; Galpin, M. R.; Struwe, W. B.; Benesch, J. L. P.; Kukura, P., Quantitative mass imaging of single biological macromolecules. *Science* **2018,** *360* (6387), 423.
21. Stetefeld, J.; McKenna, S. A.; Patel, T. R., Dynamic light scattering: a practical guide and applications in biomedical sciences. *Biophysical reviews* **2016,** *8* (4), 409-427.
22. Harding, S. E.; Jumel, K., Light Scattering. *Current Protocols in Protein Science* **1998,** *11* (1), 7.8.1-7.8.14.
23. Stetefeld, J.; McKenna, S. A.; Patel, T. R., Dynamic light scattering: a practical guide and applications in biomedical sciences. *Biophys Rev* **2016,** *8* (4), 409-427.
24. Van Holde, K. E.; Johnson, W. C.; Ho, P. S., *Principles of Physical Biochemistry*. Upper Saddle River: Pear son Education: 2006.
25. Berne, B. J.; Pecora, R., Dynamic Light Scattering: with Applications to Chemistry, Biology, and Physics. **2000**.
26. Russel, W. B.; Saville, D. A.; Schowalter, W. R., *Colloidal Dispersions*. New York: Cambridge Univ. Press: 1991.
27. Oguzhan Avci; Maria I. Campana; Celalettin Yurdakul; Ünlü, M. S., Pupil function engineering for enhanced nanoparticle visibility in wide-field interferometric microscopy. *Optica* **2017,** *4*, 247-254.
28. Cavicchi, R. E.; King, J.; Ripple, D. C., Measurement of Average Aggregate Density by Sedimentation and Brownian Motion Analysis. *Journal of Pharmaceutical Sciences* **2018,** *107* (5), 1304-1312.

29. Erickson, H. P., Size and shape of protein molecules at the nanometer level determined by sedimentation, gel filtration, and electron microscopy. *Biol Proced Online* **2009,** *11*, 32-51.
30. Anyfantakis, M.; Geng, Z.; Morel, M.; Rudiuk, S.; Baigl, D., Modulation of the Coffee-Ring Effect in Particle/Surfactant Mixtures: the Importance of Particle–Interface Interactions. *Langmuir* **2015**.
31. li, H.; Buesen, D.; Williams, R.; Henig, J.; Stapf, S.; Mukherjee, K.; Freier, E.; Lubitz, W.; Winkler, M.; Happe, T.; Plumeré, N., Preventing the Coffee-Ring Effect and Aggregate Sedimentation by in-Situ Gelation of Monodisperse Materials. *Chemical Science* **2018,** *9*.
32. Espargaró, A.; Castillo, V.; de Groot, N. S.; Ventura, S., The in Vivo and in Vitro Aggregation Properties of Globular Proteins Correlate With Their Conformational Stability: The SH3 Case. *Journal of Molecular Biology* **2008,** *378* (5), 1116-1131.
33. Jungbauer, A.; Kaar, W., Current status of technical protein refolding. *Journal of Biotechnology* **2007,** *128* (3), 587-596.
34. Mannall, G. J.; Titchener-Hooker, N. J.; Dalby, P. A., Factors affecting protein refolding yields in a fed-batch and batch-refolding system. *Biotechnology and Bioengineering* **2007,** *97* (6), 1523-1534.
35. Burgess, R. R., Chapter 17 Refolding Solubilized Inclusion Body Proteins. In *Methods in Enzymology*, Burgess, R. R.; Deutscher, M. P., Eds. Academic Press: 2009; Vol. 463, pp 259-282.
36. Hao, Y.; Chu, J.; Wang, Y.; Zhuang, Y.; Zhang, S., The inhibition of aggregation of recombinant human consensus interferon-α mutant during Pichia pastoris fermentation. *Applied Microbiology and Biotechnology* **2007,** *74* (3), 578-584.
37. Bahrami, A.; Shojaosadati, Seyed A.; Khalilzadeh, R.; Mohammadian, J.; Farahani, Ebrahim V.; Masoumian, Mohammad R., Prevention of human granulocyte colony-stimulating factor protein aggregation in recombinant Pichia pastoris fed-batch fermentation using additives. *Biotechnology and Applied Biochemistry* **2009,** *52* (2), 141-148.
38. Seefeldt, M. B.; Kim, Y.-S.; Tolley, K. P.; Seely, J.; Carpenter, J. F.; Randolph, T. W., High-pressure studies of aggregation of recombinant human interleukin-1 receptor antagonist: thermodynamics, kinetics, and application to accelerated formulation studies. *Protein science : a publication of the Protein Society* **2005,** *14* (9), 2258-2266.
39. Considine, T.; Patel, H. A.; Singh, H.; Creamer, L. K., Influence of binding conjugated linoleic acid and myristic acid on the heat- and high-pressure-induced unfolding and aggregation of β-lactoglobulin B. *Food Chemistry* **2007,** *102* (4), 1270-1280.
40. Shukla, A. A.; Gupta, P.; Han, X., Protein aggregation kinetics during Protein A chromatography: Case study for an Fc fusion protein. *Journal of Chromatography A* **2007,** *1171* (1), 22-28.

41. Adachi, K.; Ding, M.; Asakura, T.; Surrey, S., Relationship between beta4 hydrogen bond and beta6 hydrophobic interactions during aggregate, fiber or crystal formation in oversaturated solutions of hemoglobin A and S. *Archives of biochemistry and biophysics* **2009,** *481* (2), 137-144.
42. Olsen, S. N.; Andersen, K. B.; Randolph, T. W.; Carpenter, J. F.; Westh, P., Role of electrostatic repulsion on colloidal stability of Bacillus halmapalus alpha-amylase. *Biochimica et Biophysica Acta (BBA) - Proteins and Proteomics* **2009,** *1794* (7), 1058-1065.

References for Chapter 6

1. Milech, N.; Longville, B. A.; Cunningham, P. T.; Scobie, M. N.; Bogdawa, H. M.; Winslow, S.; Anastasas, M.; Connor, T.; Ong, F.; Stone, S. R.; Kerfoot, M.; Heinrich, T.; Kroeger, K. M.; Tan, Y. F.; Hoffmann, K.; Thomas, W. R.; Watt, P. M.; Hopkins, R. M., GFP-complementation assay to detect functional CPP and protein delivery into living cells. *Sci Rep* **2015,** *5*, 18329.
2. Hermanson, G. T., Functional targets. In *Bioconjugate Techniques*, Second ed.; Academic Press: Rockford, Illinois, 2008; p 1233.
3. Cabantous, S.; Terwilliger, T. C.; Waldo, G. S., Protein tagging and detection with engineered self-assembling fragments of green fluorescent protein. *Nat Biotechnol* **2005,** *23* (1), 102-7.
4. Cabantous, S.; Waldo, G. S., In vivo and in vitro protein solubility assays using split GFP. *Nature Methods* **2006,** *3*, 845.
5. Strausberg, R. L.; Strausberg, S. L., Overview of protein expression in Saccharomyces cerevisiae. *Curr Protoc Protein Sci* **2001,** *Chapter 5* (1), Unit5 6.
6. Sánchez-Martínez, C.; Pérez-Martín, J., Dimorphism in fungal pathogens: Candida albicans and Ustilago maydis—similar inputs, different outputs. *Current Opinion in Microbiology* **2001,** *4* (2), 214-221.
7. Lehmann, M.; Wyss, M., Engineering proteins for thermostability: the use of sequence alignments versus rational design and directed evolution. *Current Opinion in Biotechnology* **2001,** *12* (4), 371-375.
8. Adhikari, S.; Leissa, J. A.; Karlsson, A. J., Beyond function: Engineering improved peptides for therapeutic applications. *AIChE Journal* **2020,** *66* (3), e16776.
9. Song, J. K.; Rhee, J. S., Simultaneous Enhancement of Thermostability and Catalytic Activity of Phospholipase A1 by Evolutionary Molecular Engineering. *Applied and Environmental Microbiology* **2000,** *66* (3), 890-894.
10. Yokobayashi, Y.; Weiss, R.; Arnold, F. H., Directed evolution of a genetic circuit. *Proc Natl Acad Sci U S A* **2002,** *99* (26), 16587-91.
11. Giger, L.; Caner, S.; Obexer, R.; Kast, P.; Baker, D.; Ban, N.; Hilvert, D., Evolution of a designed retro-aldolase leads to complete active site remodeling. *Nat Chem Biol* **2013,** *9* (8), 494-498.
12. Reetz, M. T.; Carballeira, J. D.; Vogel, A., Iterative saturation mutagenesis on the basis of B factors as a strategy for increasing protein thermostability. *Angew Chem Int Ed Engl* **2006,** *45* (46), 7745-51.
13. Reetz, M. T.; Carballeira, J. D., Iterative saturation mutagenesis (ISM) for rapid directed evolution of functional enzymes. *Nat Protoc* **2007,** *2* (4), 891-903.
14. Fjell, C. D.; Jenssen, H.; Hilpert, K.; Cheung, W. A.; Pante, N.; Hancock, R. E.; Cherkasov, A., Identification of novel antibacterial peptides by chemoinformatics and machine learning. *J Med Chem* **2009,** *52* (7), 2006-15.

15. Khosravian, M.; Faramarzi, F. K.; Beigi, M. M.; Behbahani, M.; Mohabatkar, H., Predicting antibacterial peptides by the concept of Chou's pseudo-amino acid composition and machine learning methods. *Protein Pept Lett* **2013,** *20* (2), 180-6.
16. Sanders, W. S.; Johnston, C. I.; Bridges, S. M.; Burgess, S. C.; Willeford, K. O., Prediction of cell penetrating peptides by support vector machines. *PLoS Comput Biol* **2011,** *7* (7), e1002101.
17. Nielsen, H.; Brunak, S.; von Heijne, G., Machine learning approaches for the prediction of signal peptides and other protein sorting signals. *Protein Eng* **1999,** *12* (1), 3-9.
18. Khosravian, M. K. F., Fateme; Mohammad Beigi, Majid; Behbahani, Mandana; Mohabatkar, Hassan, Predicting Antibacterial Peptides by the Concept of Chou's Pseudo-amino Acid Composition and Machine Learning Methods. *Protein and Peptide Letters* **2013,** *20*, 180-186(7).
19. Lee, E. Y.; Lee, M. W.; Fulan, B. M.; Ferguson, A. L.; Wong, G. C. L., What can machine learning do for antimicrobial peptides, and what can antimicrobial peptides do for machine learning? *Interface focus* **2017,** *7* (6), 20160153-20160153.
20. Agrawal, P.; Bhalla, S.; Chaudhary, K.; Kumar, R.; Sharma, M.; Raghava, G. P. S. In silico approach for prediction of antifungal peptides *Frontiers in microbiology* [Online], 2018, p. 323. PubMed. http://europepmc.org/abstract/MED/29535692 https://doi.org/10.3389/fmicb.2018.00323 https://europepmc.org/articles/PMC5834480 https://europepmc.org/articles/PMC5834480?pdf=render (accessed 2018).
21. King, M. D.; Long, T.; Andersen, T.; McDougal, O. M., Genetic Algorithm Managed Peptide Mutant Screening: Optimizing Peptide Ligands for Targeted Receptor Binding. *Journal of Chemical Information and Modeling* **2016,** *56* (12), 2378-2387.
22. Fan, L.; Sun, J.; Zhou, M.; Zhou, J.; Lao, X.; Zheng, H.; Xu, H., DRAMP: a comprehensive data repository of antimicrobial peptides. *Scientific reports* **2016,** *6*, 24482-24482.
23. Gupta, S.; Kapoor, P.; Chaudhary, K.; Gautam, A.; Kumar, R.; Open Source Drug Discovery, C.; Raghava, G. P. S., In silico approach for predicting toxicity of peptides and proteins. *PloS one* **2013,** *8* (9), e73957-e73957.
24. Altschul, S. F.; Gish, W.; Miller, W.; Myers, E. W.; Lipman, D. J., Basic local alignment search tool. *Journal of Molecular Biology* **1990,** *215* (3), 403-410.
25. Adhikari, S.; Alahmadi, T. I.; Gong, Z.; Karlsson, A. J., Expression of Cell-Penetrating Peptides Fused to Protein Cargo. *J Mol Microbiol Biotechnol* **2018,** *28* (4), 159-168.
26. Simeoni, F., Insight into the mechanism of the peptide-based gene delivery system MPG: implications for delivery of siRNA into mammalian cells. *Nucleic Acids Res* **2003,** *31* (11), 2717-2724.

27. Gong, Z.; Ikonomova, S. P.; Karlsson, A. J., Secondary structure of cell-penetrating peptides during interaction with fungal cells. *Protein Sci* **2018,** *27* (3), 702-713.
28. Gong, Z.; Doolin, M. T.; Adhikari, S.; Stroka, K. M.; Karlsson, A. J., Role of charge and hydrophobicity in translocation of cell-penetrating peptides into Candida albicans cells. *AIChE Journal* **2019,** *65* (12).